Hydrodynamic analysis of a dual-body Wave Energy Converter device with two different Power Take-off configurations

Julio Cesar de Souza Filho

Thesis to obtain the Master of Science Degree in

Naval Architecture and Ocean Engineering

Examination Committee:

President:	Prof. Ângelo Teixeira
Supervisor:	Dr. Kourosh Rezanejad
Co-supervisor:	Prof. Dr. Carlos Guedes Soares
Members:	Prof. Shan Wang
	Dr. Kourosh Rezanejad

October 2021

TÉCNICO LISBOA

Hydrodynamic analysis of a dual-body Wave Energy Converter device with two different Power Take-off configurations

Julio Cesar de Souza Filho

Acknowledgements

I would like to express my gratitude for my supervisor, Kourosh Rezanejad, who guided and supported me during these strange times that we are living.

I would also like to thank my parents, Julio and Inês, and my sisters, Juliana and Daniela, who always supported me and made all of this path possible, thank you very much for it.

Finally, I would like to thank my Italian, Brazilian and Croatian friends that shared all this period with me. I appreciated every part of it guys, thanks. A special thanks to the person that lived through all of this with me, Vivi, it would not be so fun without you, and for this I am really thankful.

Abstract

The aim of the present thesis is to improve of the efficiency of dual body wave energy converters by changing the configuration of the power take-off installed. This is done by optimizing two different configurations for the wave energy converter (power take-off in between the floater and the submerged body, and power take-off in between submerged body and sea bottom) to be installed in the region of Pico-Azores.

The study is considered to be important as a higher efficiency means less cost to generate energy, being this one of the main barriers of the usage of wave energy converters nowadays.

The analyzes begin with the modeling of the bodies of each wave energy converter in NEMOH, that is a software that allows the calculation of the hydrodynamical coefficients of the bodies (floaters and submerged bodies).

With all the hydrodynamical coefficients calculated it is possible to create a dynamical model in frequency domain that optimizes and compares the maximum efficiency of the two configurations.

After that, using previous researches that carried out similar calculations, the model is validated by entering all the input parameters equal to the ones in the researches and comparing the outputs (hydrodynamical coefficients, absorbed power, efficiency, and also sea spectrum creation). All outputs are found to be similar and so the model is considered to be validated.

Finally, the presentation of the results is done. The comparison is made for three different combinations of bodies geometries (cylinder-sphere, cylinder-cylinder, and sphere-sphere, for the floater and submerged body respectively). The second configuration is considered more efficient, having an average improvement in the efficiency of 10.85%.

It is also found that the second configuration is optimized for smaller bodies when compared to the first one.

Keywords:

Wave Energy Converter, Power Take-off, Power Take-off configuration, harvesting energy, energy generation, Power Take off efficiency, Dual Body Wave Energy Converter, hydrodynamical analyses

Resumo

O objetivo da presente tese é estudar a melhora na eficiência de conversores de energia de onda de dois corpos por meio da mudança da configuração do PTO instalada. Isto foi feito por meio da optimização de duas configurações de conversores de onda (PTO entre o flutuador e o corpo submerso, e PTO entre o corpo submerso e o fundo do oceano) a serem instalados na região de Pico-Açores.

O estudo é considerado importante uma vez que uma maior eficiência significa um custo menor para a geração de energia, sendo esta uma das maiores barreiras para o uso de conversores de energia de onda nos dias de hoje.

A análise começa com a criação do modelo dos corpos de cada um dos conversores de onda no software NEMOH. Tal programa permite o cálculo dos coeficientes hidrodinâmicos dos copos (flutuadores e corpos submersos).

Com todos os coeficientes hidrodinâmicos calculados foi possível criar um modelo dinâmico no domínio da frequência de forma a optimizar e comparava as máximas eficiências de cada configuração.

Após isso, com resultados de pesquisas prévias, o modelo foi validado iniciando os cálculos com os mesmos valores das pesquisas e comparando os valores de saída (coeficientes hidrodinâmicos, potência absorvida, eficiência e espectro de mar). Todas as saídas foram consideradas similares aos valores presentes nas pesquisas e, sendo assim, o modelo foi considerado validado.

Por fim, é feita a apresentação dos resultados. A comparação foi feita para três diferentes combinações de geometrias dos corpos (cilindro-esfera, cilindro-cilindro, esfera-esfera para o flutuador e o corpo submerso respectivamente). A segunda configuração foi considerada mais eficiente, tendo um acréscimo médio na eficiência de 10.85%.

Foi identificado também que a segunda configuração é optimizada para corpos menores quando comparada com a primeira configuração.

Palavras Chave:

Conversor de Energia de ondas, Power Take-off, Configuração do Power Take-off, geração de energia, captação de energia, eficiencia do Power Take-off, Gerador de Energia de onda de dois corpos, análise hidrodinâmica

Table of Contents

List of Figures

List of Tables

Symbology:

m_i: Mass of the i body

A_{ij}: Added mass caused by the j body in the i body.

b_{ij}: Radiation damping caused by the j body in the i body.

F_{ei}: Exciting force acting on the body i.

x_i: Position in heave-axis of the body i.

$\dot{x}_1$: Velocity in heave-axis of the body i.

$\ddot{x}_1$: Acceleration in heave-axis of the body i.

k_{pto}: Stiffness of the PTO system.

c_{pto}: Damping coefficient of the PTO system.

b_{visci}: Viscous damping acting on the body i.

k_s: Hydrostatical stiffness of the floating body.

i: Imaginary unitary number.

k_m: Stiffness of the mooring system.

ω: Frequency.

c_d: Drag Coefficient of the body

V_{max}: Maximum velocity reached for the body in heave direction.

ρ: Fluid density.

L: Width of the buoy.

A_c: Area of the buoy in heave direction.

g: Gravity.

$Z(i\omega)$: Impedance Matrix.

H: Wave height.

c_g: Group velocity of the incoming waves.

D_{epth}: Water depth.

κ: Wave number

S: Spectrum of irregular waves.

WEC: Wave Energy Converter

Chapter 1. Introduction

In this Chapter the background/motivation and also the objective of the development of this thesis are explained, also it is shown the importance of studies in the area of wave energy converters (WEC). Then, the structure of the thesis is described.

Finally, a literature review is done presenting some works already done in the area and defining some classifications and discretization of the main components of a wave energy converter and its importance.

1.1. Background and Motivation

The world consumption of energy is rapidly increasing since the 1950's (due to different reasons, such as population, industrialization and urbanization growth) and the majority of research in the area shows this will continue in the next years.

According to the U.S. Energy Information Administration's (2019), energy consumption will raise by nearly 50 percent till 2050. The projection made by EIA (U.S. Energy Information Administration) also shows that the main primary energy source production will be renewable, such as wave energy. The forecast can be seen in Figure 1.

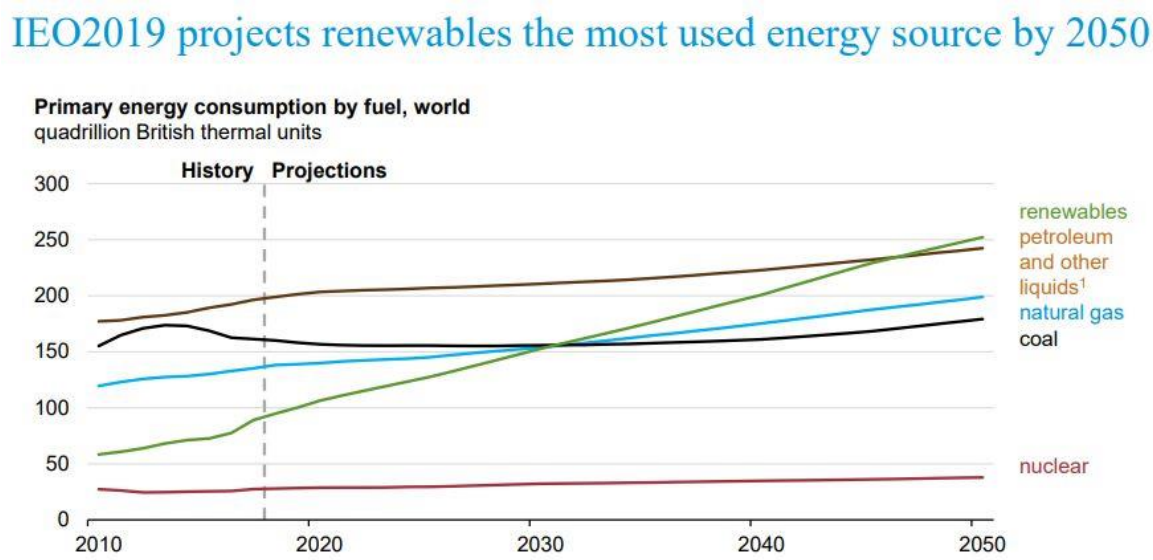

Figure 1:IEO projection of energy source in the world 2019 (Walton 2019)

The exploration of wave energy started recently (R&D started around 1970's and demonstrations of wave energy converter devices around 1980's) so there is still a lot of development to be done in order to optimize its efficiency and lower the costs of installation and operation. Moreover, Mørk et al. (2010) has estimated that the global availability of gross power of wave energy is about 3.7 TW, while the installed capacity around the end of 2016 was only 12 MW, (OES 2016). To understand the dimension of the power availability, it would represent 32412 TWh in one year (ignoring loses due to lack of perfect efficiency), and the world consumption of energy in 2019 was 173340 TWh, (Ritchie 2017).

Now it is possible to affirm that, besides the potential to represent near 20% of worlds consumption, wave energy is hugely underused (less than 1% of its potential). That means that any improve in the field could significantly increase the worlds power generation, something that will almost undeniably be one of the problems for the future years.

Also, it is important to remember the environmental effect of using wave energy instead of non-renewable ones. As it is renewable, it does not pollute the environment as strongly as some

traditional energy sources (as coal or oil for example), also, is not as dangerous to deal as nuclear energy.

The recent estimates made by OES (2017) shows that the ocean energy sector is expected to quickly grow in the next years, reaching a total of 300 GW by 2050 and so saving 500 million tonnes of CO2 emissions and creating approximately 680000 jobs.

It is possible to say now that there are several good reasons and needs to continue the studies in the field of wave energy exploration. Following that idea, the present thesis was developed with the motivation of continuing the previous research study carried out by Rezanejad and Guedes Soares (2018) to improve the efficiency of a dual body wave energy converter.

Rezanejad and Guedes Soares (2018) proved analytically that using the PTO system (linear damper) between the fixed support and intermediate mass of a general dual mass oscillatory system can inherently increase the efficiency (of capturing the energy of the excitation source) compared to the system which PTO is installed between the two masses. The main motivation of this study is to extend the study of Rezanejad and Guedes Soares (2018) specifically for dual body point absorbers based on linear wave theory.

1.2. Objectives

The objective of this thesis is to find out if it is possible to improve the efficiency of a two-body wave energy converter (installed in the coast of Azores Island – Portugal) by changing the configuration of its PTO system (the first configuration consists of the PTO being installed between the two bodies, the second configuration consists of the PTO being installed between the submerged body and sea bottom).

The main desire is to optimize both configurations varying it geometrical, PTO and mooring parameters in a range of values (more explanations about how it was done in the chapter Mathematical Model). And then prove that the second configuration is better than the first one in terms of harvesting energy efficiency.

That is of paramount importance, as improving the efficiency of a Wave Energy Converter means in other worlds reducing the cost to generate energy. And the reduction of the cost of the energy produced by Wave energy converters is one of the main challenges in the field today, as the technology to install it already exists, being the reduction of it cost one of the main objectives of study in the field nowadays

Firstly, a common configuration for the two-body WEC (Power Take Off unit placed between the two floaters) is analyzed and optimized. This analyzes is carried out for three different shapes of the geometries of the bodies (the floater and the submerged body are respectively: cylinder-sphere, cylinder-cylinder, sphere-sphere).

The optimization was done for each one of the three cases (cylinder-sphere, cylinder-cylinder, sphere-sphere) by varying the geometrical parameters (radius, draft, height) of both bodies and also the parameters of the power take off unit and mooring system. Then, the best combination of them in terms of power absorbing efficiency in irregular waves was chosen as the optimal one.

Secondly, using the same procedure described, a different configuration for the wave energy converter (Power Take Off unit placed between sea bottom and the fully submerged body) is analyzed. Also, the best ones in terms of efficiency are pointed out.

Finally, the comparison between the two configurations is presented. In the end it has been proven that the second configuration is the best in terms of efficiency in harvesting wave energy, as it was desired. Hence, the application of the second configuration would reduce the energy production costs significantly (which is one of the main barriers nowadays on the way of industrial development of Wave Energy Converter devices). Therefore, it might be helpful to promote the application of WECs.

1.3. Structure of the Thesis

This thesis is structured in the following Sections:

Chapter 1: Introduction

This Chapter is dedicated to describing the objective that was the main guide of the present thesis, and also give the initial background and motivation that led to the develop of this research, giving a general idea on why it is important to research in the field of wave energy.

Also in this chapter, there is the literature review. It was dedicated to present several different papers related to wave energy converters. Starting by two different types of classification of Wave Energy Converters, and then going to different methods of optimization, different power take-off systems and control methods that improve the efficiency and power absorption of the converters.

This is considered important due to the fact that shows that more people already studied the subject, and every knowledge should be build considering the previous knowledge already built, this way there is a progression and cooperation in order to achieve greater results.

Chapter 2: Description of the mathematical model

This Chapter is dedicated to present the formulation and mathematical model used to develop the code and the analyzes.

The development of it was done carefully finding papers with similar calculations at every step of the model, so, this way the reliability of the calculations is higher due to the fact that someone already did some similar analyzes and found good and trustful results.

All the equations were chosen to be present here in order to have a better organization and a better way to take a look at how everything was developed. If it were not like this it would be hard to find in the text which equation or consideration is being used.

At the end of this chapter a description of the code created in order to do the optimization is presented, this description was done as carefully as possible once it is one of the main objectives of the present study (once a better efficiency means a cheaper cost to generate electricity using wave energy converters).

Chapter 3: Validation of the model.

This chapter is dedicated to the validation of the model created. In order to do so several papers with results similar to the ones obtained by the present thesis were found.

Then, using the same input parameters of the papers found, the output results were compared, named they are the hydrodynamical coefficients for both one and two bodies WEC, power absorption in regular wave, efficiency in irregular waves and development of the sea state spectrum. This was done in order to raise the reliability of the results obtained in the present thesis, once as more reliable the results are the better.

Chapter 4 : Results and discussion

This Chapter is dedicated to present and discuss all the results obtained in the present thesis, some analyzes in order to better understand the results are also done.

The goal of this section was to find the better way to present and analyzes the results, as there are different possible ways to do so. This chapter also presents a comparison of all the efficiencies found in the thesis, a final analyzes of which geometry is better is made, guaranteeing that the present thesis has a reasonable conclusion

Chapter 5: Conclusion and future work

This Chapter is dedicated to summarizing all the achievements of the present thesis, making some considerations of what was expected and what was achieved. Also, there are

considerations about possible future research in the field and possible ways of improving the reliability and applicability of the present thesis.

Chapter 2. Literature Review

In this section, the classification of different wave energy converters is presented according to two different methods of classification. After that, a more detailed description about components (power-take-off and mooring system) is done. Then, some different control systems and optimization methods are showed and briefly described.

Finally, some considerations about environmental predictions are made in order to prove that unless something is done to change, the world will face several conditions due to the rise of global temperature, that means that finding/making cheaper clean energy sources, as renewable energy, is one of the main goals of humanity in the next decades

A wave energy converter is a device that captures energy from the waves and converts it into electrical energy.

Normally, the wave energy is harvested by the movements of the device. There are several different types of WECs and therefore they can be classified into different groups.

One of the possible classifications is by the distance to the shoreline, studied by Cruz (2008); Falcão (2010); Guedes Soares et al (2012), classifying them into onshore, near shore and offshore.

Another one is the one used by The European Marine Energy Center LTD (EMEC) and also Guedes Soares et al (2012). In which the device is classified into 8 different types: attenuator, oscillating wave surge converter, oscillating water column, overtopping/terminator device, submerged pressure differential, bulge wave, rotating mass, point absorber and others.

Due to the high usage of both, the two classifications are going to be presented.

2.1. Classification based on the distance to the shoreline

Figure 2 shows the different places that the WEC can be installed and the power availability in each of those places.

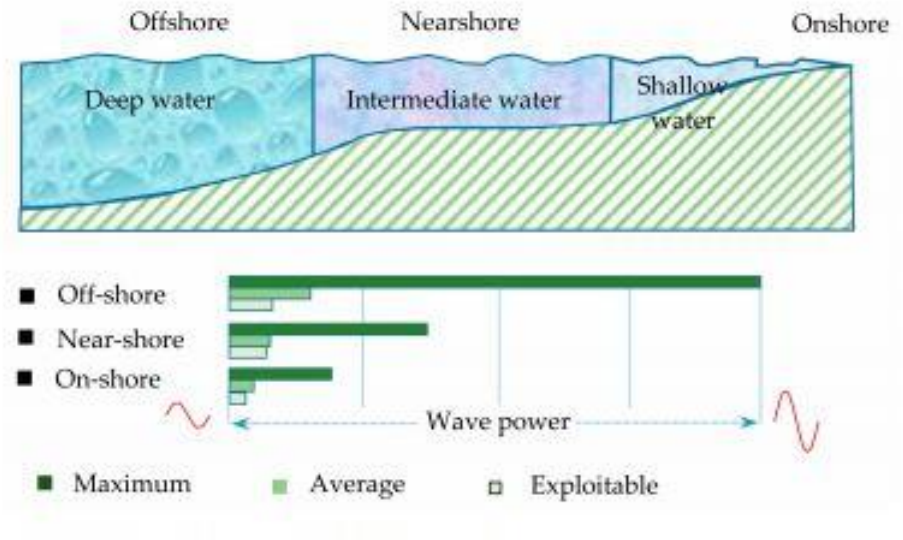

Figure 2:Position of the WEC and energy available (Guedes Soares et al 2012).

Onshore WECs are usually fixed or embedded to the shoreline, this brings the advantage of easier and cheaper installation and maintenance. Also, it does not require complex mooring systems or long lengths of underwater transmission cables. Although, in the shorelines the waves carry less energy and also some geometrical restriction maybe applied in order to preserve the

landscape near the coast, (Guedes Soares et al 2012). One famous kind of onshore WEC is the Seawave Slot-Cone Generator (SSG), (Zhao et al. 2019).

The near shore WECs are usually installed in water depths around 10m-25m and a distance around 500m from the shoreline. Although floating near shore devices exists, usually they are bottom-mounted. This kind of device has harder and more expensive installation and maintenance then the onshore ones (however, it stills a lot easier and cheaper than the offshore ones) but is exposed to waves carrying more energy. An example of it is WaveRoller.

The offshore devices are in areas far away from the shoreline and water depths over 40m (Deepwater). This kind of device usually is installed floating or near-surface and receives the most energy from the waves.

Also, it allows the installations of a farm of devices due to the great availability of sea space. However, as they are receiving high energy waves they suffer with high structural loads on the device and on its mooring system and a higher risk of being damage by a storm. These facts make them more expensive and require more complex technology to be installed and maintained, (OES 2016). An example is the Pelamis.

2.2. Classification based on EMEC.

2.2.1. Attenuator

An attenuator is a floating device which operates parallel to the dominant wave direction and effectively rides the waves. These devices capture energy from the relative motion of the two arms as the wave passes them.

These WECs work based on power absorption from pitch angle rather than on the height of oscillation; absorption efficiency drops with increasing angles, thus being self-limited and safer in high seas. (Guedes Soares et al 2012).

The schematic work concept of the attenuator can be seen in Figure 3.

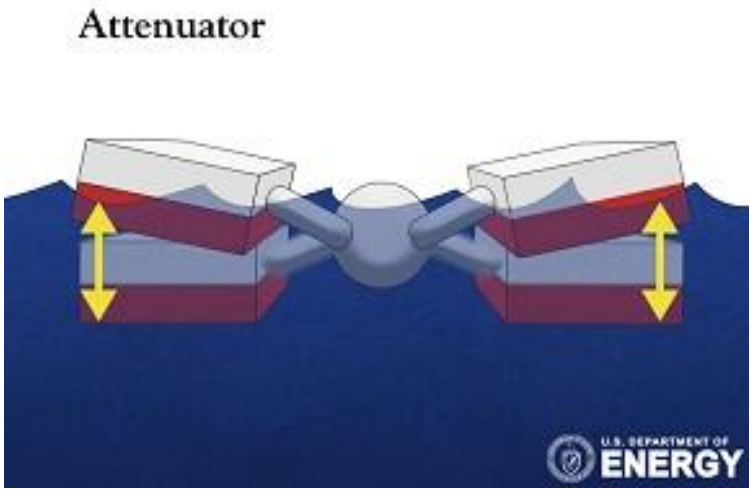

Figure 3:Attenuator WEC (Guedes Soares et al 2012).

2.2.2. Oscillating Wave Surge Converter

Oscillating wave surge converters extract energy from wave surges and the movement of water particles within them. The arm oscillates as a pendulum mounted on a pivoted joint in response to the movement of water in the waves.

The device is usually installed in locations close to the shore (as with this it is submitted to reduced wave power) so the structural loads on the structure are smaller.

Also, the exploitable power is just slightly smaller than the ones find in offshore areas. (Guedes Soares et al 2012).

The schematic work concept of the Oscillating Wave Surge Converter can be seen in Figure 4

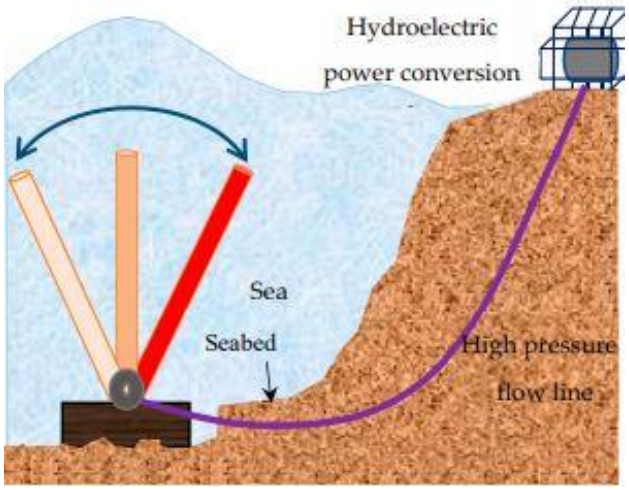

Figure 4:Oscillating Wave Surge Converter (Guedes Soares et al 2012).

2.2.3. Oscillating Water Column

These are among the first devices proposed, due to this fact there are abundant literature available to study.

An oscillating water column is a partially submerged, hollow structure. It is open to the sea below the water line, enclosing a column of air on top of a column of water. Waves cause the water column to rise and fall, which in turn compresses and decompresses the air column. This trapped air is allowed to flow to and from the atmosphere via a turbine, which usually has the ability to rotate regardless of the direction of the airflow. The rotation of the turbine is used to generate electricity.

This device, even though they have a good peak efficiency, have a low time-averaged efficiency. There are proposals to improve it, but with a high cost and delicate operation. (Guedes Soares et al 2012).The schematic work concept of the Oscillating Water Column can be seen in Figure 5.

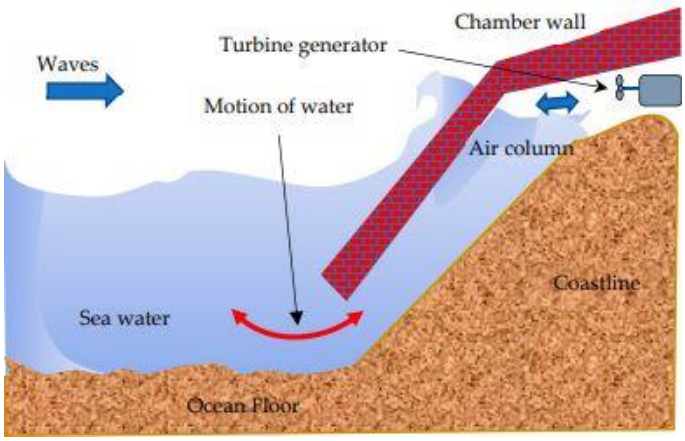

Figure 5:Oscillating Water Column (Guedes Soares et al 2012).

2.2.4. Overtopping/Terminator Device

Overtopping devices capture water as waves break into a storage reservoir. The water is then returned to the sea passing through a conventional low-head turbine which generates power. An overtopping device may use ‘collectors’ to concentrate the wave energy.

The development of this kind of device is new, so due to this fact there is not many experimental data available.

The schematic work concept of the Overtopping/Terminator Device can be seen in Figure 6.

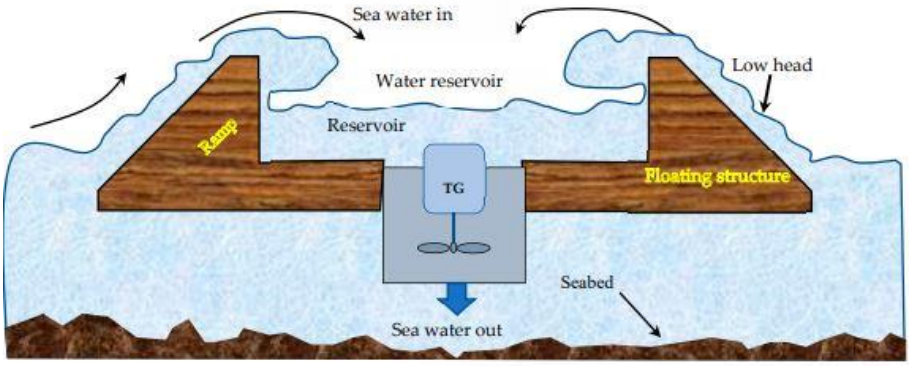

Figure 6:Terminator Device (Guedes Soares et al 2012).

2.2.5. Submerged Pressure Differential

Submerged pressure differential devices are typically located near shore and attached to the seabed. The motion of the waves causes the sea level to rise and fall above the device, inducing a pressure differential in the device. The alternating pressure pumps fluid through a system to generate electricity.

As they are located below the surface, they have better survivability and no visual impact, however this makes the cost for installation and maintenance higher. (Guedes Soares et al 2012).

The schematic work concept of the Submerged Pressure Differential can be seen in Figure 7.

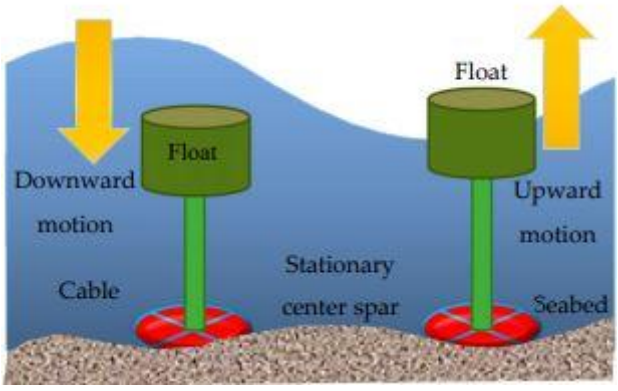

Figure 7:Submerged Pressure Differential Device (Guedes Soares et al 2012).

2.2.6. Bulge Wave

Bulge wave technology consists of a rubber tube filled with water, moored to the seabed heading into the waves. The water enters through the stern and the passing wave causes pressure

variations along the length of the tube, creating a ‘bulge’. As the bulge travels through the tube it grows, gathering energy which can be used to drive a standard low-head turbine located at the bow, where the water then returns to the sea.

Bulge wave energy converter uses entirely new principles to convert oceanic wave energy into electrical power. This type of converter is also called Anaconda wave power device, as designed by Checkmate Sea Energy Ltd. It is used to generate electricity by using abandoned oceanic waves, as shown in Figure 9.

It is made of elastic pipe, which is submerged just under the sea water surface at low pressure. One of the two sides of this elastic pipe is fixed and anchored with its head to the base. As the sea wave passes along the tube, a bulge wave is created, which moves in front of the wave. The energy is captured continuously, which is used to drive the turbine generator (TG) to produce electricity. (Farrok et al. 2020).

The schematic work concept of the Bulge Wave can be seen in Figure 8.

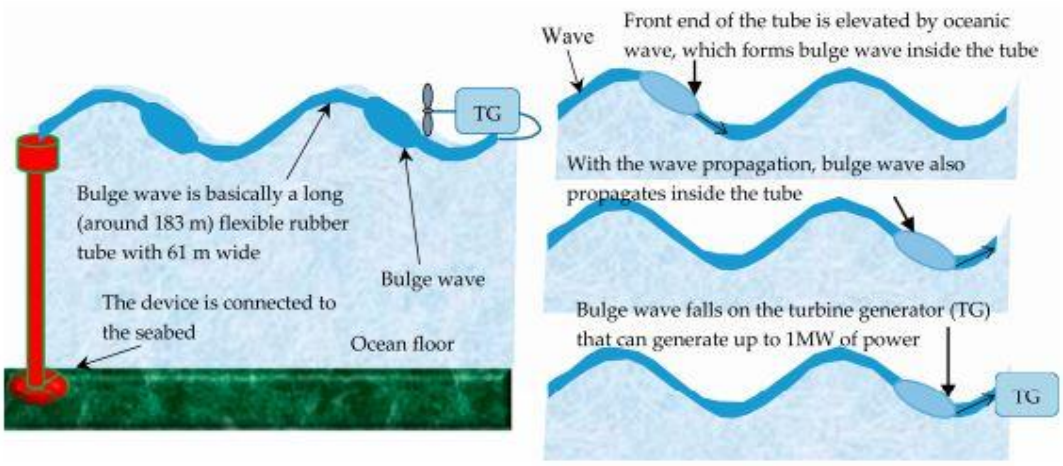

Figure 8:Bulge WEC (Guedes Soares et al 2012).

2.2.7. Rotating Mass

Two forms of rotation are used to capture energy by the movement of the device heaving and swaying in the waves. This motion drives either an eccentric weight or a gyroscope causes precession. In both cases the movement is attached to an electric generator inside the device.

Rotating mass wave power device operates the motion of wave to roll a physical heavy object (mass) that produces mechanical energy. The rotating mass receives mechanical power from the oceanic wave and supplies it to the electrical generator. (Farrok et al. 2020).

The schematic work concept of the Rotating Mass can be seen in Figure 9.

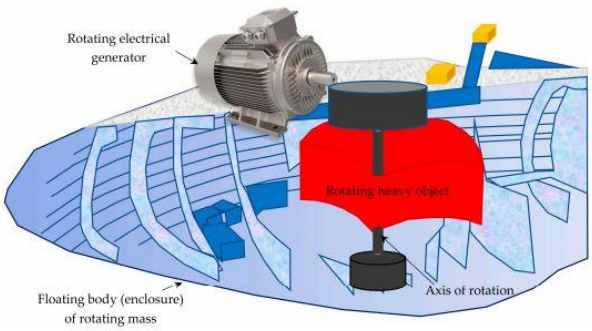

Figure 9:Rotating Mass Device (Guedes Soares et al 2012).

2.2.8. Point Absorber

As this is the WEC studied in the present thesis more considerations about it were made.

A point absorber is a floating structure which absorbs energy from all directions through its movements at/near the water surface. It converts the motion of the buoyant top relative to the base into electrical power. The main consideration about point absorbers is that it harvests energy just by the heave movement of the wave, it is considered to be fixed in all other degrees of freedom.

A point absorber can be composed by one or more bodies. For instance, in the present thesis a two bodies point absorber is considered, but there are point absorber with one body, three or so on. Al Shami et al (2019), for example, presented point absorbers composed of two, three, four and five bodies and compared them.

A point absorber is usually composed by a number of bodies (the buoys), a mooring system, that can be developed in several different ways according to the design proprieties and a power take-off system (PTO), that may take a number of forms, depending on the configuration of displacers/reactors.

In the present thesis two different locations for the PTO were studied, the PTO being installed between the two bodies and the PTO being installed between the submerged body and sea bottom). These components (PTO and mooring) are usually optimized in accordance with the place that the wave energy converter is going to be installed, there are several different methods to optimize them, a few of them are described later in this Chapter. Besides being optimized, these components can be also put under some control method, that will change its proprieties in accordance with sea conditions to maximize the energy generated, some of this control methods are also described later in this Chapter.

The schematic work concept of a kind of Point Absorber composed by one body and a heavy plate can be seen in Figure 10.

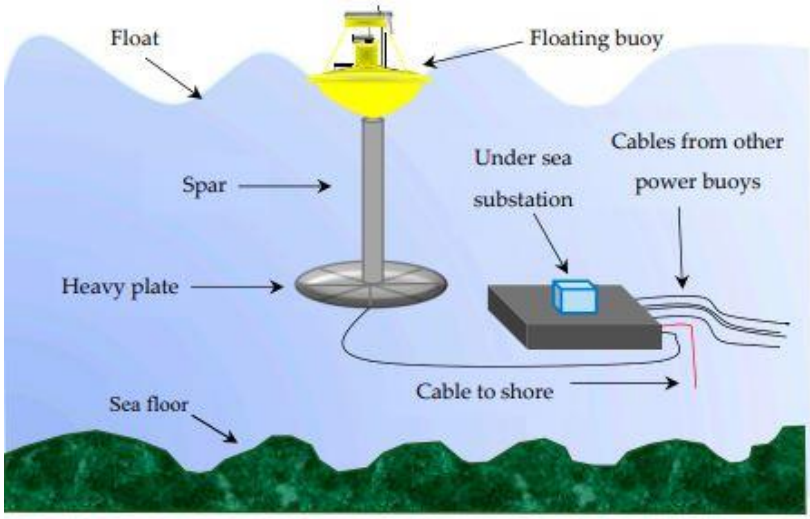

Figure 10:Point Absorber (Guedes Soares et al 2012).

2.2.9. Other

This covers those devices with a unique and quite different design to the more well-established types of technology or if information on the device's characteristics could not be determined. For example, the Wave Rotor, is a form of turbine turned directly by the waves. Flexible structures

have also been suggested, whereby a structure that changes shape/volume is part of the power take-off system.

2.3. PTO system

There can be several different kinds of PTO systems, some more complex than the others. Discussions about different kinds of PTO were made by Ahamed et al. (2020) and they are: Hydraulic motor system; Pneumatic air turbine transfer system; Hydro turbine transfer system; Direct mechanical drive systems; Direct linear electrical drive systems; Triboelectric nanogenerators; Hybrid systems.

Hydraulic motor system is the most common type of PTO for wave energy converters, it consists basically of a hydraulic cylinder, hydraulic motor, accumulator, and generator. The move of the sea waves usually moves the hydraulic ram increasing the pressure of a working hydraulic oil, then the PTO's hydraulic cylinder converts rotational motion and translational motion into energy that will move the motor installed. Then, finally the motor converts it into electrical energy.

Ther are some advantages regarding its use, it generates big amounts of power using low frequency waves and can harvest energy from the variation of the wave energy converter movement.

Usually, the waves create large forces with slow speed. In this case the hydraulic system is perfectly appropriate and has a great effectiveness on harvesting energy

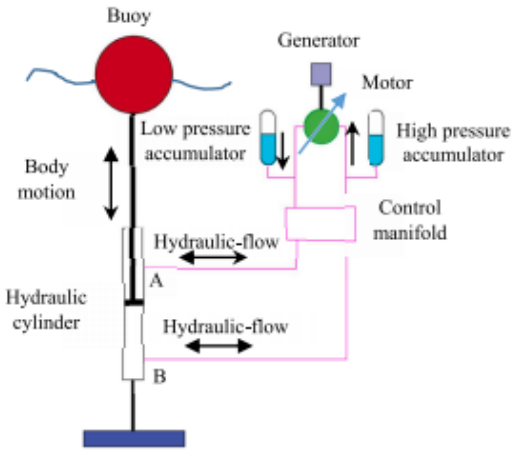

Figure 11:Schematic description of a hydraulic motor system for the PTO (Ahamed et al. 2020).

Pneumatic air turbine transfer system, the working mechanism of this type of PTO is basically sea water entering and exiting an air chamber (due to the wave motion) and compressing the air inside it. Then this pressurized air goes through a turbine attached to a generator that will generate energy

There are some advantages of using it, it converts the slow velocity of the waves into high air flow rates. Also, it's always from the corrosive sea water (due to the presence of salt) and its usually located in places that can facilitate the maintenance and change of the equipment (in case it breaks).

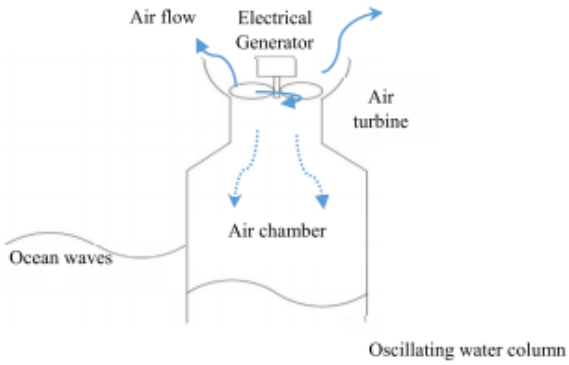

Figure 12:Schematic description of a pneumatic air turbine system for the PTO (Ahamed et al. 2020).

Hydro turbine transfer system, the system usually works by water flowing through the hydraulic turbine, which directly runs the generator that will then generate energy.

The advantages of using it is that it is a well-known technology, requiring low maintenance and having a low cost of installing. It also has a long lifetime.

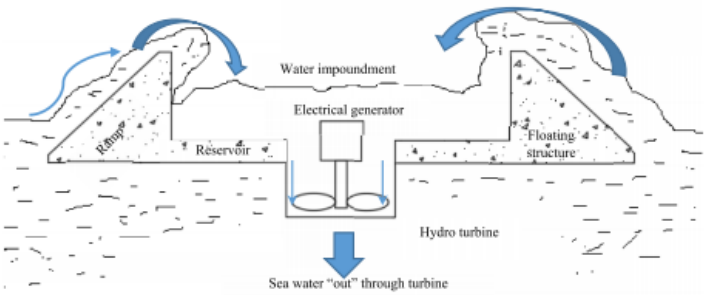

Figure 13: Schematic description of a hydro turbine system for the PTO (Ahamed et al. 2020).

Direct mechanical drive systems are composed of a mechanical transmission, a gearbox, and an electric generator (usually the electric generator is coupled with the gearbox). Then the mechanical transmission and the gearbox are used to drive the generator, which will finally generate energy.

The advantages of using this kind of system is due to the fact that it converts wave energy into electrical energy using linear-to-rotary conversion systems without any pneumatics or hydraulic systems. Therefore, it generates more energy than other systems because it has reduced frictional resistance. One of the main challenges of using this system in the present days are the high maintenance cost and short lifetime.

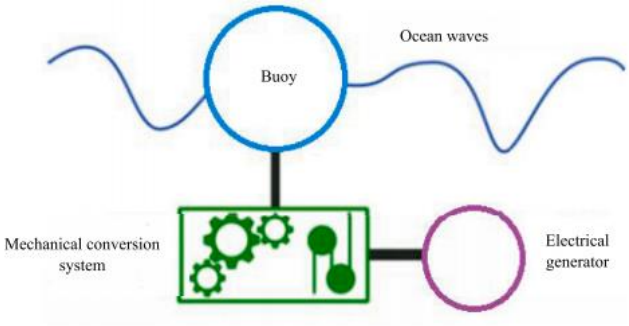

Figure 14:Schematic description of a direct mechanical drive system for the PTO (Ahamed et al. 2020).

Direct linear electrical drive systems is a system that, when placed on the seabed, consists of a translator (consisting basically on permanent magnets) and a stator (equipped with coil windings)

one of them is attached to the moving buoy and the other fixed in the seabed. The relative movement between these two parts generates than electrical energy.

The advantages of this type of PTO are that there are no losses due to any mechanical system (as there are not any involved in the process) meaning a high efficiency, also meaning a low maintenance cost, as no mechanical system needs to be fixed. Moreover, this system makes possible to easily control the parameters of the PTO.

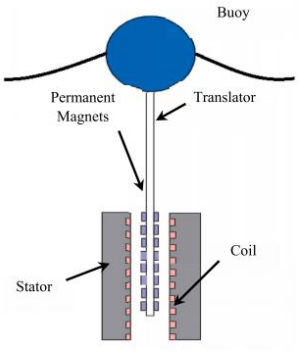

Figure 15:Schematic descriptiomn of a direct linear electrical drive system for the PTO (Ahamed et al. 2020).

Triboelectric nanogenerators is a relatively new technology, it is based on the coupling of triboelectrification and electrostatic induction. It has specific merits as it generates high power density with a high efficiency. It has low weight and low installation costs. The best advantage of this kind of system is that it can generate energy on any frequency range, so it is applicable to lots of different projects and places of operation.

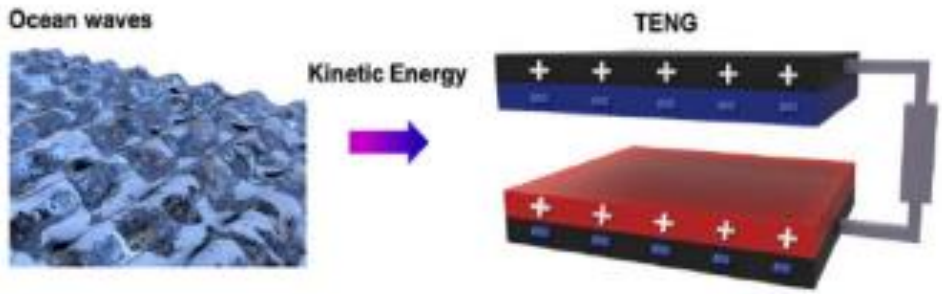

Figure 16:Schematic description of a triboelectric nanogenerators system for the PTO (Feng et al. 2018).

Hybrid systems consists in a system in which two or more PTO mechanisms are installed together and are working to generate electrical energy.

For instance, Feng et al. (2018) proposed a system that a triboelectric nanogenerator and an electromagnetic generator are working together to generate energy, this making the system more efficient, as it has two mechanisms to harvest energy. The main advantage of hybrid systems is that all the working principles can be installed in the same structure. Therefore, installation costs, maintenance costs, and mooring costs are all reduced (considering all the principles installed).

There are several other PTO systems developed, and as the study of each different type is not the main goal of the present thesis, a more detailed characterization of them is not going to be made.

In the present thesis a linear generator was considered as PTO, assuming it to be simplified as a spring and a damper. Also, in the present thesis the power take-off unit is assumed to harvest

energy just in heave direction, an assumption normally made, as in (Ruezga 2019); (Al Shami et al 2018); (Engström et al 2009); (Liang and Zuo 2016); (Al Shami et al 2019); (Cheng et al. 2015); (Al Shami et al. 2019).

2.4. Mooring System

The mooring system is one of the main components of the cost of the whole wave energy converter. Due to this fact, it's study and comprehension in order to produce better and cheaper systems are of major importance, as reducing the cost of harvesting energy using wave energy converters is one of the main goals of its studies nowadays.

In the case of free-floating systems (that's case of the wave energy converter being analyzed), the main purpose of the mooring system is to keep the structure on station (on the position that it's supposed to be) even in the worst storm conditions.

The two main components of a mooring system are the lines and the anchor. The components need to be selected by considering the mooring configuration, location to be installed and agreeing to the reliability of a long-term mooring (in the literature long term mooring is defined for floating units positioned at the same place for five or more years.

There are different kinds of anchors and lines that can be used, a brief description of the ones used for offshore structures is made (as in the present thesis an offshore unit is studied).

The lines can be made out of chain, wire rope and synthetic rope mostly, each one of them having a different price and a different application. The chain has a medium cost of installation, are able to provide a great catenary stiffness and have good bending proprieties and abrasion. They're a good fit for long term moorings but usually need to be regularly inspected. Chains have a medium cost of installation. The wire ropes, because of its elasticity, are usable in tensioned mooring applications, In the case of wire ropes extreme bending conditions should be avoided and so this should be taking into consideration when thinking about installing it. Wire ropes have low cost of installation, being that a good quality of it as it reduces the initial investment required to produce the wave energy converter. The synthetic ropes have a weight that can be considered around zero under the water. So, they are close to neutrality buoyant. Because of its weight and elasticity characteristics they're more used in deep water tether applications. Due to low experiences on using it in real conditions, the safety factor of it needs to be higher to guarantee reliability.

If any changes in axial stiffness happens after the installation a re-tensioning process is required. Axial conditions and heating at storm conditions should be avoided in the case of synthetic ropes. The cost of installation in this case is high, meaning that unless its installation would provide measurable gains in harvesting energy or reliability it shouldn't be used.

The main used anchors are gravity anchors, its horizontal holding capacity is generated by dead weight that provides friction between seabed and anchor. Drag embedment anchor, its horizontal holding capacity is generated in the main instalment direction by the embedment of the anchor in the ground. Suction anchor, horizontal and vertical holding capacity is generated by forcing a pile mechanically or from a pressure difference into the ground, providing friction along the pile and the ground. Vertical load anchor, horizontal and vertical holding capacity is generated due to a specific embedment anchor allowing loads not only in the main instalment direction. And drilled anchor, horizontal and vertical holding capacity is generated by grouting a pile in a rock with a pre-drilled hole. Each one of these anchors can be choose according to the demands of the wave energy converter project and location of installation. The gravity anchor and drag embedment anchor have a medium cost of installation, the other three described have a high cost of installation.

This fact should also be considered while installing the anchor, if the ones with high cost don't provide any measurable gains against the ones with medium cost they shouldn't be used.

There are a variety of moorings configurations developed, each one of them with a proper purpose and particular characteristics and each one of them with a different application regarding design proprieties and place of installation.

The three main types are spread mooring (where the structure in usually connected to line that's fixed in the seabed), single point mooring (where the structure is moored in a single point of a moored buoy and dynamic positioning (the proprieties of the mooring system changes according to the sea conditions guaranteeing a better efficiency of the device)

For spread mooring system the most used one is the catenary system, in which mooring lines of a free hanging Catenary Mooring arrive horizontal to the seabed so that the anchor point is only subject to horizontal forces. The restoring forces are mainly generated by the weight of the mooring lines returning the system to equilibrium. For single point mooring the most used one is catenary anchor leg, in which the floating structure is moored to a catenary moored buoy and is able to weathervane around the moored buoy.

The dynamic positioning is less used in wave energy converters installation if compared to the other two described. This is due to the fact that, despite generating a better efficiency on harvesting energy, they have a way higher cost of installation, cost of maintenance and also, they are way less reliable than the other two.

In order for them to become more normally used in the world, more research on the area should be one in order to reduce its costs of installation and maintenance and in order to improve its reliability. There are still just few research that focus mainly on the design of the mooring system for wave energy converter, so more studies in the area should be done in order to provide a better understanding on how to reduce the costs and improve harvesting energy efficiency just by changing the type or components of a mooring system.

2.5. Control systems

There are several different control methods that can be applied to the wave energy converter in order to maximize the efficiency, such as self-reacting control, (Bacelli et al. 2011), latching control, (Shadman et al. 2021), phase-control, (Sang et al 2017), electric load control, (Wang et al 2020).

Bacelli et al. (2011) developed a self-reacting control method by creating a system possible to work in real-time based on the approximation of the motion of the device and of the force exerted by the power take off unit by means of a linear combination of basic functions (for instance Fourier series, the one used in the paper).

The control, as described in the paper, is a system composed of a feed-forward part and a feedback part; the feed-forward block generates the reference trajectories for the relative velocity, the relative position, and the PTO force, that maximize the produced energy while satisfying the amplitude constraint. The feedback controller corrects the PTO force reference signal generated by the feed-forward, in order to minimize the difference between the reference motion and the actual motion of the device.

Shadman et al. (2021), developed a system based on a latching control that, as defined in his work, is the one that holds the oscillating body during some time intervals (latching duration) and releases it at a specific instant(unlatching) to make the phase of the buoy velocity equal to the wave excitation phase. It tunes the wave energy converter oscillation period to the incoming wave period. The latching control can be done either by an external system or the PTO, in the work of Shadman et al. (2021) the one used is the PTO. A schematic design of it can be seen in Figure 17.

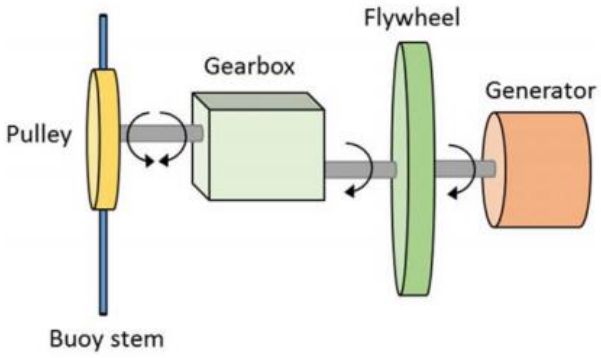

Figure 17:Schematic design of the PTO used for latching control (Shadman et al. 2020).

The mechanism of latching of the PTO is happens basically by disengaging the driveshaft from the driven shaft. This happens by the action of the flywheel when the driven shaft rotates faster than the driveshaft. A certain moment after the buoys maximum velocity occurs the disengagement happens. At that moment occurs that the velocity of the buoy begins to decrease, and it cannot reach the amplified velocity of the flywheel. There are several researches about latching control done so far, being this one of the most recent, which makes it results more impactful.

Sang et al (2017) developed a phase-control system to be installed in a slider-crank ocean wave energy converter. An AC synchronous machine was installed in the PTO unit in order to achieve a higher system performance. The control methods, as present in the paper, is a novel control methodology that ensures one-way continuous rotation at a relatively high speed and efficiency.

The proposed method does not rely on the wave motion (small or large, fast or slow) to achieve continuous rotation. To do that, the electric machine operates in two quadrants (+torque, +speed and torque, +speed) for every half cycle of a wave.

What this really entails is that in addition to harvesting energy through the electrical machine (generator mode), energy should be provided to the machine (motor mode) in some instant time from an external source such as the power grid. This way the slider crank linkage synchronizes (resonates) with the waves.

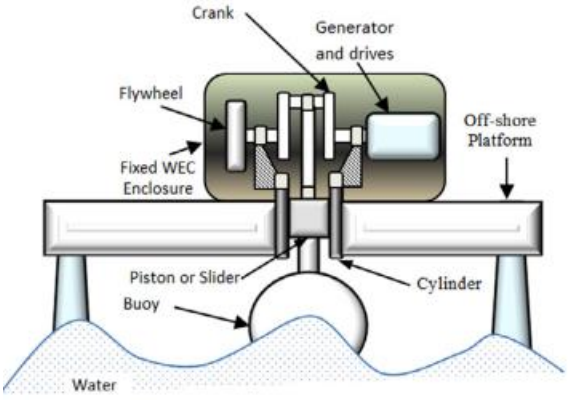

Figure 18:Schematic model of the phase control system (Sang et al 2017).

Wang et al (2020) created an electric load control system by investigating the electric dynamics and improve electric power generation of an isolated wave energy converter that uses a linear permanent magnet generator as the power take-off system, as this way the parameters of the power rake-off unit (PTO) can be easily controlled by changing the value of the resistor of the generator. To do that, a coupled fluid-mechanical-electric-magnetic-electronic mathematical model and an optimization routine were developed.

This model is used to simulate the hydrodynamic and electric response of a wave energy converter connected to specific electric loads and also used in an optimization routine that can efficiently find the optimal resistor load value for a device under regular waves or irregular wave under specific sea states.

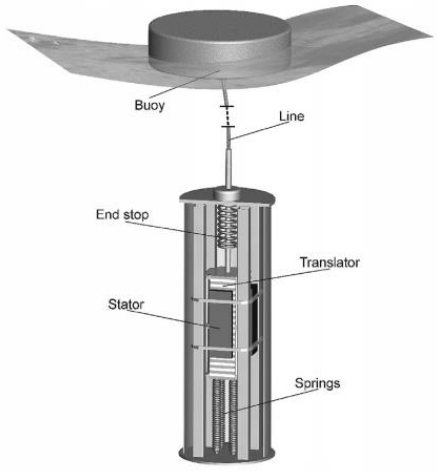

Figure 19:Schematic Model of a WEV with electric load control system (Wang et al 2020).

As it can be seen the main goal of every control method is to improve the efficiency of the wave energy converter by changing the way it acts according to the conditions of the sea. That means that if the sea changes its state the control method will change the way the Wave Energy Converter behaves and improve its efficiency.

Although they are really useful and important, the control system is not the focus of the present study. Therefore, in the present thesis none control system was adopted, they were not fully described here, but it is important to mention that they exist and are being investigated by other researchers. Also, it is important to mention that the main logic behind the development of the control systems is the same of the present thesis, make the energy generated by the wave energy converters cheaper.

2.6. PTO Optimization Studies

There are several methods of optimization being studied over the years, each one of them focusing on a different technique to do it, however all of them have the same goal, making harvest energy using wave energy converters cheaper. Due to the lack of historical research, there is no mutual agreement between researchers to define the best way and so many different authors developed different ways of doing so. Usually that's a pattern in science until an agreement between the research is reached, in this section a few of those methods were described.

Some papers focus on the usage of control methods, to optimize the PTO design for the optimal design of the incoming wave, (Bacelli et al. 2011); (Shadman et al. 2021); (Sang et al 2017); (Wang et al 2020).

Shadman et al (2021), for instance, developed a different non-predictive latching control. This was done by creating a time-domain model able to mesmerize the dynamical behavior of the wave energy converter analyzed by him taking into consideration the interaction of hydrodynamic forces and electro-mechanical forces produced by, respectively, the wave excited buoy and PTO system.

A latching control, as defined in his work, is the one that holds the oscillating body during some time intervals (latching duration) and releases it at a specific instant(unlatching) to make the phase of the buoy velocity equal to the wave excitation phase. It tunes the WEC oscillation period to the incoming wave period.

There are several researches about latching control done so far, being his one of the most recent, which makes it results more impactful. In the conclusion of his work, he achieves a gain in between 38% and 281% in power production. Although this is an incredible result, there are also some things to take into consideration before using this control method.

The installation cost of it is high if compared to control-free systems, it decreases the reliability of the system, as this method of work can overheat the generator (meaning that more frequent maintenance is required) and it reduces the lifetime of the system. So, an economical study needs to be done prior to its installation.

Some focus on the geometrical parameters in order to optimize it, (Shadman et al. 2018); (Al Shami et al 2018); (Liang and Zuo 2016).

Liang and Zuo (2016), for instance, developed an optimization system based on the geometrical proprieties of the bodies of the wave energy converter, he studied a two-body wave energy converter considering both its viscous and hydrodynamical proprieties (the viscous proprieties were approximated by linear considerations. The main idea is to develop a system in which one of the damped natural frequencies of one of the two structures present in the wave energy converter matches (or gets as close as possible to) the excitation force. This was done by modeling the dynamic behavior of the wave energy converter using a frequency domain analyzes. One of the main conclusions he reached is that the power absorbed, and efficiency of a two-body system is notably higher than a single body system with the same floating buoy structure. It´s also noted in his research that a non-optimized structure could be losing up to 80% of its power absorption capacity.

Shadman et al. (2018), for instance, developed an optimization process through linear hydrodynamic frequency domain analyses and the design of experiments (DOE) approach. Minitab was used to apply the DOE and perform statistical analysis of the optimization process. The frequency domain analysis of the system hydrodynamics was performed using ANSYS-AQWA. The diameter and draft of the floating cylinder (buoy) are considered as the geometrical parameters to be optimized. The objective of the optimization process is to determine the buoy that absorbs the maximum wave energy over the largest range of frequencies for the site's predominant waves.

Others, on the mooring system installed in the WEC, Vicente et al (2011), for instance, studied what might be, for wave energy converter floating point absorber, the optimal mooring configuration parameters, respecting certain pre-established acceptable intervals and using a time-domain model that considers the non-linearities introduced by the mooring system.

And some focus on the numbers of degrees of freedom, Al Shami et al (2019), for instance, studied the effects of increasing the number of freedoms of a point absorber wave energy converter. Both cylindrical and spherical shapes for the bodies were considered. The analyzes started at a simple two bodies wave energy converter (two degrees of freedom) then adding one body at the time until it reaches a five bodies wave energy converter (five degrees of freedom) while always keeping the volume and the mass of the system always constant. The analyzes was done considering linearized drag force and viscous damping effects. It was found by the end of the study that increasing the degrees of freedom for the system with cylindrical bodies would decrease the resonant frequency and also the captured power. While for the case of the spherical bodies, increasing the degrees of freedom would also decrease the resonant frequency but would greatly increase the captured power.

Also, due to the big importance of the subject, there are complete PhD thesis focused on that, (Ricci 2012).

One of the goals of the present thesis is to optimize the geometrical and design parameters in order to maximize the efficiency for a certain area in the ocean (as mentioned before, this means reducing the cost to generate energy), this was done by creating a code in MatLab, using also a software called NEMOH, to perform several analyses

More explanations about how the code was developed, which considerations were made and which kind of analyzes was done are in Chapter Mathematical Model, being the presentation and description of different optimization methods the goal of this section.

2.7. Environmental Considerations

As said already in the section Background and Motivation, the environmental safety is one of the main reasons why the studies and development of renewable energy, such as wave energy, is so important nowadays. In this section some descriptions are presented in order to prove that the environmental safety is indeed of great importance.

Unless the pollution reduces significantly in the next decades, the world might face some severe consequences. The goal of this section is to present some of these severe scenarios described by other researches, also describing what would avoid these scenarios.

Firstly, it is important to highlight that Hausfather et al. (2020) studied the efficiency of the models used to predict the climate changes of the few past decades, the models analyzed were published between 1970s and late 2000s. The models were compared to the observed values of global mean surface temperature changes. It was found out that most of the models are very skilled in predicting changes in the surface temperature, most of them returning a precise prediction when compared to the real observed values. That being said, once it known that the models are trustful it is possible to analyze what are their predictions for our future next decades.

Tamir et al (2021), recently analyzed cities around the world and developed a model to predict the temperature rise by the year of 2100. It was found that the surface temperature will rise around 4 degrees Celsius by the year of 2100. This increase should cause severe problems for our civilization.

Zheng et al (2021) studied the main effects of climate change in the vegetation of Wuwei, China. It was found out that if the temperature rises more than 1,5 degrees Celsius the region could face desertification.

So, considering the rise of 4 degrees predicted by Tamir et al. (2021), it is possible to assume that this region will face desertification unless something is done. A region suffering desertification means less area to cultivate food, less area usable to live, less water available. That, combine with the imminent populational rise, will produce hunger in a dangerous level.

Zheng et al. (2021) also shows that there are many other studies like the one he did for different areas with the same conclusion, temperature rise will implicate in desertification of regions. For instance, Getzin et al. (2016) made similar predictions for the region of Australia, and Getzin et al. (2015) did the same prediction for the Region of Namibia, Africa. So, it can be assumed that the desertification caused by climate change would be face almost all around the world.

Vidhee et al (2021) studied the effect of climate change in the flooding of cities in India. The flood would be caused by mean sea level rise. It was found out that unless the temperature rise stays below 2 degrees Celsius 42 Indian cities will face severe conditions regarding flooding. It is said that a possible way to reduce the consequences is to keep vegetations in the cities that would act like a sponge. However, Zheng et al. (2021) already showed that the world will face desertification is different areas due to climate change.

Jiejie Sun et al. (2021) studied how the temperature rise would affect the productivity of P. deltoides, a species of plant commonly used to reforest regions in the world due to its high productivity. It was found out that if the predictions of temperature change became true, the productivity of this species will notably decrease. This would cause a decrease in the ability of human race to reforest regions. The possible way to reduce this effect would be to artificially irrigate the regions to be reforested, and this would cost a great amount of money.

All being said it is possible to notice that if the predictions for temperature rise becomes true the world will face several bad scenarios. The main way to avoid it is the reduction of CO2 emissions in the world. One of the possible ways to do it, and one of the most effective also, is to change

the regular energy sources (such as coal, fossil fuel) to renewable ones (such as wave energy, the focus of the present studies).

Aderinto et al. (2018). investigated the main challenges that the industry of wave energy converters is facing right now when it comes to growing and installing more devices around the world. The most important problem was considered to be the fact that this technology is a nascent stage. That mean that the cost of maintenance, installation and also energy generation are still high and need to be developed. So, the only way to do it is keeping producing studies in the area, for instance some can study the mooring systems, some can study the PTO systems and so on.

Knowing this it is possible to affirm that it is of main importance to make wave energy converters more used around the world, and one way of doing so is making this kind of energy cheaper, as right now one of the main barriers of its usage is its price. That means that the studied being done in the present thesis is significant and more research in the field should be done in order to avoid the scenario previously presented.

Chapter 3. Mathematical Model

The goal of these section is to describe a mathematical model (using both a BEM (boundary element method) solver software, NEMOH (Babarit, A. et al 2015), and a code created in MatLab) that allows the calculation of the efficiency/Power Absorbed, both in regular and irregular waves, of the two models/configurations of the WEC's considered in the present thesis. Figures and explanations of both models are presented in this section in convenient moments.

With this model correctly developed it is possible to optimize the efficiency based on the variation of the WEC's parameters, that being the goal of this thesis. So, it is vital that this model is as reliable as possible. The main guarantee of the reliability of the model is obtained by carrying out a process of validation of all the results obtained that were already similarly calculated by other papers and researchers.

There are different ways to create a model that describes the WEC's in Figure 21 and Figure *22*. One possible way is to develop the time domain analyzes like the one developed by Cheng et al (2015). However, in the present thesis the analyzes was carried out using a frequency domain analyzes, like the ones proposed by Al Shamiet et al (2018); Liang and Zuo (2016); Al Shami et al (2019) (it is important to notice that as three authors developed the model in the same way it must be at least a reliable one).

There are pros and cons for each of the two methods, as described in (Al Shami et al. 2019). The frequency domain is simple and take less computational effort, although it cannot model non-linear forces and interactions, so these should be simplified in the case of using this model.

The time domain model demands more computational effort, but it is able to represent higher order waves, complex mooring, non-linear wave excitation forces, etc. So, in the case these kinds of calculations being important these should be the model used.

The description of the model will be done in parts, firstly by the description of the BEM solver NEMOH, then the dynamic model of both configurations and finally the calculations of efficiency and power absorbed for both regular and irregular waves.

All the calculations will be described together with reliable papers in which similar calculations were made, because by doing this the reliability of the results obtained is higher

3.1. BEM solver NEMOH

In order to create the dynamic model in frequency domain and carry out the necessary calculations it is necessary to calculate the frequency-dependent hydrodynamic parameters of the two bodies (added mass, radiation damping, and wave forces).

There are some programs specialized in this calculation, for example WAMIT and NEMOH, a comparison between the two of them was made by Penalba et al (2017) showing good agreement between them. So, NEMOH was the one chosen due to the fact that is an open source program and so it brings two advantages.

Firstly, it is free (no need for a license) and secondly it is possible to download the code of the program and integrate it with the MatLab code, so all the procedure is automatized.

NEMOH is a program based on the linear and second-order potential theory. To proceed with the calculations the velocity potential and fluid pressure on the submerged surfaces of the bodies are determined with the boundary element method.

Finally, the program solves the equations and from this solution obtains the hydrodynamic parameters. NEMOH require some inputs in order to work and proceed with the calculations, a mesh file with the discretization of the panels for both bodies, conditions of the sea (like water depth, wave height, distance between the bodies and draft of the floating buoy) and values assumed for gravity and ρ.

Further examples of input parameters and results are given in the Section Discussion of Results, as the goal of this section is just to present the model created, how it was developed, and how it works.

3.1.1. Equations and Assumptions of NEMOH

In order to proper perform the calculations NEMOH makes some assumption, as it is described by the developer of the code in (Babarit and Delhommeau 2015). The assumptions are inviscid fluid, incompressible and irrotational flow (which means the velocity derivates from a velocity potential and the pressure is obtained from Bernoulli formula).

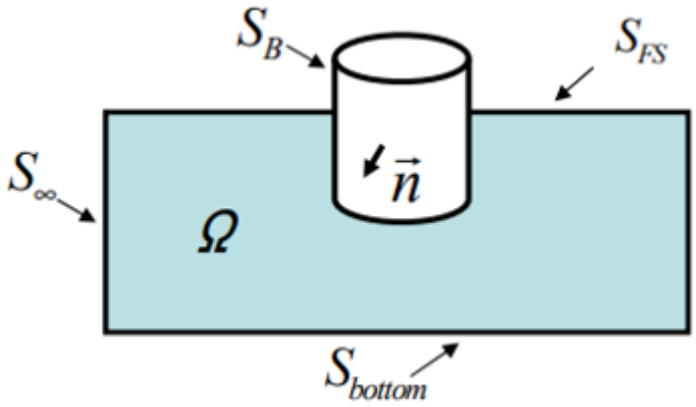

Figure 20: Model of the body to explain NEMOH equations

The governing equation that is solved is Laplace equation. It is solved by including the boundary conditions for the bodies (using BEM method). In order to facilitate the comprehension of the equations Figure 20 is presented.

$$\nabla^2\varphi = 0 \tag{1}$$

Where φ is the corresponding potential function of the fluid flow.

The boundary conditions can be described by (being M the point considered for the calculations):

$$\Delta\phi = 0;\ \ M \in \Omega \tag{2}$$

$$\frac{\partial\phi}{\partial n} = \vec{V}\vec{n};\ M \in S_B \tag{3}$$

$$\frac{\partial\phi}{\partial n} = 0;\ M \in S_{bottom} \tag{4}$$

$$\frac{\partial n}{\partial t} + \vec{\nabla}n\,\vec{\nabla}\phi = 0;\ \ M \in S_{FS} \tag{5}$$

$$\frac{\partial\phi}{\partial t} + gn + 0.5\left(\vec{\nabla}\phi\right)^2 = 0;\ \ M \in S_{FS} \tag{6}$$

Using all the boundaries conditions it is possible then to solve the Laplace equation and so solve the problem for the hydrodynamical coefficients.

3.2. Dynamic Model of First Geometry

Firstly, it is important to clarify that the movement of the dual body WEC is restricted to heave and the two bodies are coupled due to the PTO forces, so the system has two degrees of freedom (heave movement for the buoy and heave movement for the submerged body). The dynamic model of the system can be seen in Figure 21.

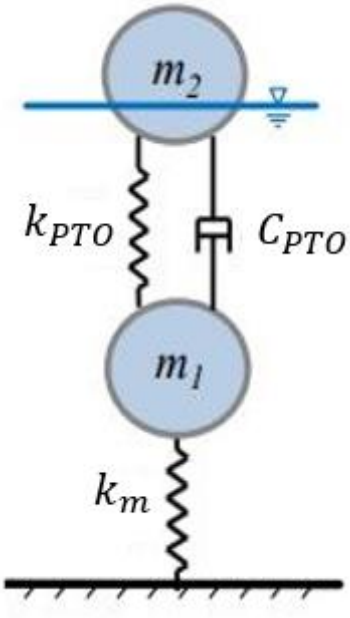

Figure 21:Dynamic Model of First Configuration

The model is based on the linear wave theory, meaning small wave amplitudes and small body motions were considered. As described before, the analyzes was developed in frequency domain.

The parameters c_{pto}, K_{pto}, K_m are PTO damping and stiffness; and mooring/interconnection stiffness respectively.

The hydrodynamic parameters (added mass, radiation damping and excitation force) for both the buoy and the submerged body were calculated using the BEM solver software NEMOH.

In order to create the model, Newton's second law was applied for both bodies.

$$\mathrm{M}\ddot{\mathrm{x}} = \sum \mathrm{F}_{\mathrm{external}} \tag{7}$$

For the first body, also considering the interaction between the two bodies, equation (7) becomes:

$$\mathrm{m}_1\ddot{\mathrm{x}}_1 + \mathrm{A}_{11}\ddot{\mathrm{x}}_1 + \mathrm{A}_{12}\ddot{\mathrm{x}}_2 + \mathrm{b}_{11}\dot{\mathrm{x}}_1 + \mathrm{b}_{12}\dot{\mathrm{x}}_2 + \mathrm{b}_{\mathrm{visc1}}\dot{\mathrm{x}}_1 + \mathrm{c}_{\mathrm{pto}}(\dot{\mathrm{x}}_1 - \dot{\mathrm{x}}_2) + \mathrm{k}_{\mathrm{pto}}(\mathrm{x}_1 - \mathrm{x}_2) + \mathrm{k}_{\mathrm{s}}\mathrm{x}_1 = \mathrm{F}_{\mathrm{e1}} \tag{8}$$

Where:

$$\mathrm{k}_{\mathrm{s}} = \rho \mathrm{g} \mathrm{A}_{\mathrm{c}} \tag{9}$$

In order to use the frequency domain instead of time domain the excitation wave is assumed to be a regular sinusoid and the buoy displacement assumed harmonic.

Then it is possible to consider, as in (Al Shamiet al 2018); (Liang and Zuo 2016); (Al Shami et al 2019); (Cheng et al. 2015), that the exciting force and buoy displacement can be expressed as:

$$F_{e1} = F_1 e^{i\omega t} \tag{10}$$

And

$$x_1 = X_1 e^{i\omega t} \tag{11}$$

Where F_1 is calculated using NEMOH. Substituting equations (10) and (11) in equation (8) it becomes:

$$\begin{aligned} -\omega^2(m_1 + A_{11})X_1 - \omega^2 A_{12}X_2 + i\omega b_{11}X_1 + i\omega b_{12}X_2 + i\omega b_{visc1}X_1 + i\omega c_{pto}(X_1 - X_2) \\ + k_{pto}(X_1 - X_2) + k_s X_1 = F_1 \end{aligned} \tag{12}$$

Analogously, the equation for the submerged body became:

$$\begin{aligned} -\omega^2(m_2 + A_{22})X_2 - \omega^2 A_{21}X_1 + i\omega b_{22}X_2 + i\omega b_{21}X_1 + i\omega b_{visc2}X_2 + i\omega c_{pto}(X_2 - X_1) \\ + k_{pto}(X_2 - X_1) - k_m X_2 = F_2 \end{aligned} \tag{13}$$

Denoting the matrices:

$$M = \begin{bmatrix} m_1 + A_{11} & A_{12} \\ A_{21} & m_2 + A_{22} \end{bmatrix} \tag{14}$$

$$C = \begin{bmatrix} b_{11} + b_{visc1} + c_{pto} & b_{12} - c_{pto} \\ b_{21} - c_{pto} & b_{22} + b_{visc2} + c_{pto} \end{bmatrix} \tag{15}$$

$$K = \begin{bmatrix} k_s + k_{pto} & -k_{pto} \\ -k_{pto} & k_{pto} - k_m \end{bmatrix} \tag{16}$$

$$X = \begin{bmatrix} X_1 \\ X_2 \end{bmatrix} \tag{17}$$

$$F = \begin{bmatrix} F_1 \\ F_2 \end{bmatrix} \tag{18}$$

It is possible now to model the system as:

$$Z(i\omega) = -\omega^2 M + i\omega C + K \tag{19}$$

Where Z is the impedance matrix and can be written as:

$$Z(i\omega) = \begin{bmatrix} Z_{11} & Z_{12} \\ Z_{21} & Z_{22} \end{bmatrix} \tag{20}$$

With:

$$Z_{11} = -\omega^2(m_1 + A_{11}) + i\omega(b_{11} + b_{visc1} + c_{pto}) + k_s + k_{pto} \tag{21}$$

$$Z_{12} = -\omega^2 A_{12} + i\omega(b_{12} - c_{pto}) - k_{pto} \tag{22}$$

$$Z_{21} = -\omega^2 A_{21} + i\omega(b_{21} - c_{pto}) - k_{pto} \quad (23)$$

$$Z_{22} = -\omega^2(m_2 + A_{22}) + i\omega(b_{22} + b_{visc2} + c_{pto}) + k_{pto} - k_m \quad (24)$$

The solution for the equations (21), (22), (23) and (24) can now be written as:

$$X = Z(i\omega)^{-1}F \quad (25)$$

3.3. Considerations About Viscous Damping

The calculations of b_visc2 was carried out following the same approach as (Al Shami et al 2019); (Siow et al. 2014).

Which means considering the viscous damping to have a linear behavior. It is important to say that both analyzes were done in frequency domain (been the consideration of linearized viscous damping the best way to perform its calculations in this domain).

The viscous damping is calculated using Drag force equation as given by Morison with the assumption that the fluid has a much higher velocity than the structure, so the term $V_{StructureZ}$ is ignored.

$$b_{visc2} = 0.5\rho A_c c_d * |V_{FluidZ} - V_{StrctueZ}| * (V_{FluidZ} - V_{StructureZ}) \quad (26)$$

Where V_{FluidZ} is the fluid velocity at z direction and $V_{StrctueZ}$ is the structure velocity at z direction.

The equation is then linearized by using the Fourier series linearization method. In terms of linearizing the model V_{FluidZ} is considered to be the maximum velocity reached by the fluid.

Then the equation then becomes:

$$b_{visc2} = 0.5\rho A_c c_d \frac{8}{3\pi} V_{max} \quad (27)$$

Where c_d is the drag coefficient. It varies according to the geometry of the body and common values used can be found in Siow et al. (2014). Also, for a bigger range of data, Cengel Cimbala (2010) was used.

3.4. Dynamic Model of Second Geometry

The development of the dynamic model of the second geometry is analogous to the first one. The dynamic model can be seen in Figure 22.

The variable k_m in this case is the connection stiffness between the two floaters, this variable was created like this to provide a fair comparison between the two configurations, as this way both configurations have the same number of variables in the model.

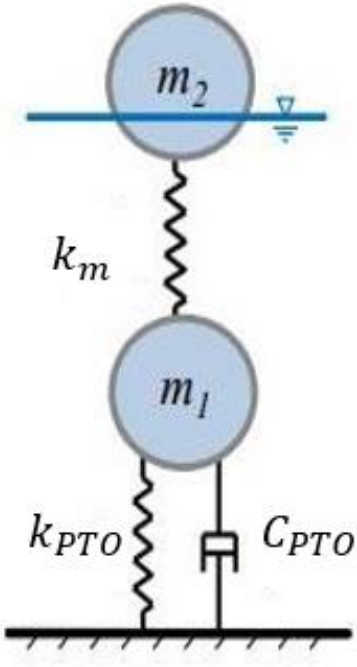

Figure 22:Dynamic Model of Second Configuration

The equations of motion for this configuration became:

For the first body:

$$-\omega^2(m_1 + A_{11})X_1 - \omega^2 A_{12}X_2 + i\omega b_{11}X_1 + i\omega b_{12}X_2 + i\omega b_{visc1}X_1 + k_m(X_1 - X_2) + k_s X_1 = F_1 \quad (28)$$

For the second body:

$$-\omega^2(m_2 + A_{22})X_2 - \omega^2 A_{21}X_1 + i\omega b_{22}X_2 + i\omega b_{21}X_1 + i\omega b_{visc2}X_2 - i\omega c_{pto}X_2 + k_m(X_2 - X_1) - k_{pto}X_2 = F_2 \quad (29)$$

Then, the impedance matrix became:

$$Z_{11} = -\omega^2(m_1 + A_{11}) + i\omega(b_{11} + b_{visc1}) + k_s + k_m \quad (30)$$

$$Z_{12} = -\omega^2 A_{12} + i\omega(b_{12}) - k_m \quad (31)$$

$$Z_{21} = -\omega^2 A_{21} + i\omega(b_{21}) - k_m \quad (32)$$

$$Z_{22} = -\omega^2(m_2 + A_{22}) + i\omega(b_{22} + b_{visc2} - c_{pto}) - k_{pto} + k_m \quad (33)$$

And finally, the solution is now calculated the same way of the first geometry:

$$X = Z(i\omega)^{-1}F \quad (34)$$

3.5. Power and Efficiency for Regular Waves

The efficiency for regular waves is defined as the ratio between the power absorbed by the WEC and the maximum power available to be absorbed in the income wave. The calculation is carried out for each different frequency of incoming waves.

$$\eta(\omega) = \frac{P_{avg}(\omega)}{P_{max\_wave}(\omega)} \tag{35}$$

The calculation of the power absorbed for each frequency of income wave can be calculated as in (Al Sham et al 2018); (Liang and Zuo 2016); (Al Shami et al 2019); (Cheng et al. 2015). It is important to notice that they are different for the first and second geometry, as the PTO (which generates the power) is placed in different places. For the first geometry it generates power in relation to the relative motion between the two bodies, for the second, in relation to the absolute motion of the second body.

For the first configuration:

$$P_{avg}(\omega) = \frac{1}{T}\int_0^T c_{pto}(\dot{x}_1 - \dot{x}_2)dt = 0.5\omega^2 c_{pto} abs(X_1 - X_2) \tag{36}$$

For the second configuration:

$$P_{avg}(\omega) = \frac{1}{T}\int_0^T c_{pto}(\dot{x}_2)dt = 0.5\omega^2 c_{pto} abs(X_2) \tag{37}$$

And the maximum power available in the wave to be absorbed by the WEC according to Dean and Darimple (2010) can be calculated as the total energy per wave per unit width times the group velocity.

$$P_{max\_wave}(\omega) = Ec_g(\omega) \tag{38}$$

Where:

$$E = 0.5\rho g H^2 L \tag{39}$$

And

$$c_g(\omega) = 0.5\frac{\omega}{\kappa}\left(1 + (2\kappa(\omega)D_{epth})/(\sinh 2\kappa(\omega)D_{epth})\right) \tag{40}$$

And κ is the wave number, calculated by Dean and Darimple (2010) as:

$$g\kappa(\omega)\tanh\kappa(\omega) * D_{epeth} = \omega \tag{41}$$

The calculation of the wave number must be an iterative process, however as the MatLab software were used a simple command 'vpasolve' was enough to reach the desired results.

3.6. Power and Efficiency for Irregular Waves

The calculation for irregular waves depends on the sea state of the place where the WEC is installed.

The parameters taken into considerations are the significant wave high (H_s) and energy wave period (T_e), more considerations about the Sea State are about to be made in the next section. The efficiency can then be calculated as described in (Liang and Zuo 2016); (Cheng et al. 2015).

$$\eta = \frac{P_{avg\_irr}}{P_{max\_wave\_irr}} \tag{42}$$

It is possible to notice that unlike in regular waves, the final efficiency is one number independent on the income wave frequency.

The calculation of absorbed and available power in irregular waves depends on the constructions of a sea spectra. The one chosen in this model was Pierson-Moskowitz spectra:

$$S(\omega) = 526 H_s^2 T_e^{-4} \omega^{-5} e^{-1054 T_e^{-4} \omega^{-4}} \tag{43}$$

Now, both the absorbed and available power can be written as:

$$P_{irr} = \int_0^{\infty} P_{reg}(\omega)\, S(\omega) d\omega \cong \sum P_{reg}(\omega)\, S(\omega) \Delta\omega \tag{44}$$

3.7. Sea State

The place considered for the WEC to be installed is Pico-Azores. The states of the sea were found in (Matos et al 2015). The study modeled the Sea State in Pico and the results found can be seen in Figure 23.

Hs (m) \ TP (s)	2.5	4	5.5	7	8.5	10	11.5	13	14.5
9.0	0	0	0	0	0	0	1	0	0
8.0	0	0	0	0	0	0	7	1	0
7.0	0	0	0	0	0	34	35	0	1
6.0	0	0	0	0	81	155	41	17	3
5.0	0	0	0	36	635	339	145	57	32
4.0	0	0	12	1336	1365	728	359	117	11
3.0	0	3	1622	3590	2133	1351	556	51	0
2.0	0	3333	6329	3829	2774	999	100	1	0
1.0	8775	7633	1804	1491	591	55	12	9	3
0.0									

Figure 23:Description of Sea State Pico-Azores (Matos et al 2015).

The values seen in Figure 23 are the occurrence of each Sea State. So, dividing all of the cells by the total amount of occurrences registered it is possible to reach a percentage of each sea state. This was made in MatLab, and the final results obtained can be seen in Figure 24.

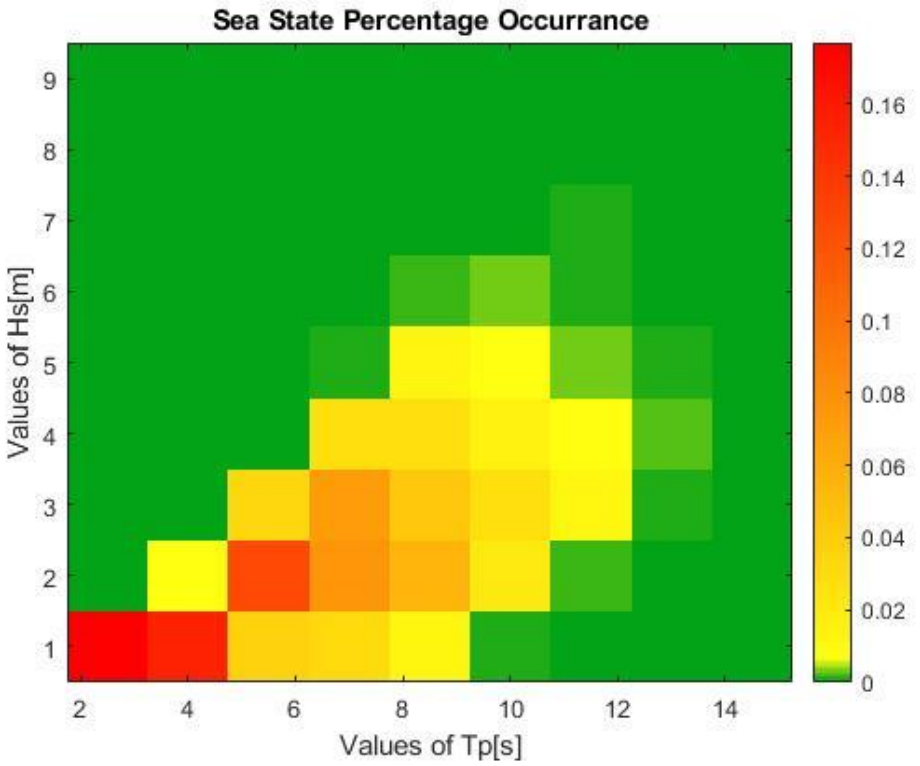

Figure 24:Description of Sea State Percentage Occurrence in Pico-Azores

The calculations of the final Sea Spectrum were carried based on (Falcão et al 2002), a study also about Pico-Azores.

The calculation of each Spectrum was calculated following the description previously done in this current chapter.

With occurrence of each Sea State, the total spectrum is now the sum of all the spectrum of each sea state times its percentage of occurrence.

$$S(\omega) = \sum S_{SeaState}(\omega) * Occurence \tag{45}$$

3.8. Parametrical Optimization

The parametrical optimization process is one of the main goals of this thesis, as this is the part responsible for guaranteeing that the best efficiency is reached, resulting in less cost to produce energy in a determined area.

Firstly, three different combinations of geometrical shapes were defined to be analyzed (cylinder-sphere, cylinder-cylinder, sphere-sphere for the floater and the submerged body respectively).

All the three combinations were analyzed for both the first configuration (PTO between the two bodies) and second configuration (PTO between submerged body and sea bottom)

The process described in the next lines was caried out for all the three configurations combined with both first and second configurations of the PTO, so it was carried out six times.

For example, the process can be carried out for the case of cylinder-sphere using the first configuration of the PTO, cylinder-sphere using the second configuration of the PTO, cylinder-cylinder using the first configuration of the PTO and so on.

The process consists in the creation of loops in MatLab involving both the NEMOH software and codes created to perform the dynamical analyzes and optimization of the system (resulting in the calculation of absorbed power and efficiency).

First, the shape of the bodies being analyzed are defined (for example cylinder-sphere). Then, different mesh geometries are created, using a MatLab loop, in the correct file to be inputted input in NEMOH (as much as the operator decides to input, as more geometries are set more computational time to run the program is needed). NEMOH then outputs the hydrodynamical coefficients that are stored in a '. MAT' file by the MatLab loop.

The meaning of this different meshes created is to set different sizes of the bodies to be analyzed. So, for example, it is analyzed for the case cylinder-sphere (using the first PTO configuration) for different sizes of the cylinder combined with different sizes of the sphere (each one of these combinations generating a different output in NEMOH).

For example, one of this meshes could contain data about a cylinder-sphere WEC with a cylinder with 2 meters radius and 1 meter draft combined with a sphere with 2 meter radius, another one of this meshes could contain a cylinder with 1 meter radius and 0.5 meter of draft combined with a sphere with 1 meter radius, and so on (as many as the operator decides to set).

Then, a range of values of PTO and mooring parameters (c_{pto}, K_{pto}, K_m) are defined and will be used to optimize the efficiency.

After, a loop proceeds to the calculation of efficiency and power absorbed (following the model described in this chapter) for all the different meshes (different combinations of bodies sizes) combined with all the different parameters (c_{pto}, K_{pto}, K_m).

Finally, the code points which is the best geometrical configuration and mooring and PTO parameters (c_{pto}, K_{pto}, K_m) that reached the maximum efficiency for the case analyzed.

For example, if the case been analyzed was cylinder-sphere using the first configuration of the PTO, the code would, in this stage, point which combination of mesh (sizes of the buoy and the submerged body) and mooring and PTO parameters (c_{pto}, K_{pto}, K_m) generated the maximum efficiency, being this the optimum case.

In Figure 25 a flowchart better explaining the way the optimization process works can be seen.

For instance, the case decided to be analyzed could be sphere-sphere. So, the loop on the top could be initialized with two different geometry sizes, sphere-sphere with both 1 meter radius and another one with 2 meters radius each. For that case, after the first loop finishes its calculations, two different groups of results with hydrodynamical coefficients would be stored in .MAT files.

Using each of that .MAT files, the second flow performs the dynamical calculation for both the first and second configurations of the PTO. Also, for each of this PTO's configurations the system tries all the values of mooring and PTO parameters (c_{pto}, K_{pto}, K_m) using a pre-defined range of values. The final output of this loop is the results of the best case for each scenario consider. So, the program would output the dynamical calculations (power, efficiency in regular and irregular waves) for both PTO configurations using the parameters that generated the maximum efficiency possible. Having this results a final comparison between the two PTO's shows which one is better in terms of efficiency. For instance, following the example, the best case for the sphere-sphere with the first PTO configuration could've been both with 1 meter radius and generated 40% of efficiency; and for the second configuration with the PTO the one of both with 2 meters and generated 47% of efficiency. In that fictional example, the second configuration would've been considered better for the case sphere-sphere due to the fact that is has a higher best efficiency.

The geometries selected and the results obtained are presented in the chapter Discussion of Results, being the goal of the present chapter just the description of the generic model used.

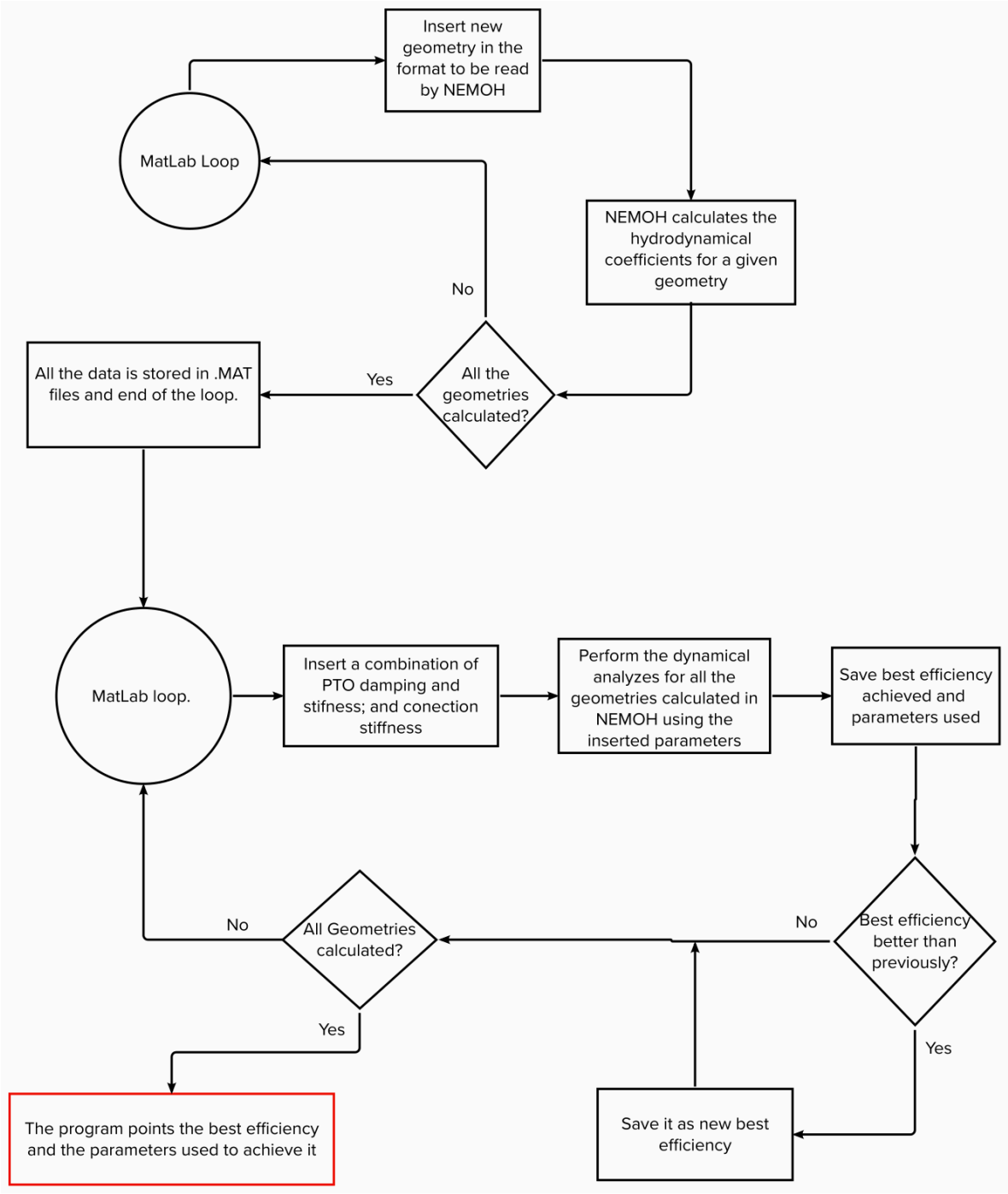

Figure 25:Flowchart of how optimization process works

Chapter 4. Validation

The validation of the results was done in four parts. The objective of each of these parts is to compare the obtained values with the ones from existing papers.

Firstly, a single body wave energy converter was modeled using the exact same dimensions and parameters of one of the devices modeled in (Ruezga 2019), the parameters compared in this case were all the hydrodynamical coefficients, the absorbed power and the RAO.

Secondly, a two-body wave energy converter was modeled following the same dimensions and parameters of the model in (Al Shami et al 2019) the parameters compared were the hydrodynamical coefficients for both bodies and the absorbed power.

Then, the validation for irregular waves was carried out following the same structure and sea conditions presented in (Engström et al 2009), the comparison made here was with the captured width radio presented in the paper and the one calculated.

Finally, the Spectrum of the Sea State considered was compared with the one described in (Falcão et al 2002), as they are both modeling the same place (Pico-Azores) and so they should return the same value.

All comparisons ended up showing similar values between the obtained results and the papers, which increases the reliability of the conclusions of the present thesis.

Also, it is important to say that by doing the validation it's also guaranteed that the analyzes follows a certain logic, starting by validating simper geometries and cases, as the single body analyzes, until it evolves to more complexes analyzes, like two body devices in irregular waves, which is one of the main analyzes done in the present thesis

The mathematical theory and equations used in the calculations were already described in Section Mathematical Model, being the presentation of the validation the only goal of this chapter.

4.1. Single Body Wave Energy Converter

The structure considered is a cylindrical single body wave energy converter with a PTO system in reference to the seabed. The dynamical simplified model considered is shown in Figure 26

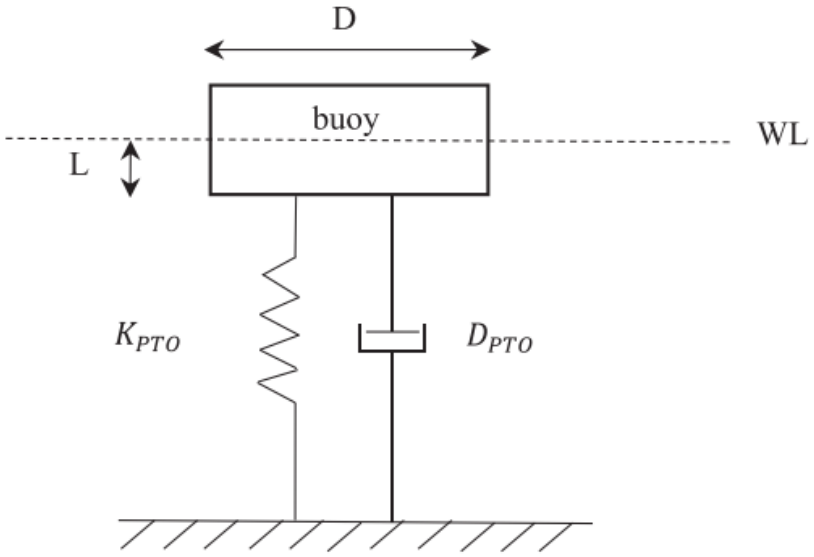

Figure 26:Dynamic Model of the Single Body WEC Considered (Ruezga 2019).

The analysis was carried considering 40 frequencies in a range from 0.05 rad/s to 4 rad/s and the parameters/dimensions of the analysis were the same as (Ruezga 2019).

Table 1:Parameters Considered for Validation of Single Body WEC

Parameters Used	
Wave Height [m]	1
Water Depth [m]	25
PTO Damping [KNs/m]	20
Restoring Stiffness [KN/m]	5
Buoy Parameter	
Diameter [m]	2.5
Draft [m]	1
Mass [Kg]	2.0E+04

The mesh of the structure was done using the pre-processor of NEMOH and considering 735 panels and 2940 nodes. It is important to emphasize that in order to continue the calculations in NEMOH only half of the body needs to be discretized as it is axisymmetric.

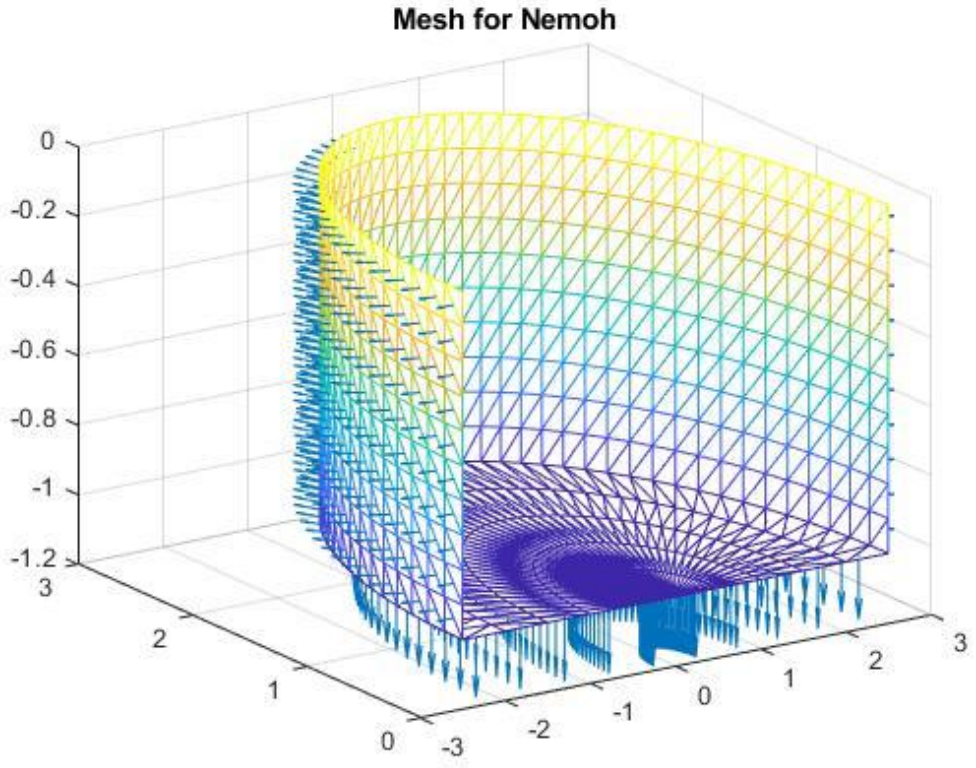

Figure 27:Mesh for the Buoy - Validation of Single Body WEC

Then, using the main processor and solver of NEMOH, the hydrodynamic coefficients (added mass, radiation damping and excitation force) were obtained and compared with the ones obtained in (Ruezga 2019).

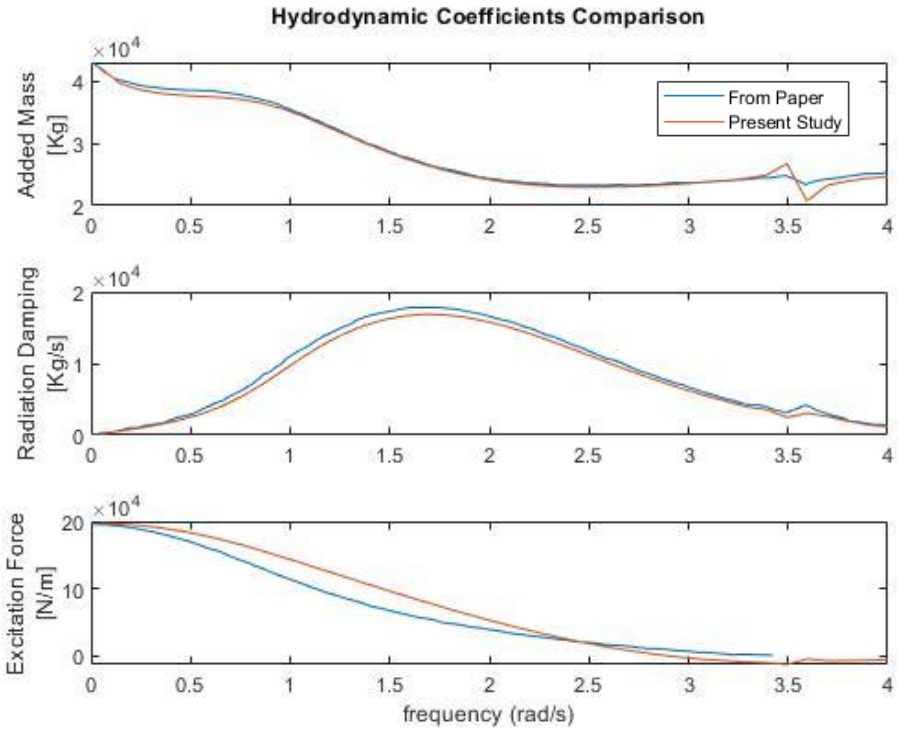

Figure 28:Hydrodynamic Coefficients Comparison for Validation Single Body WEC

In the possession of the hydrodynamic coefficients the calculations of the absorbed power and RAO were carried out.

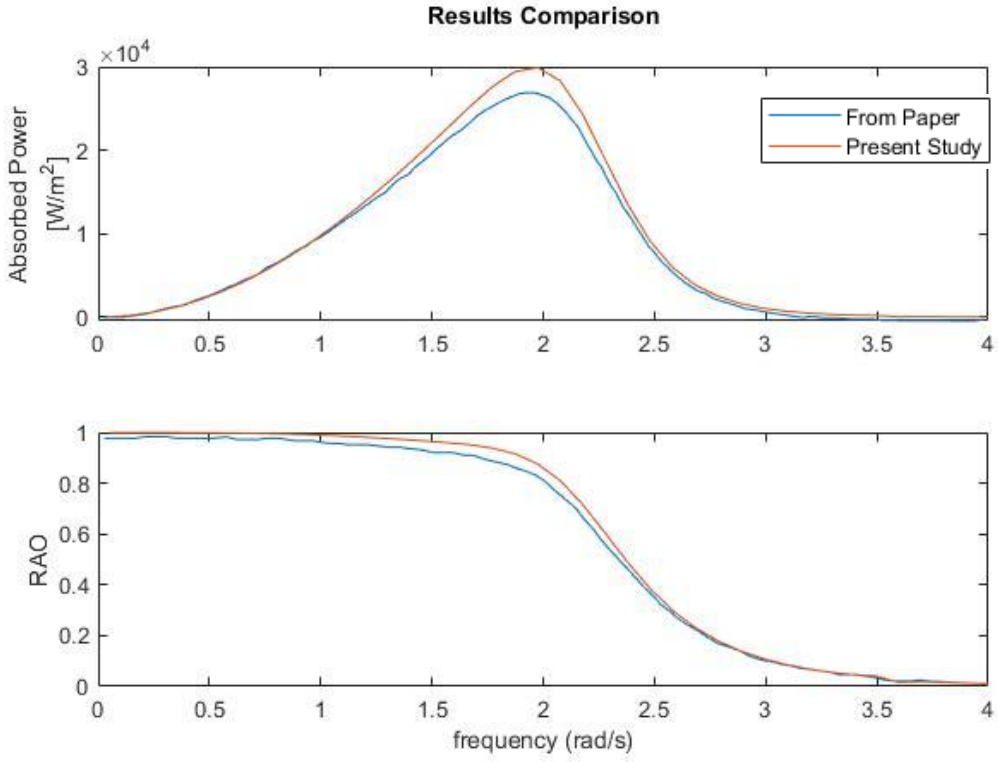

Figure 29:RAO/Absorbed Power Comparisons for Validation Single Body WEC

As it is possible to see all the comparisons show similar values between the papers and the calculations. That mean that the main goal of this section was successfully achieved.

55555

4.2. Dual Body Wave Energy Converter

The structure considered is a cylindrical buoy and a sphere submerged body to compose the dual body wave energy converter with a PTO system in located in between the two bodies. The dynamical simplified model considered is shown in Figure 30.

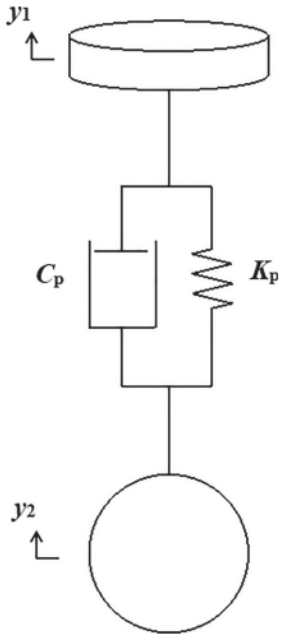

Figure 30:Dynamic Model of the Dual Body WEC Considered (Al Shami et al 2019).

The analysis was carried considering 40 frequencies in a range from 0.05 rad/s to 3 rad/s and the parameters/dimensions of the analysis were the same as (Al Shami et al 2019).

Table 2:Parameters Considered for Validation of Dual Body WEC

Parameters Used	
Wave Height [m]	1
Water Depth [m]	400
PTO damping [Ns/m]	250000
PTO stiffness [N/m]	100000
Buoy Parameters	
Diameter [m]	1.5
Height [m]	0.8
Mass [Kg]	2898
Draft [m]	0.4
Submerged Body Parameters	
Radius [m]	1.105
Mass [Kg]	5792
Depth [m]	20

The mesh of the structure was done using the pre-processor of NEMOH. Two bodies were meshed and after the analyses was done using both of the meshes. The buoy was modeled using 686 panels and 2744 nodes. The submerged body was modeled using 980 panels and 3920 nodes.

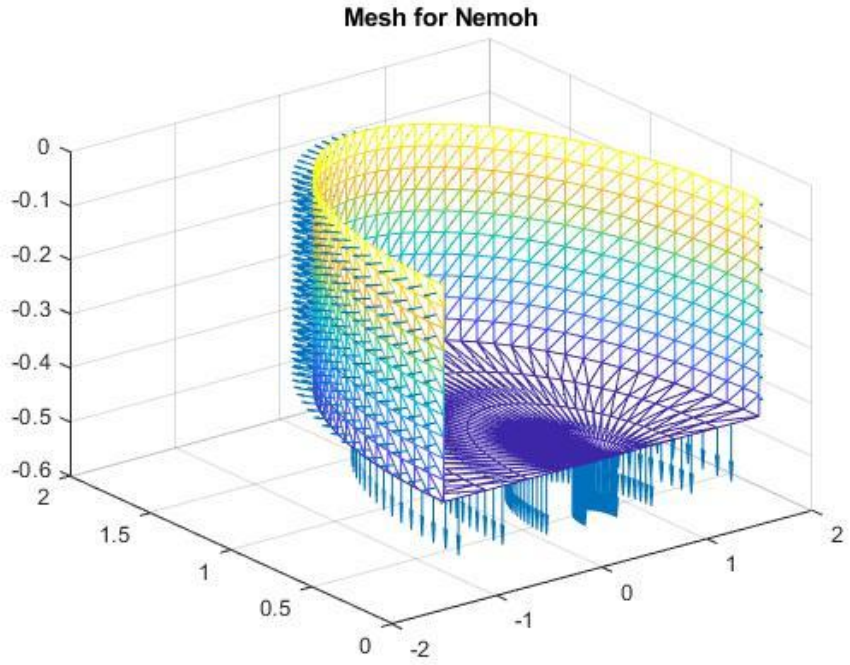

Figure 31:Mesh for the Buoy for Validation of Dual Body WEC

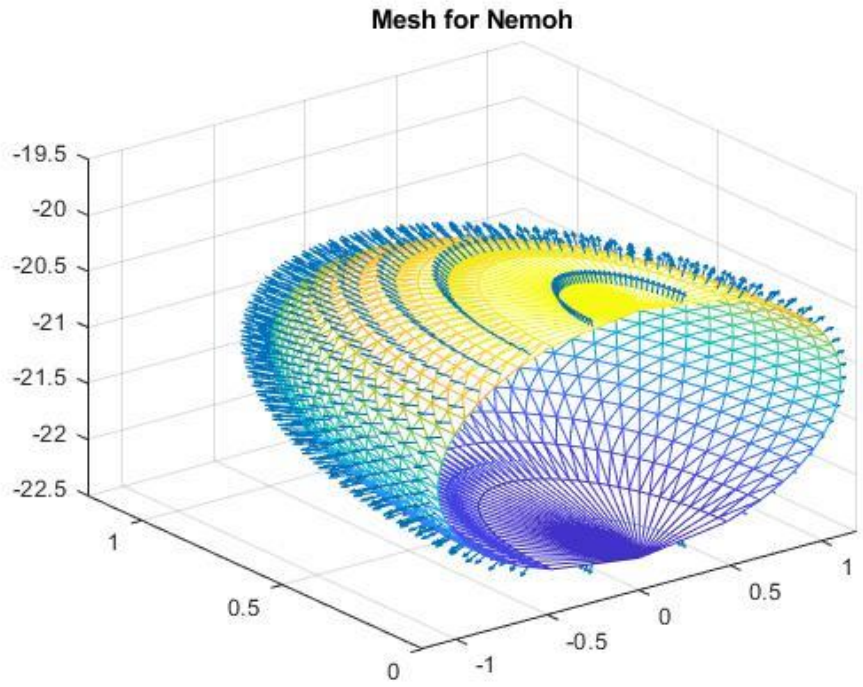

Figure 32:Mesh for Submerged Body for Validation of Dual Body WEC

Then, using the main processor and solver of NEMOH, the hydrodynamic coefficients (added mass, radiation damping and excitation force) were obtained for both buoy and submerged body and compared with the ones obtained in (Al Shami et al 2019).

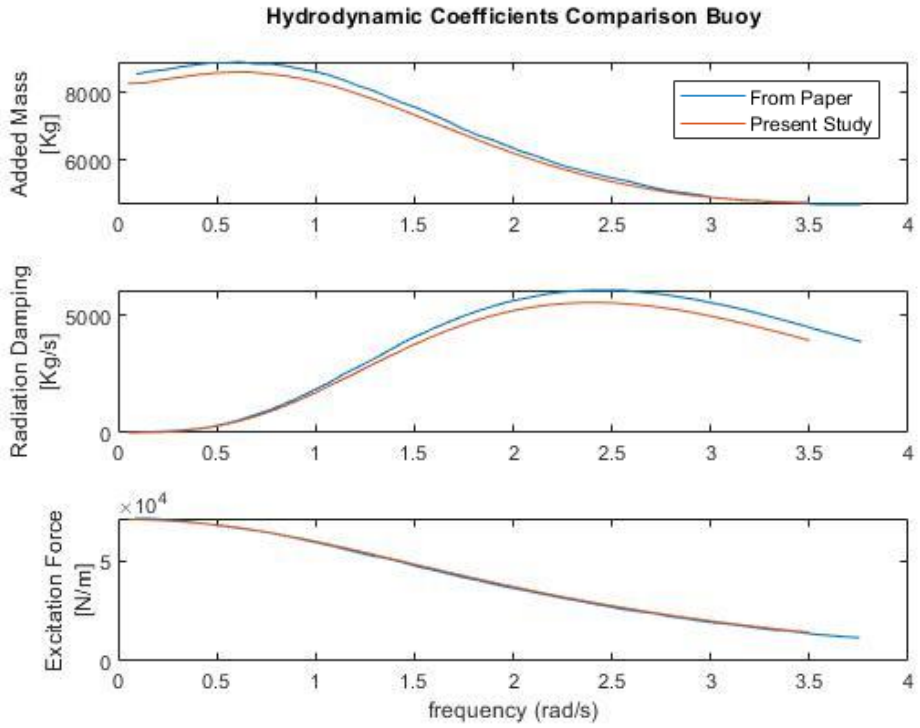

Figure 33:Hydrodynamic Coefficients Comparison for the Buoy for Validation of Dual Body WEC

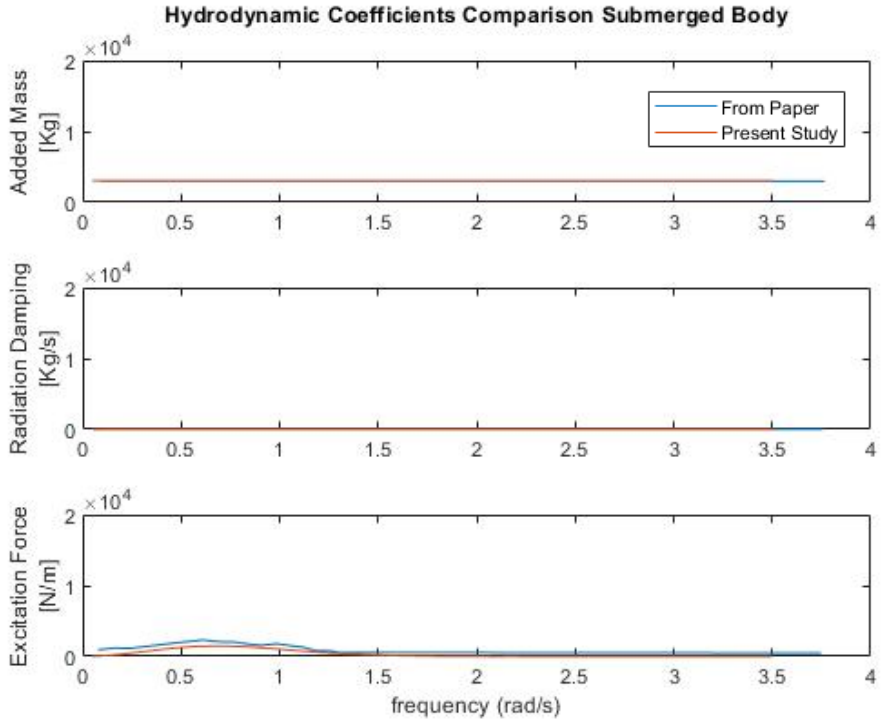

Figure 34:Hydrodynamic Coefficients Comparison for the Submerged Body for Validation of Dual Body WEC

In the possession of the hydrodynamic coefficients the calculations of the absorbed power were carried out and compared with the values obtained in Al Shami et al (2019). The results of the comparison are showed in Figure 35.

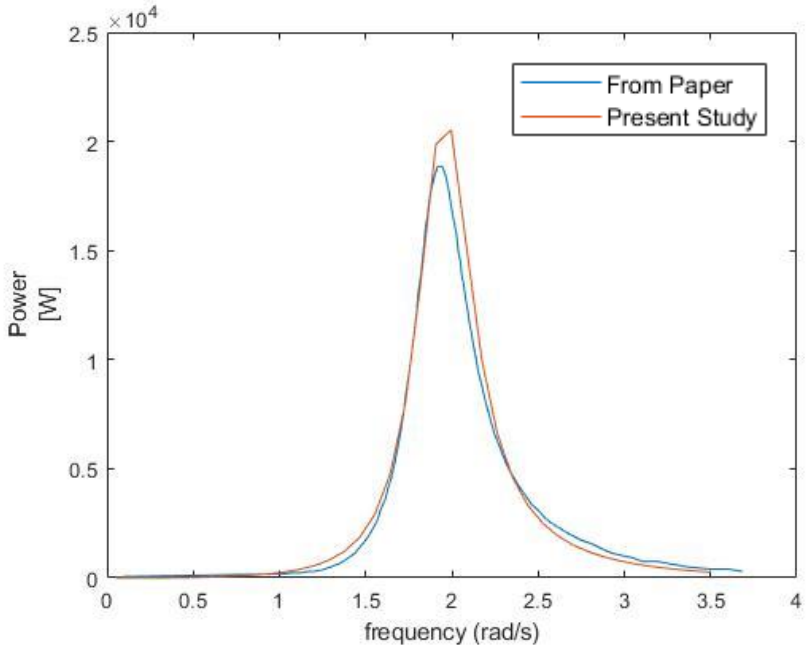

Figure 35:Average Absorbed Power Comparison for Validation of Dual Body WEC

As it is possible to see all the comparisons show similar values between the papers and the calculations for both the submerged body and the buoy. That proofs that the results achieved in this paper are reliable.

Analyzing the graphics one absorbed power for both cases validated so far it is possible to make some comments.

For the case of the one-body wave energy converter it is possible to notice that the curve of absorbed power reaches a peak around the frequency with the value of 2 rad/s (seen in Figure 29). Looking at dual body system, it is possible to see that it reaches its peak around the value of 2 rad/s (seen in Figure 35).

The reason for that is that this is the natural resonant frequency of each of these systems, and if the frequency of the incoming wave coincides with the resonant natural frequency, the system will show a maximum of power absorption in that point.

The further away from the value of resonant frequency of the system the frequency of the wave goes, the less amount of energy is absorbed.

It is also good to notice that besides showing a good agreement in the values the validation process also showed a good agreement in the natural resonant frequency.

4.3. Irregular Waves

The structure considered is a cylindrical buoy and a sphere submerged body to compose the dual body wave energy converter with a PTO system in located in between the submerged body and the sea bottom. The dynamical simplified model considered is shown in Figure 36.

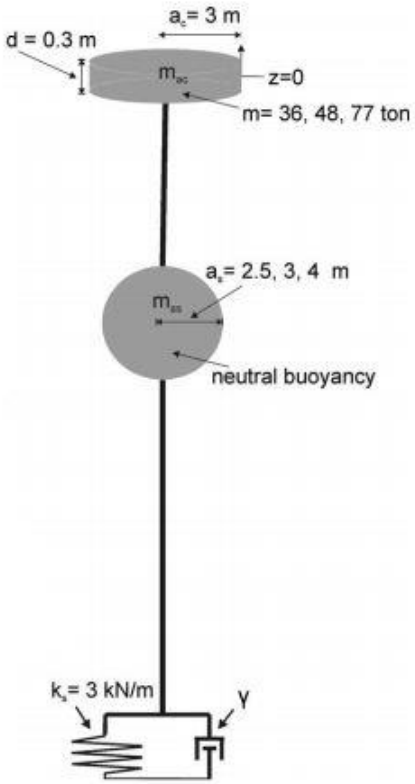

Figure 36:Dynamic Model of the Dual Body WEC Considered (Engström et al 2009).

The analysis was carried considering 40 frequencies in a range from 0.05 rad/s to 3 rad/s and the parameters/dimensions of the analysis were the same as (Engström et al 2009).

Table 3:Parameters Considered for Validation of Irregular Waves

Parameters Used	
Significant Wave Height [m]	1
Water Depth [m]	400
PTO Stiffness [N/m]	3000
Buoy Parameters	
Diameter [m]	3
Draft [m]	0.3
Submerged Body Parameters	
Radius [m]	3
Depth [m]	20

The mesh of the structure was done using the pre-processor of NEMOH. Two bodies were meshed and after the analyses was done using both of the meshes. The buoy was modeled using 686 panels and 2744 nodes. The submerged body was modeled using 980 panels and 3920 nodes.

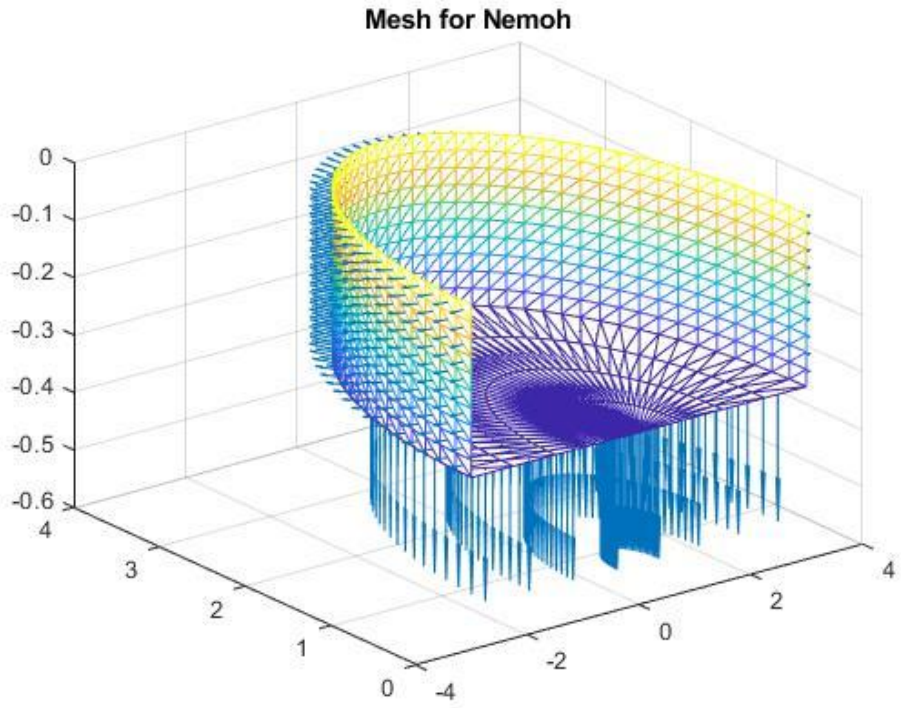

Figure 37:Mesh for the Buoy for Validation of Irregular Waves

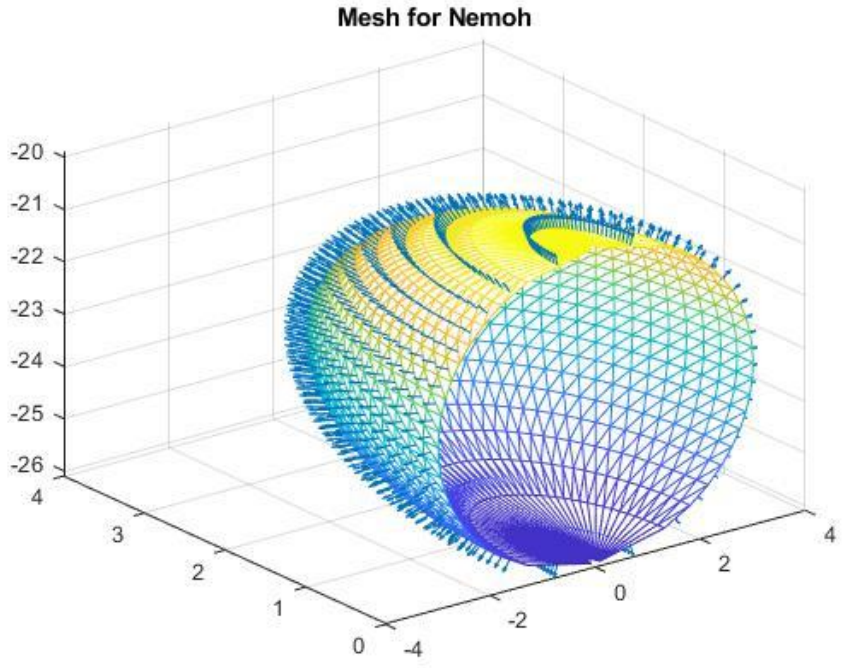

Figure 38:Mesh for the Submerged Body for Validation of Irregular Waves

Then, using the main processor and solver of NEMOH, the hydrodynamic coefficients (added mass, radiation damping and excitation force) were obtained for both buoy and submerged body. As these coefficients are not presented in (Engström et al 2009), (and they were already validated before), the only validation here is for the capture width ratio. This comparison is good because

it depends on all the other calculations (hydrodynamical coefficients, power absorption, sea state definition and so on), so once this is right it means everything before also was.

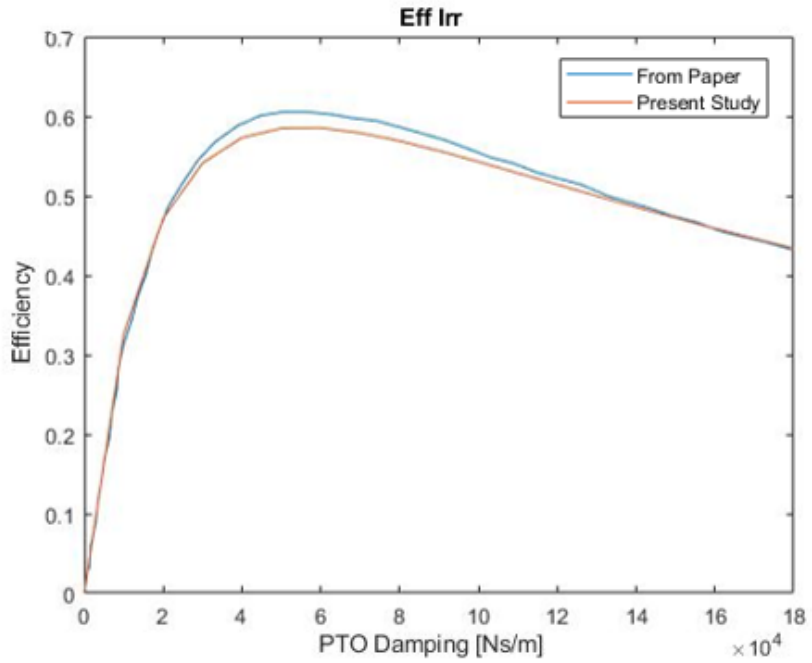

Figure 39:Efficiency in Irregular Waves Comparison for Validation of Irregular Waves

As it is possible to notice the comparison shows similar values between the calculations and the data presented in the paper. That means that the calculations done are reliable.

4.4. Sea State Spectrum

The place chosen in the present thesis is Pico-Azores, the same place as (Falcão et al 2002), so the resultant Spectrum was compared with the one presented by Falcão et al (2002). All the calculations used to create the Spectrum are already presented in the Section Mathematical Model, and as already said there the spectrum used was Pierson-Moskowitz spectra.

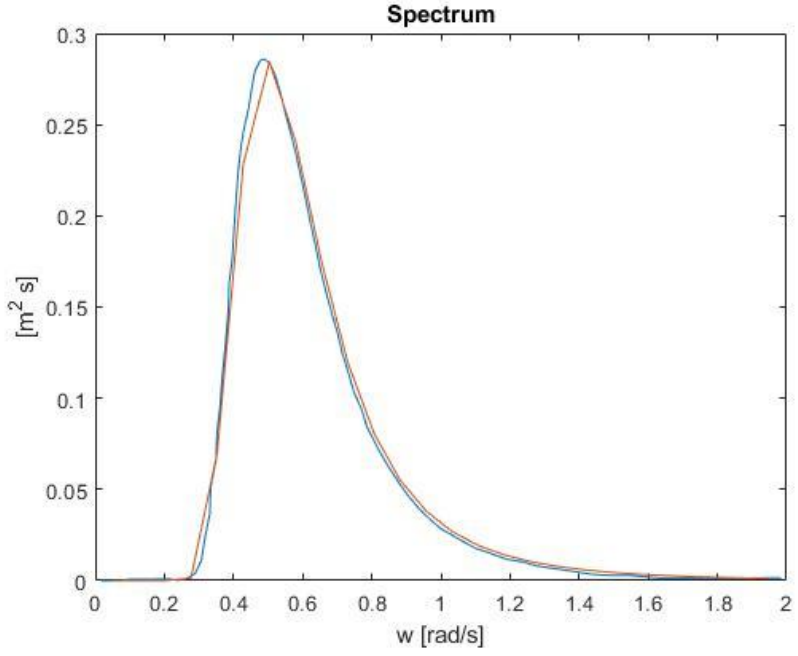

Figure 40:Sea Spectrum Comparison for Validation of Sea State

As it can be seen in Figure 40 the values obtained by the paper and by the present thesis are quite similar, showing again that the results obtained are reliable.

The meaning of the peak in the Spectrum graphic is the frequency that happens the most in the considered place (Pico-Azores). So, that means that the frequency around 0.55~0.6 rad/s is the one that happens the most in the considered place. In a deeper analyzes it is possible to affirm that a system that operates with natural resonant frequency in a value closer to that frequency (0.55-0.6 rad/s) will probably have a better energy generation than a system operating in a natural resonant frequency far away from this value.

This happens due to the fact that already explained that a system generates the most energy when the frequency of the incoming waves and the natural resonant frequency of the system are closer. So, if a system has a natural frequency close to the frequency that happens the most in a specific sea state that means that this system will operate more time in a peak of energy generation, meaning that it will probably generate more energy than a system working with natural frequency far away from that value.

Chapter 5. Discussion of Results

The Optimization Process was carried out for 3 different combinations of bodies (cylinder-sphere, cylinder-cylinder, sphere-sphere for the floater and the submerged body respectively). For each of these combinations' different sizes of the bodies are considered alongside with a range of values of PTO and mooring parameters (c_{pto}, K_{pto}, K_m) that are going to be optimized for each combination.

This process follows all the steps already better described and properly explained in the chapter Mathematical Model. Being the goal of this chapter only the presentation and discussion of the results obtained.

The values of the parameters (c_{pto}, K_{pto}, K_m) and body sizes chosen were defined by looking at already existing papers and seeing which values are commonly used in these kinds of wave energy converters. For each one of these combinations the analyzes for both configurations were carried out.

The first comparison is between the optimized first configuration (PTO between the two bodies) and the second configuration (PTO between submerged body and sea bottom) using the same parameters as the optimized first configuration.

The second comparison is the opposite, the optimized parameters for the second configuration and the first configuration using the same parameters as the optimized second configuration. A comparison between the maximum efficiency obtained for each optimized configuration was made at the end of the calculation for each combination (cylinder-sphere, cylinder-cylinder, sphere-sphere).

Finally, an analyzes of all the efficiencies obtained was carried out and it was proven that the second configuration is indeed more efficient than the first one in all the cases tested in the present thesis. To simplify computational time required all cylinders were modeled in NEMOH using 686 panels and 2744 nodes and all the spheres using 980 panels and 3920 nodes.

5.1. Sea State Azores-Pico

The location analyzed in the present thesis is Pico-Azore-Portugal. The considered Sea State (Matrix of occurrence of each combination of Ts and Hs) is the one obtained by Matos et al (2015). The calculations are already presented in chapter Mathematical Model.

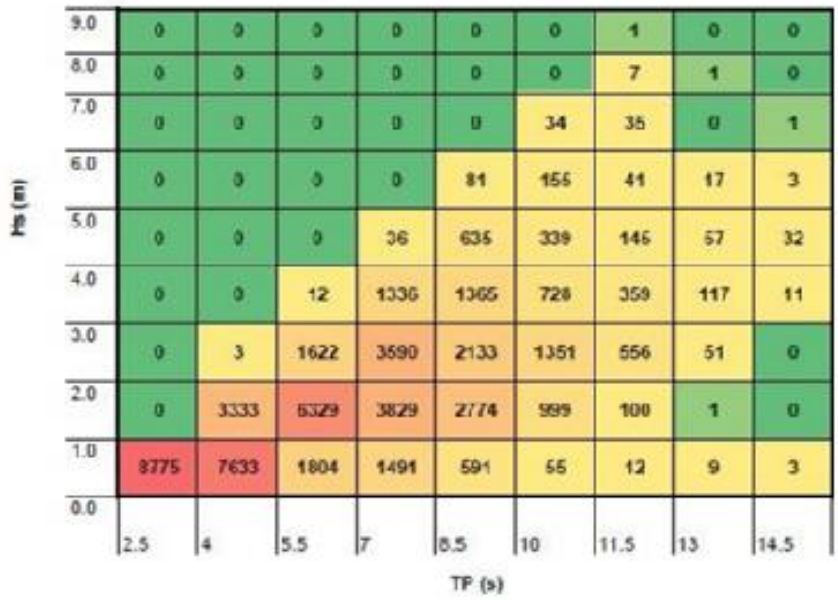

Figure 41: Occurence of each Sea State in Pico-Azores (Matos et al 2015).

The spectrum used, as already described is Pierson-Moskowitz spectra. The final Spectrum can be seen in Figure 42.

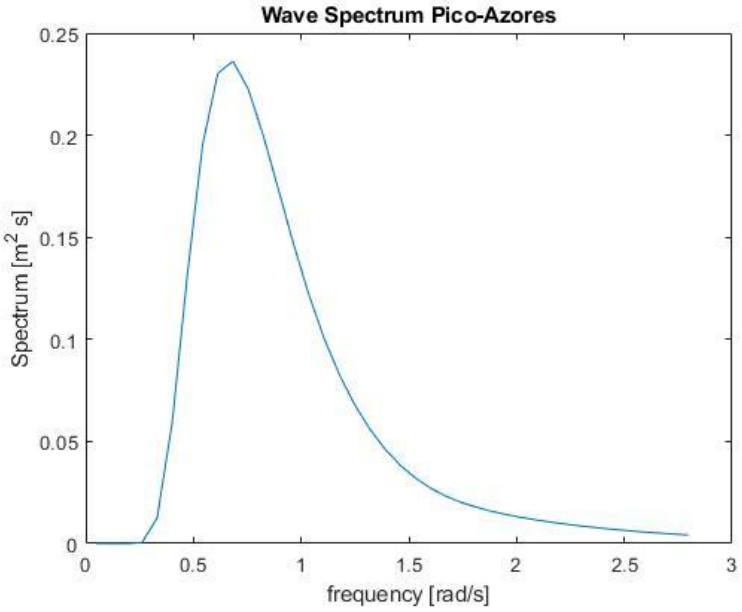

Figure 42:Spectrum Pico-Azores

5.2. Cylinder-Sphere

To perform the calculations and the optimization process nine different combinations of geometrical parameters were chosen.

In order to also optimize the PTO and mooring system, the values of PTO and mooring parameters were set to vary based on the available literature, common values were the ones chosen.

After that, the optimization process (the one explained in Figure 25) is carried out and the results are presents for every geometrical combination and the best parameters of PTO and mooring system.

The presentation of the hydrodynamic coefficients is made in this section due to the fact that they are the same for both configurations, as it just depends on the geometry of the bodies.

Table 4:Different Combinations of Geometrical Parameter Used (Cylinder-Sphere)

Configuration Number	Buoy Radius [m]	Buoy Draft [m]	Submerged Body Radius [m]	Distance Between Bodies [m]
1	1	0.5	1	10
2	2.5	0.5	1	10
3	2.5	1	1	10
4	2.5	1	3	10
5	4	1	3	10
6	6	1	3	10
7	4	1	1	10
8	6	1	1	10
9	6	2	3	10

Table 5:Parameters Variation for Optimization (Cylinder-Sphere)

Mooring and PTO parameters			
Parameter	Starting Value	Ending Value	Step
PTO Damping [Ns/m]	10000	300000	10000
Equivalent PTO Stiffness [N/m]	10000	140000	10000
Mooring Stiffness/ Floaters Interconnection Stiffness [N/m]	10000	140000	10000

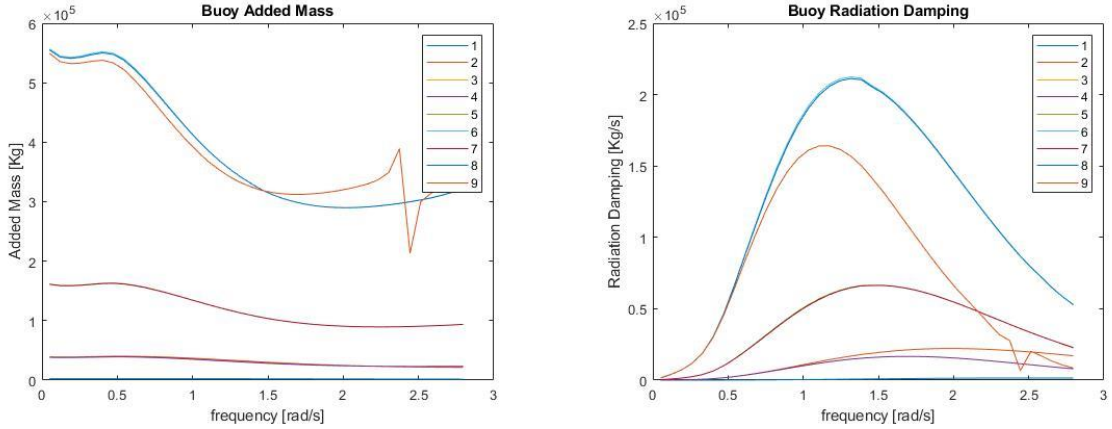

(a) *(b)*

Figure 43:(a)Buoy Added Mass (Cylinder-Sphere), (b) Buoy Radiation Damping (Cylinder-Sphere)

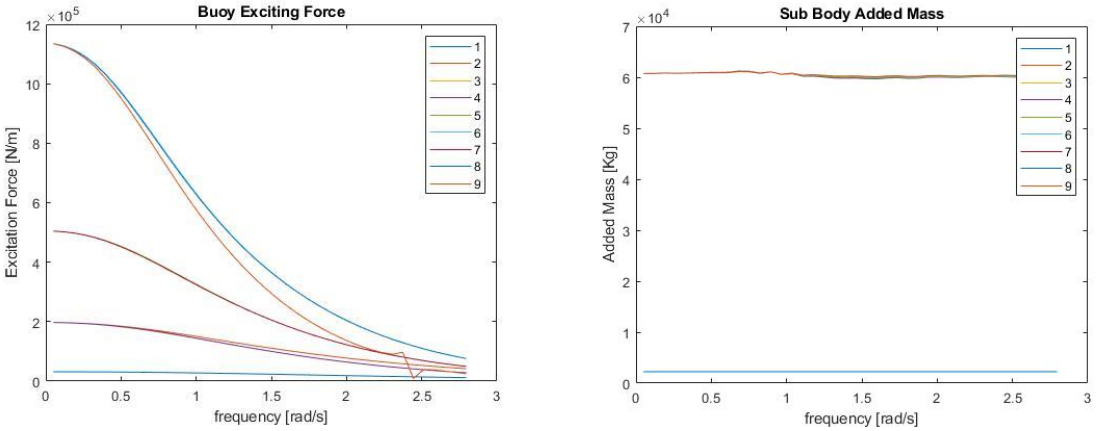

(a) *(b)*

Figure 44:(a) Buoy Exciting Force (Cylinder-Sphere), (b) Submerged Body Added Mass (Cylinder-Sphere)

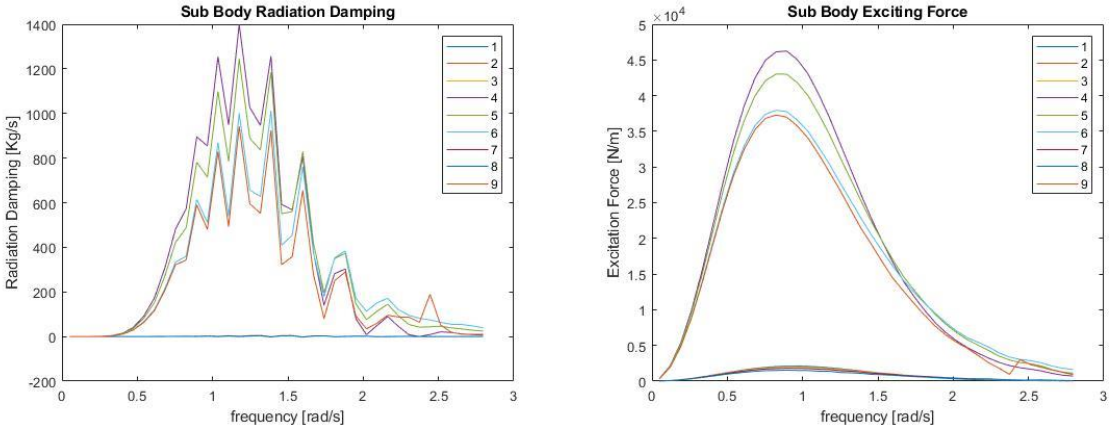

(a) *(b)*

Figure 45: (a) Submerged Body Radiation Damping (Cylinder-Sphere), (b) Submerged Body Exciting Force (Cylinder-Sphere)

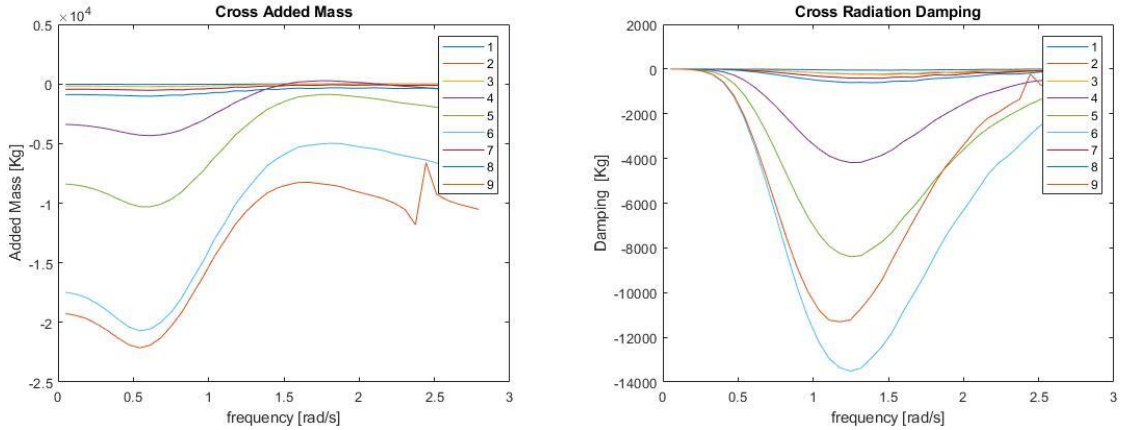

(a) *(b)*

Figure 46: (a) Cross Added Mass (Cylinder-Sphere), (b) Cross Radiation Damping (Cylinder-Sphere)

5.2.1. Results for Optimized First Configuration

The presentation and comparison of results in this section was carried out using the parameters for the optimized first configuration for both configurations. These values were obtained following the optimization process described in the Chapter 3Mathematical Model

Table 6:Opitmal Parameters First Configuration (Cylinder-Sphere)

Optimal Parameters	
Buoy Radius [m]	2.5
Buoy Draft [m]	1
Submerged Body Radius [m]	3
PTO Damping [Ns/m]	280000
Equivalent PTO Stiffness [N/m]	140000
Mooring Stiffness/ Floaters Interconnection Stiffness [N/m]	50000
b_{visc2} [Ns/m]	1.42E+04

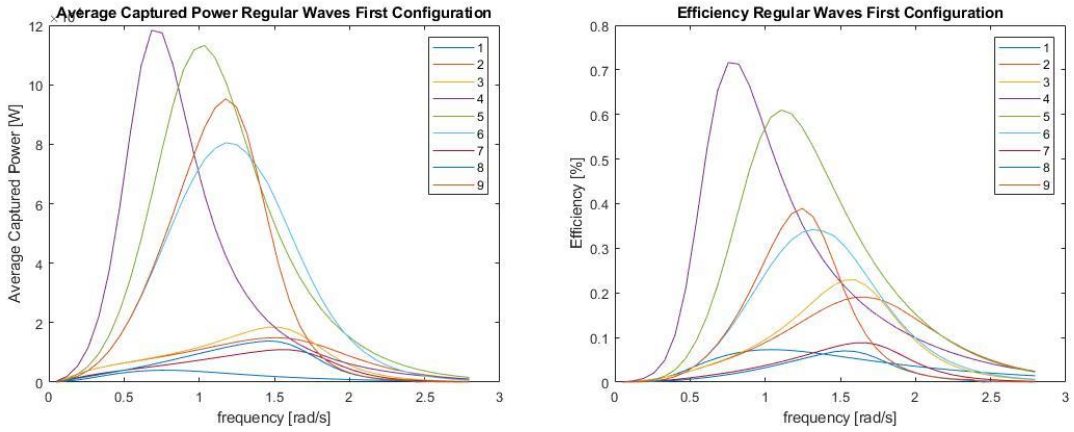

(a) *(b)*

Figure 47: (a) Average Captured Power Regular Waves First Configuration (Cylinder-Sphere), (b) Efficiency Regular Waves First Configuration (Cylinder-Sphere)

Table 7:Absorbed Power and Efficiency for First Configuration in Irregular Waves (Cylinder-Sphere)

Irregular Waves First Configuration		
Geometry	Absorbed Power [W]	Efficiency
1	5.42E+02	5.08%
2	1.56E+03	5.86%
3	1.66E+03	6.22%
4	1.26E+04	47.07%
5	1.15E+04	26.83%
6	7.73E+03	12.07%
7	1.03E+03	2.42%
8	1.24E+03	1.93%
9	8.02E+03	12.54%

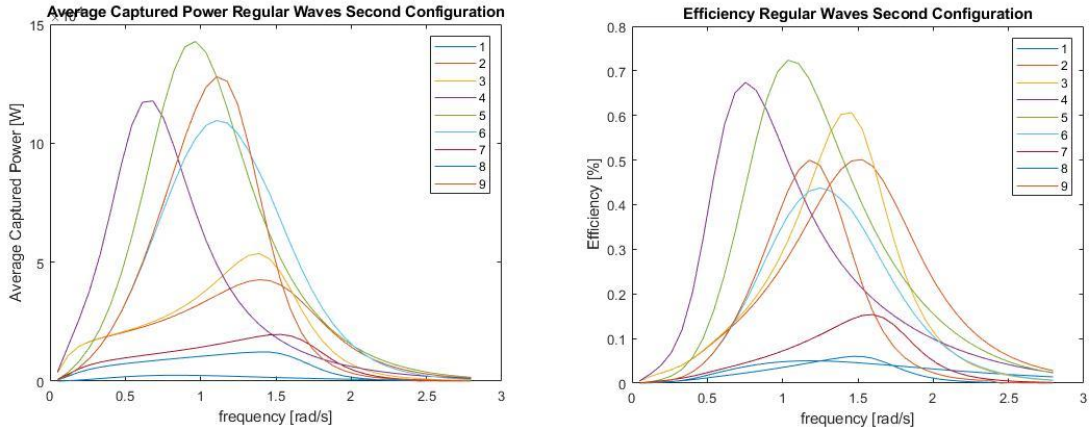

(a) *(b)*

Figure 48:(a) Average Captured Power Regular Waves Second Configuration (Cylinder-Sphere), (b) Efficiency Regular Waves Second Configuration (Cylinder-Sphere)

Table 8:Absorbed Power and Efficiency for Second Configuration in Irregular Waves (Cylinder-Sphere)

Irregular Waves Second Configuration		
Geometry	Absorbed Power [W]	Efficiency
1	3.44E+02	3.22%
2	4.57E+03	17.15%
3	4.93E+03	18.50%
4	1.31E+04	48.99%
5	1.56E+04	36.45%
6	1.14E+04	17.85%
7	2.08E+03	4.86%
8	1.48E+03	2.31%
9	1.19E+04	18.60%

5.2.2. Results for Optimized Second Configuration

The presentation and comparison of results in this section was carried out using the parameters for the optimized second configuration for both configurations. These values were obtained following the optimization process described in the chapter Chapter 3Mathematical Model

Table 9:Opitmal Parameters Second Configuration (Cylinder-Sphere)

Optimal Parameters	
Buoy Radius [m]	1
Buoy Draft [m]	0.5
Submerged Body Radius [m]	1
PTO Damping [Ns/m]	60000
Equivalent PTO Stiffness [N/m]	100000
Mooring Stiffness/ Floaters Interconnection Stiffness [N/m]	20000
b_{visc2} [Ns/m]	2.28E+03

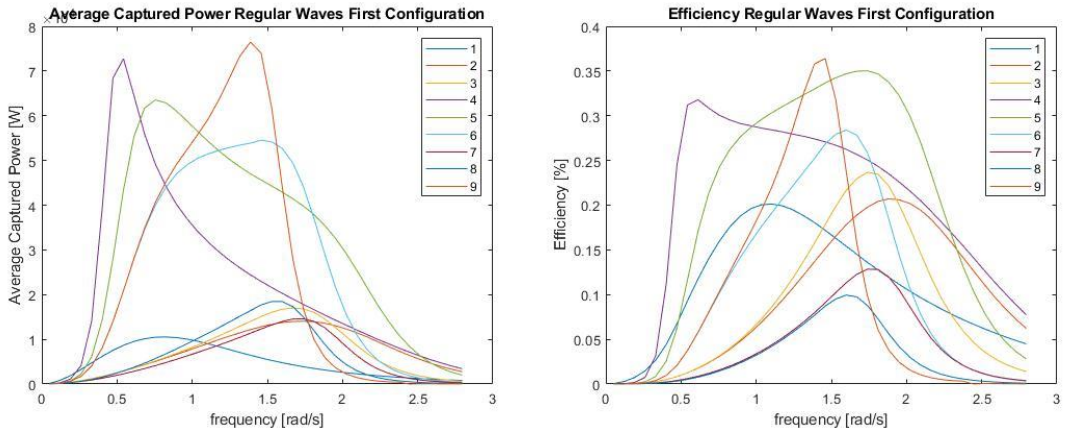

(a) *(b)*

Figure 49:(a) Average Captured Power Regular Waves First Configuration (Cylinder-Sphere), (b) Efficiency Regular Waves First Configuration (Cylinder-Sphere)

Table 10:Absorbed Power and Efficiency for First Configuration in Irregular Waves (Cylinder-Sphere)

Irregular Waves First Configuration		
Geometry	Absorbed Power [W]	Efficiency
1	1.44E+03	13.48%
2	1.09E+03	4.07%
3	1.13E+03	4.25%
4	7.38E+03	27.68%
5	8.50E+03	19.91%
6	6.21E+03	9.70%
7	9.14E+02	2.14%
8	1.22E+03	1.90%
9	6.56E+03	10.26%

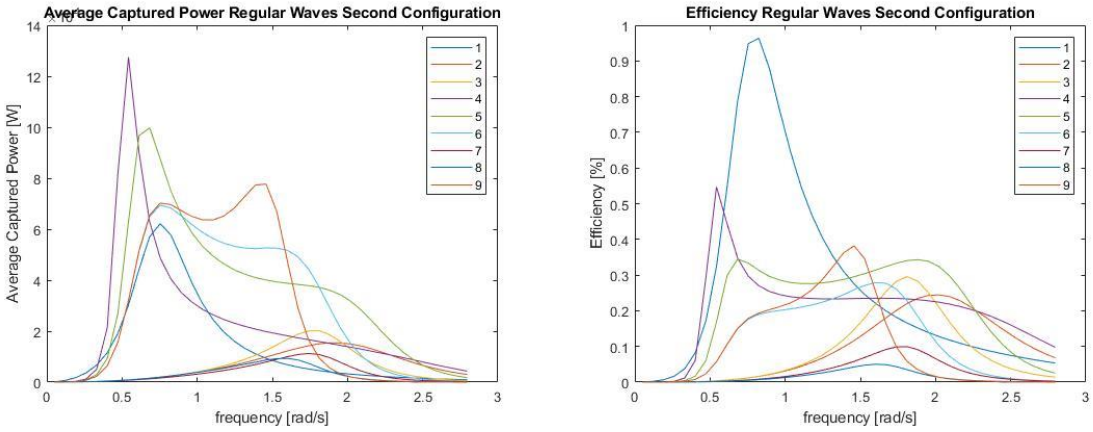

(a) *(b)*

Figure 50:(a) Average Captured Power Regular Waves Second Configuration (Cylinder-Sphere), (b) Efficiency Regular Waves Second Configuration (Cylinder-Sphere)

Table 11:Absorbed Power and Efficiency for Second Configuration in Irregular Waves (Cylinder-Sphere)

Irregular Waves Second Configuration		
Geometry	Absorbed Power [W]	Efficiency
1	5.91E+03	55.43%
2	6.35E+02	2.38%
3	6.83E+02	2.56%
4	8.35E+03	31.29%
5	1.04E+04	24.43%
6	8.51E+03	13.29%
7	4.66E+02	1.09%
8	4.95E+02	0.77%
9	8.91E+03	13.92%

5.2.3. Analyzes

Firstly, when looking at the comparison between the two configurations using the parameters of the optimized first configuration it is possible to see that the second configuration is already slightly better. The maximum efficiency for the first one is 47,07% against 48,99% for the second.

Also, it is possible to notice that the highest efficiency was obtained for the same geometrical combination (number four in Table 4). However, for the second configurations, despite the fourth having the best efficiency it is the fifth that generates more power in irregular waves.

Comparing just the power generated by the most efficient combination of geometrical parameters (which in this case makes sense as they have the same bodies dimensions), the second has also a slightly higher value, 1.31E+04 W against 1.26E+04 W.

Secondly, when comparing the two configurations using the optimized parameters of the second configuration it is possible to notice that the second configuration has also a higher value (in this case not slightly higher, but quite higher) than the first one, as it was expected, 55.43% for the second against 27.68% for the first.

Unlike the first case, now the maximum efficiency was obtained for different combinations of geometrical parameters.

The second configuration has the highest efficiency for the first combination in Table 4 and the first has the highest efficiency for the fourth combination (interesting to notice that this is the same configuration that has the highest efficiency in the first comparison).

Thirdly, comparing the average efficiency of all geometrical configurations using both the optimized parameters of the first and second configuration, the second configuration presents better efficiency in both cases.

The average efficiency using the first optimized configuration parameters is 13.34% for the first configuration and 18.66% for the second.

Using the optimized parameters of the second configuration, the average efficiency for the first configuration is 10.38% against 16.13% for the second.

Finally, and most important (as usually when installing a wave energy converter, the optimum configuration is the one chosen), when comparing both optimized configurations the second configuration produces 55,43% efficiency against 47.07% in the first configuration, that represents an improvement of 8.36%, which is a good improvement in the operation of the WEC.

If we compare just the power generated by the two most efficient cases the first configuration has a higher power absorption, which also makes senses, as the bodies of the fourth combination are way bigger than the bodies of the first combination (as it can be seen in Table 12).

The fact mentioned above is not a problem, as a WEC with bigger bodies are more expensive and should usually produce more energy.

Also, it is possible (and common) to install more than one WEC in the same location, being the efficiency of it the most important parameter to take into consideration when considering which WEC to install. For this case (cylinder-sphere) it is now proved that the second configuration is more efficient than the first one, being this the main goal of the present thesis, as it was already mentioned in the Section Objectives.

Table 12:Comparison Between Optimized Bodies for First and Second Configurations (Cylinder-Sphere)

	First Configuration Optimized bodies	Second Configuration Optimized bodies
Buoy Radius [m]	2.5	1
Buoy Draft [m]	1	0.5
Submerged Body Radius [m]	3	1

5.3. Cylinder-Cylinder

To perform the calculations and the optimization process eleven different combinations of geometrical parameters were chosen.

In order to also optimize the PTO and mooring system, the values of PTO and mooring parameters were set to vary based on the available literature, common values were the ones chosen.

After that, the optimization process is carried out and the results are presents for every geometrical combination and the best parameters of PTO and mooring system.

The presentation of the hydrodynamic coefficients is made in this section due to the fact that they are the same for both configurations, as it just depends on the geometry of the bodies.

Table 13:Different Combinations of Geometrical Parameter Used (Cylinder-Cylinder)

Configuration Number	Buoy Radius [m]	Buoy Draft [m]	Submerged Body Radius [m]	Submerged Body Height [m]	Distance Between Bodies [m]
1	1	0.5	1	1	10
2	1	1	1	1	10
3	1	1	2.5	1	10
4	1	1	2.5	2	10
5	2.5	1	1	1	10
6	2.5	2	1	1	10
7	2.5	1	2.5	2	10
8	2.5	2	2.5	2	10
9	2.5	2	4	2	10
10	4	2	2.5	2	10
11	4	2	4	2	10

Table 14:Parameters Variation for Optimization (Cylinder-Cylinder)

Mooring and PTO parameters			
Parameter	Starting Value	Ending Value	Step
PTO Damping [Ns/m]	10000	300000	10000
Equivalent PTO Stiffness [N/m]	10000	140000	10000
Mooring Stiffness/ Floaters Interconnection Stiffness [N/m]	10000	140000	10000

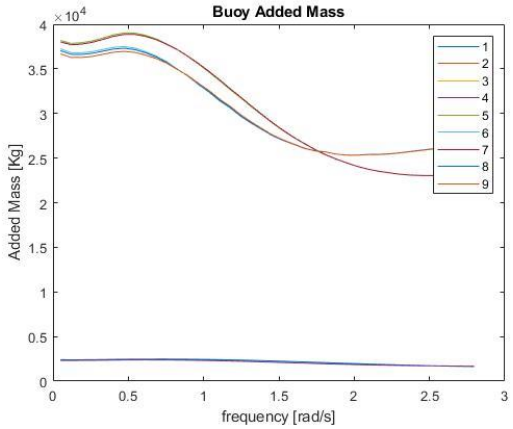

(a)

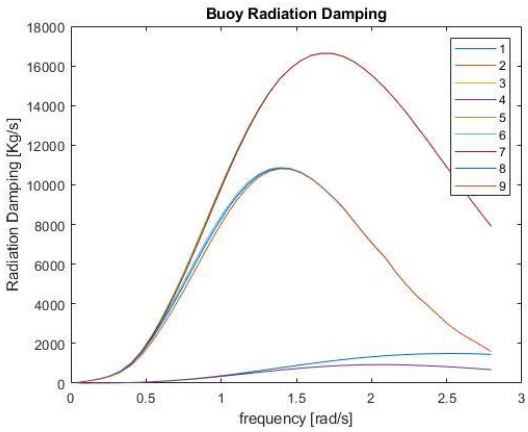

(b)

Figure 52:(a) Buoy Added Mass (Cylinder-Cylinder), (b) Buoy Radiation Damping (Cylinder-Cylinder)

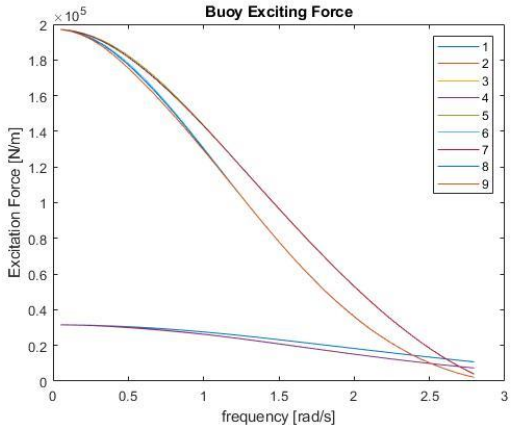

(a)

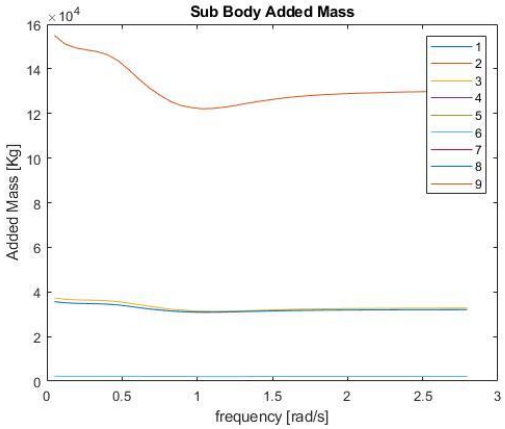

(b)

Figure 51:(a) Buoy Exciting Force (Cylinder-Cylinder), (b) Submerged Body Added Mass (Cylinder-Cylinder)

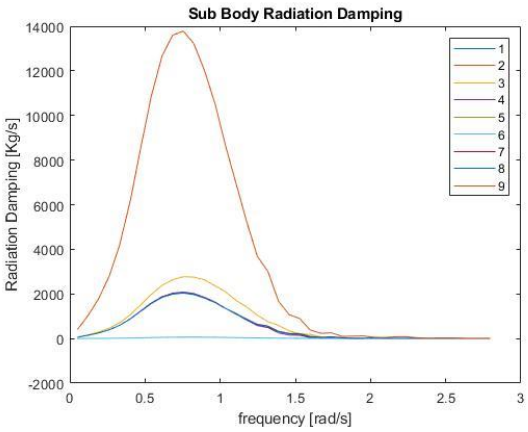

(a)

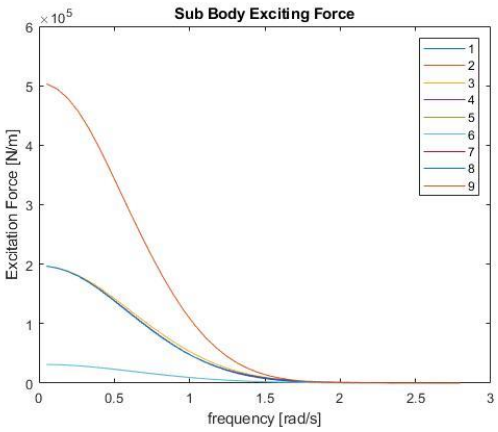

(b)

Figure 53:(a) Submerged Body Radiation Damping (Cylinder-Cylinder), (b) Submerged Body Exciting Force (Cylinder-Cylinder)

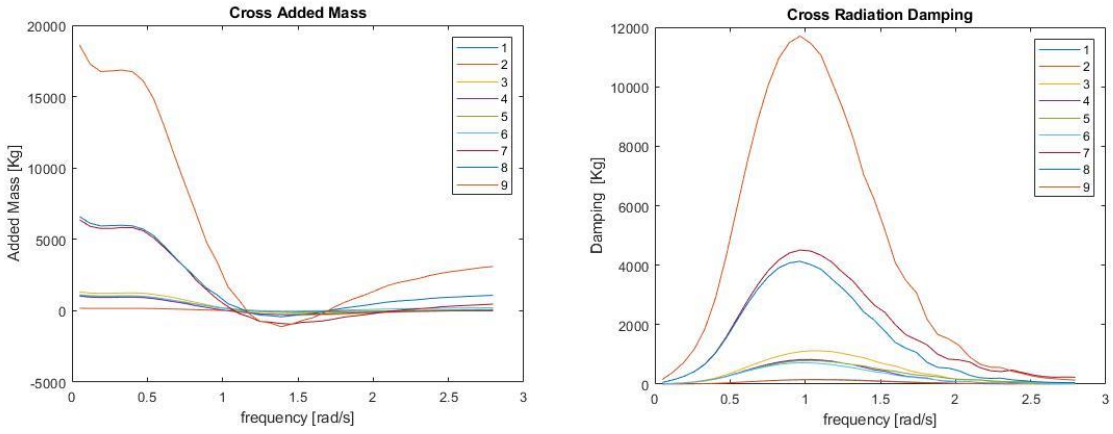

(a) *(b)*

Figure 54:(a) Cross Added Mass (Cylinder-Cylinder), (b) Cross Radiation Damping (Cylinder-Cylinder)

5.3.1. Results for Optimized First Configuration

The presentation and comparison of results in this section was carried out using the parameters for the optimized first configuration for both configurations. These values were obtained following the optimization process described in the chapter Chapter 3Mathematical Model

Table 15:Opitmal Parameters First Configuration (Cylinder-Cylinder)

Optimal Parameters	
Buoy Radius [m]	2.5
Buoy Draft [m]	2
Submerged Body Radius [m]	4
Submerged Body Heigth [m]	2
PTO Damping [Ns/m]	260000
Equivalent PTO Stiffness [N/m]	10000
Mooring Stiffness/ Floaters Interconnection Stiffness [N/m]	20000
b_{visc2} [Ns/m]	3.27E+04

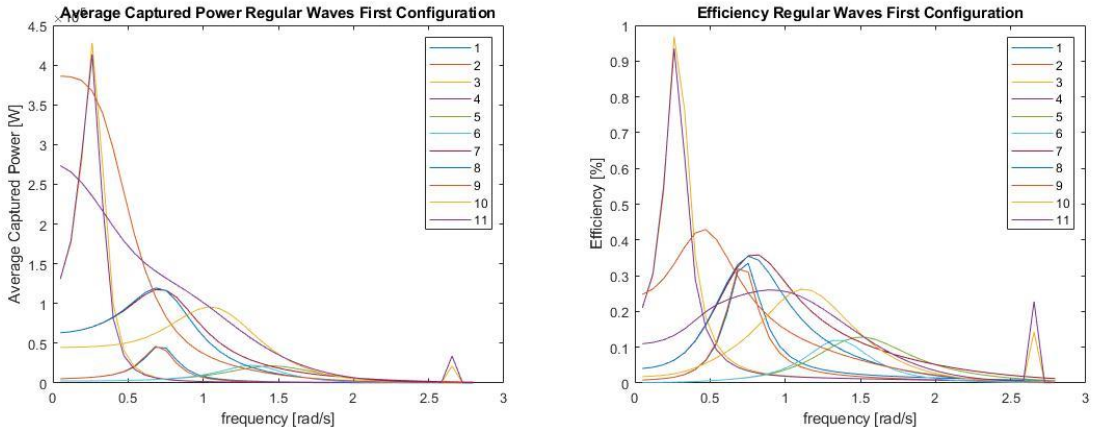

(a) *(b)*

Figure 55:(a) Average Captured Power Regular Waves First Configuration (Cylinder-Cylinder), (b) Efficiency Regular Waves First Configuration (Cylinder-Cylinder)

Table 16:Absorbed Power and Efficiency for First Configuration in Irregular Waves (Cylinder-Cylinder)

Irregular Waves First Configuration		
Geometry	Absorbed Power [W]	Efficiency
1	3.30E+03	30.89%
2	3.16E+03	29.58%
3	1.88E+03	17.62%
4	1.60E+03	14.99%
5	1.28E+03	4.80%
6	1.28E+03	4.78%
7	1.34E+04	50.21%
8	1.28E+04	47.95%
9	1.46E+04	54.86%
10	1.07E+04	25.13%
11	1.90E+04	44.41%

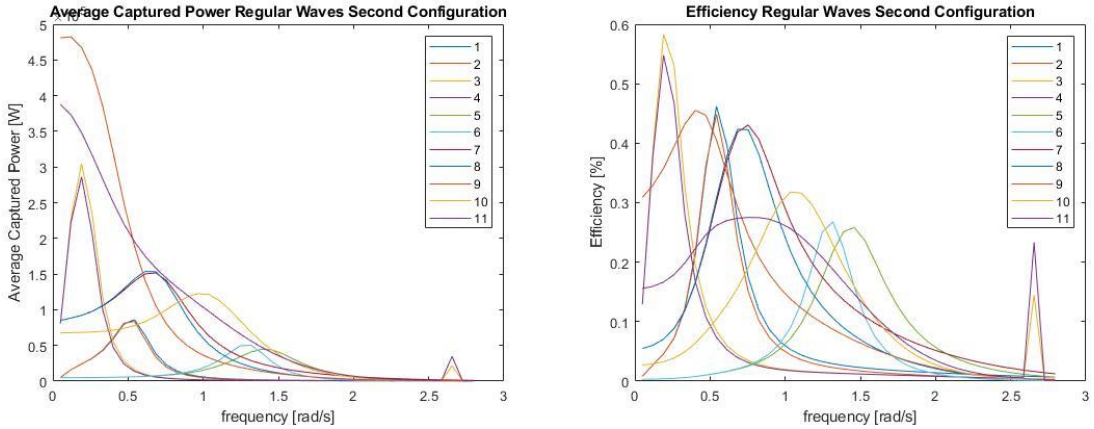

(a) *(b)*

Figure 56:(a) Average Captured Power Regular Waves Second Configuration (Cylinder-Cylinder), (b) Efficiency Regular Waves Second Configuration (Cylinder-Cylinder)

Table 17:Absorbed Power and Efficiency for Second Configuration in Irregular Waves (Cylinder-Cylinder)

Irregular Waves Second Configuration		
Geometry	Absorbed Power [W]	Efficiency
1	4.78E+03	44.84%
2	4.46E+03	41.82%
3	1.31E+03	12.27%
4	1.15E+03	10.77%
5	2.26E+03	8.47%
6	2.36E+03	8.87%
7	1.64E+04	61.32%
8	1.57E+04	58.68%
9	1.48E+04	55.33%
10	1.44E+04	33.83%
11	2.12E+04	49.66%

5.3.2. Results for Optimized Second Configuration

The presentation and comparison of results in this section was carried out using the parameters for the optimized second configuration for both configurations.

Table 18:Opitmal Parameters Second Configuration (Cylinder-Cylinder)

Optimal Parameters	
Buoy Radius [m]	2.5
Buoy Draft [m]	1
Submerged Body Radius [m]	2.5
Submerged Body Heigth [m]	2
PTO Damping [Ns/m]	300000
Equivalent PTO Stiffness [N/m]	140000
Mooring Stiffness/ Floaters Interconnection Stiffness [N/m]	20000
b_{visc2} [Ns/m]	5.23E+03

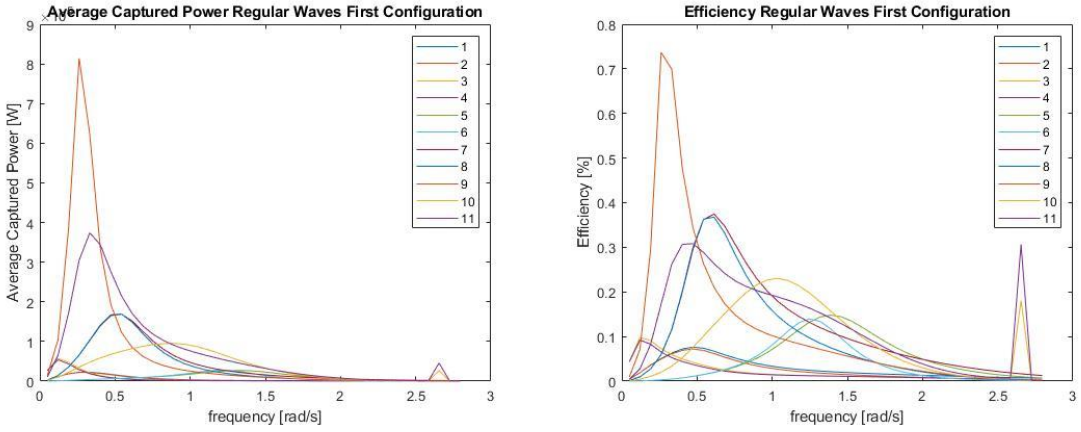

(a) *(b)*

Figure 57:(a) Average Captured Power Regular Waves First Configuration (Cylinder-Cylinder),(b) Efficiency Regular Waves First Configuration (Cylinder-Cylinder)

Table 19:Absorbed Power and Efficiency for First Configuration in Irregular Waves (Cylinder-Cylinder)

Irregular Waves First Configuration		
Geometry	Absorbed Power [W]	Efficiency
1	1.14E+03	10.68%
2	1.04E+03	9.73%
3	5.58E+02	5.23%
4	5.04E+02	4.72%
5	2.15E+03	8.06%
6	2.14E+03	8.03%
7	1.44E+04	53.87%
8	1.35E+04	50.67%
9	1.06E+04	39.69%
10	1.24E+04	28.99%
11	1.99E+04	46.73%

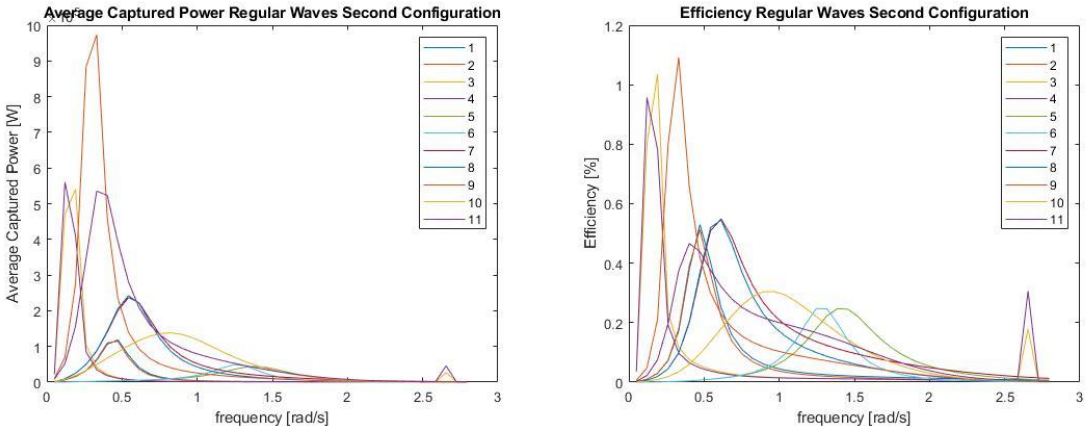

(a) *(b)*

Figure 58:(a) Average Captured Power Regular Waves Second Configuration (Cylinder-Cylinder), (b) Efficiency Regular Waves Second Configuration (Cylinder-Cylinder)

Table 20:Absorbed Power and Efficiency for Second Configuration in Irregular Waves (Cylinder-Cylinder)

Irregular Waves Second Configuration		
Geometry	Absorbed Power [W]	Efficiency
1	4.29E+03	40.17%
2	3.95E+03	37.02%
3	6.79E+02	6.36%
4	5.99E+02	5.62%
5	2.15E+03	8.05%
6	2.23E+03	8.35%
7	1.86E+04	65.67%
8	1.77E+04	62.20%
9	1.23E+04	46.08%
10	1.67E+04	39.22%
11	2.43E+04	56.94%

5.3.3. Analyzes

Firstly, when looking at the comparison between the two configurations using the parameters of the optimized first configuration it is possible to see that the second configuration is already better. The maximum efficiency for the first one is 54.86% against 61.32% for the second.

Also, it is important to notice that in this case both configurations reach the optimum efficiency for different geometrical parameters (number 9 in Table 13 for the first optimization and number 7 for the second optimization). It is interesting to notice that the second configuration reaches higher values of efficiency with a smaller buoy.

Secondly, when comparing the two configurations using the optimized parameters of the second configuration it is possible to notice that the second configuration has also a higher value than the first one, as it was expected, 65.66% for the second against 53.87%%for the first.

Also, it is possible to notice that the highest efficiency was obtained for the same geometrical combination (number seven in Table 13).

Comparing just the power generated by the most efficient combination of geometrical parameters (which in this case makes sense as they have the same bodies dimensions), the second also has a higher value, 1.86E+04 W against 1.44E+04 W.

Thirdly, comparing the average efficiency of all geometrical configurations using both the optimized parameters of the first and second configuration, the second configuration presents better efficiency in both cases.

The average efficiency using the first optimized configuration parameters is 29.57% for the first configuration and 35.08% for the second.

Using the optimized parameters of the second configuration, the average efficiency for the first configuration is 24.22% against 34.43% for the second.

Finally, and most important (as usually when installing a wave energy converter, the optimum configuration is the one chosen), when comparing both optimized configurations the second configuration produces 65.67% efficiency against 54.86% in the first configuration, that represents an improvement of 10.81%, which is a good improvement in the operation of the WEC.

Now an interesting fact, even though the first optimized configuration has a higher dimension of the bodies. It is the second optimized configuration that generates more power, 1.86E+04 against 1.46E+04. For this case (cylinder-cylinder) it is now proved that the second configuration is more efficient than the first one, being this the main goal of the present thesis, as it was already mentioned in the Section Objectives.

Table 21::Comparison Between Optimized Bodies for First and Second Configurations (Cylinder-Cylinder)

	First Configuration Optimized bodies	Second Configuration Optimized bodies
Buoy Radius [m]	2.5	2.5
Buoy Draft [m]	2	1
Submerged Body Radius [m]	4	2.5
Submerged Body Heigth [m]	2.5	2

5.4. Sphere-Sphere

To perform the calculations and the optimization process seven different combinations of geometrical parameters were chosen.

In order to also optimize the PTO and mooring system, the values of PTO and mooring parameters were set to vary based on the available literature, common values were the ones chosen.

After that, the optimization process is carried out and the results are presents for every geometrical combination and the best parameters of PTO and mooring system.

The presentation of the hydrodynamic coefficients is made in this section due to the fact that they are the same for both configurations, as it just depends on the geometry of the bodies.

Table 22:Different Combinations of Geometrical Parameter Used (Sphere-Sphere)

Configuration Number	Buoy Radius [m]	Submerged Body Radius [m]	Distance Between Bodies [m]
1	1	1	10
2	1	2	10
3	2	1	10
4	2	2	10
5	2	3	10
6	3	1	10
7	3	3	10

Table 23:Parameters Variation for Optimization (Sphere-Sphere)

Mooring and PTO parameters			
Parameter	Starting Value	Ending Value	Step
PTO Damping [Ns/m]	10000	300000	10000
Equivalent PTO Stiffness [N/m]	10000	140000	10000
Mooring Stiffness/ Floaters Interconnection Stiffness [N/m]	10000	140000	10000

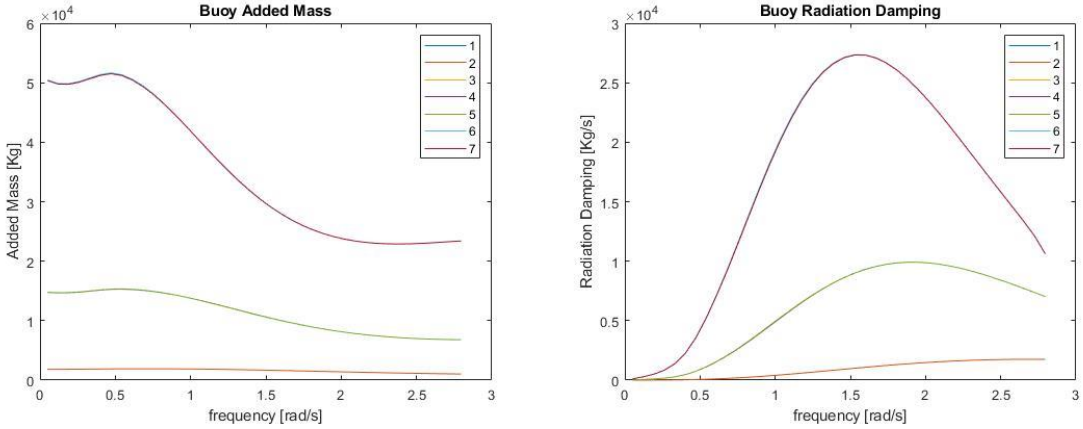

(a) *(b)*

Figure 59:(a) Buoy Added Mass (Sphere-Sphere), (b) Buoy Radiation Damping (Sphere-Sphere)

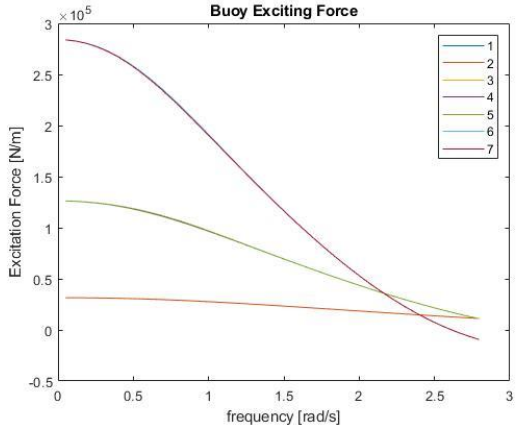

(a)

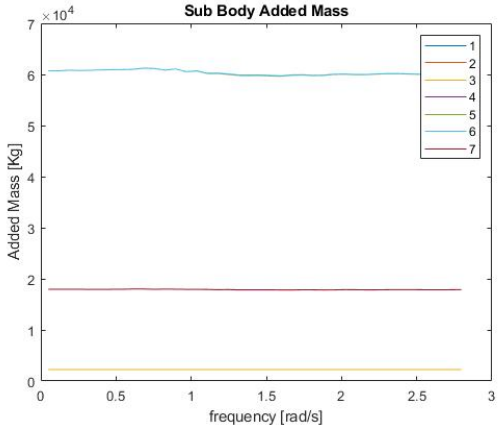

(b)

Figure 60:(a) Buoy Exciting Force (Sphere-Sphere), (b) Submerged Body Added Mass (Sphere-Sphere)

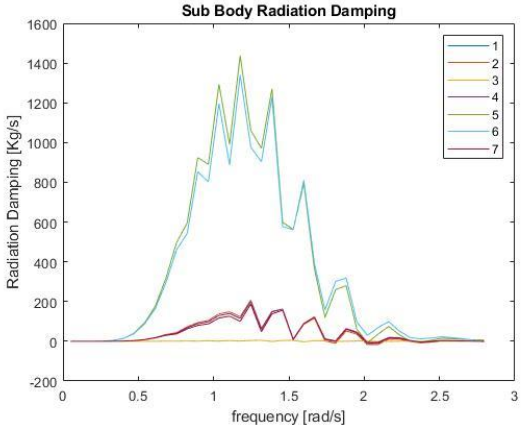

(b)

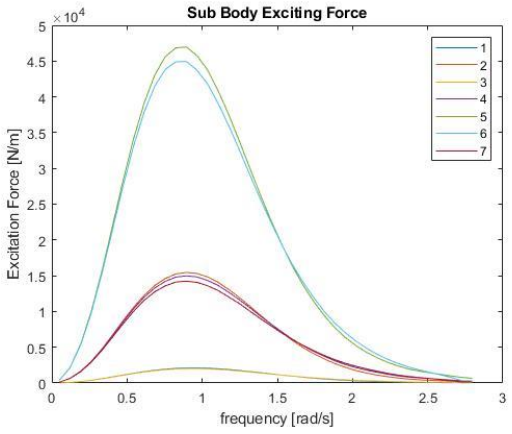

(b)

Figure 62:(a) Submerged Body Radiation Damping (Sphere-Sphere), (b) Submerged Body Exciting Force (Sphere-Sphere)

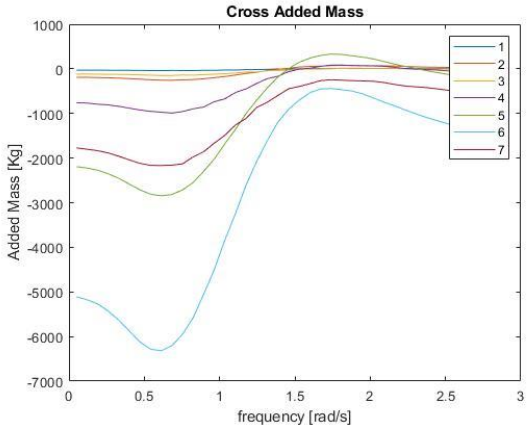

(a)

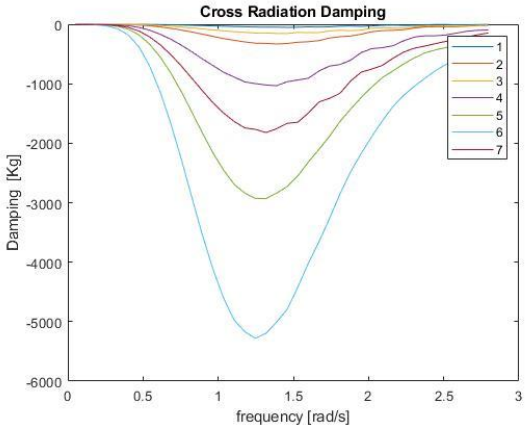

(b)

Figure 61:(a) Cross Added Mass (Sphere-Sphere), (b) Cross Radiation Damping (Sphere-Sphere)

5.4.1. Analyzes of Hydrodynamical Coefficient Results

In this section an analyzes about the hydrodynamical coefficients extracted with NEMOH is carried out.

The analyzes was decided to be carried out in this part of the chapter due to the fact that now all the hydrodynamical coefficients of all the bodies studied are already presented in the sections before that one.

The first consideration that is possible to make while analyzing the hydrodynamical coefficients is that the radiation damping for the submerged body, if the submerged body is a sphere, is neglectable for the cases analyzed. As it is possible to see the values of radiation damping for the submerged body has a magnitude around 10^3 while the values of radiation damping for the buoy has a magnitude around 10^5, meaning it is neglectable

Another conclusion is that the values of added mass for the buoy increases as the size of the buoy increases.

Although this is true, in the case of the cylinder being the buoy, it was noticed that increasing the radius of the buoy produces a way bigger increase in the added mass than increasing the draft of the buoy. It was also noticed that cylinders with similar size of spheres produces a higher added mass than spheres.

It is also possible to conclude that increasing the buoy radius increases the excitation force, in the case of the buoy being a cylinder it was noticed that increasing the draft decreases the excitation force.

This behavior can be explained due to the fact that increasing the draft causes a decrease in the radiating capabilities, this is explained by the fact that the extra submerged part of the buoy reduces its interaction with the waves, and so the excitation force of the incoming waves decreases.

The explanation mentioned above is the same to the fact that the buoy's radiation damping increases with the increase of the radius of the buoy but, in the case of cylindrical body, it decreases with the increase oh the draft.

It can be clearly noticed that spheres have way smaller radiation damping if compared to cylinders, this is due to the fact that the shape of cylinders offers less resistance to the fluid flow around them, causing less radiation.

The submerged added mass is almost constant in the wave frequency. Also, as it was expected it values rises as the size of the body rises. Again, in the case of the cylinder, the rise produced by increasing the radius was way higher than the rise produced by increasing the draft.

The submerged excitation force increases as the size of the body increases, which was expected.

Similar conclusions regarding the analyzes of hydrodynamical coefficients of bodies with different shoes and sizes were reached by Elie et al. (2019)

5.4.2. Results for Optimized First Configuration

The presentation and comparison of results in this section was carried out using the parameters for the optimized first configuration for both configurations. These values were obtained following the optimization process described in the Chapter Mathematical Model

Table 24: Optimal Parameters First Configuration (Sphere-Sphere)

Optimal Parameters	
Buoy Radius [m]	2
Submerged Body Radius [m]	3
PTO Damping [Ns/m]	300000
Equivalent PTO Stiffness [N/m]	110000
Mooring Stiffness/ Floaters Interconnection Stiffness [N/m]	10000
b_{visc2} [Ns/m]	2.05E+04

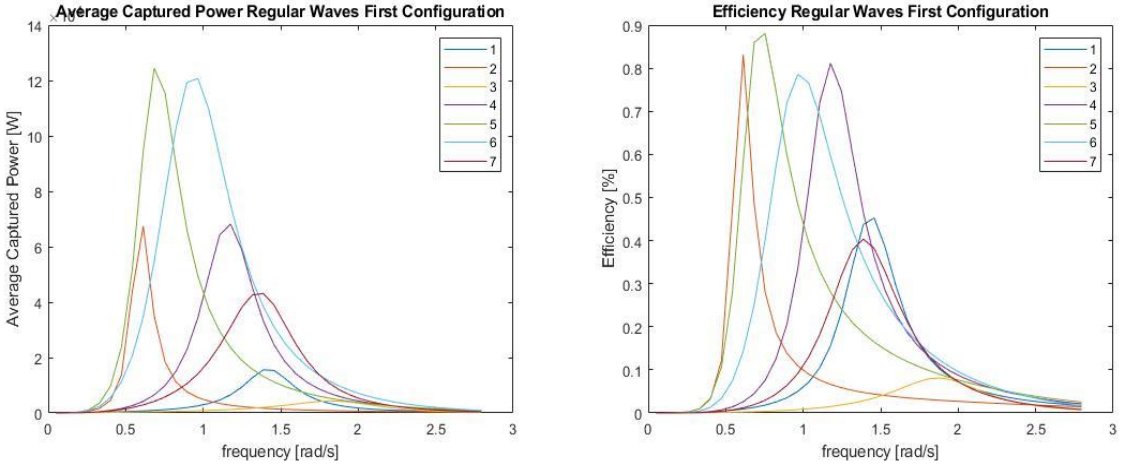

(a) *(b)*

Figure 63:(a) Average Captured Power Regular Waves First Configuration (Sphere-Sphere), (b) Efficiency Regular Waves First Configuration (Sphere-Sphere)

Table 25:Absorbed Power and Efficiency for First Configuration in Irregular Waves (Sphere-Sphere)

Irregular Waves First Configuration		
Geometry	Absorbed Power [W]	Efficiency
1	4.99E+02	4.68%
2	3.15E+03	29.51%
3	1.52E+02	0.71%
4	3.28E+03	15.39%
5	9.96E+03	46.67%
6	1.02E+04	31.85%
7	1.96E+03	6.13%

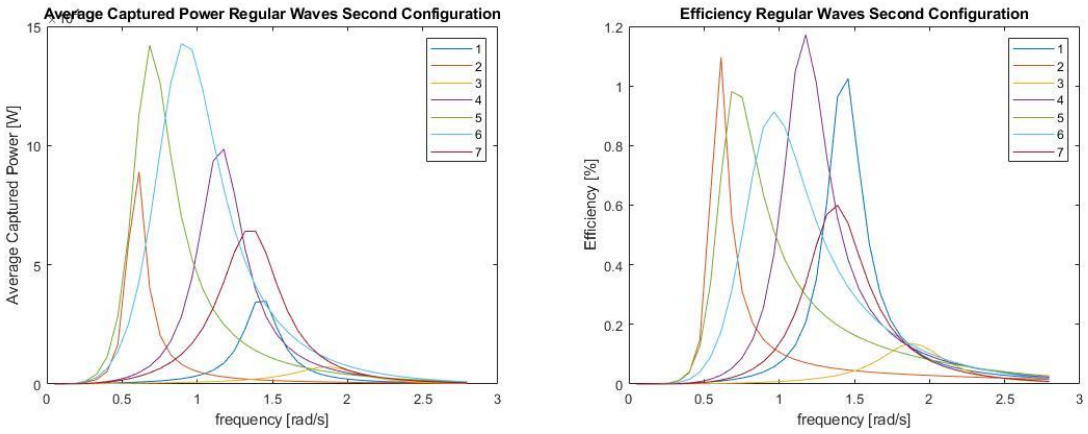

(a) *(b)*

Figure 64:(a) Average Captured Power Regular Waves Second Configuration (Sphere-Sphere), (b) Efficiency Regular Waves Second Configuration (Sphere-Sphere)

Table 26:Absorbed Power and Efficiency for Second Configuration in Irregular Waves(Sphere-Sphere)

Irregular Waves Second Configuration		
Geometry	Absorbed Power [W]	Efficiency
1	7.64E+02	7.16%
2	3.89E+03	36.42%
3	1.71E+02	0.80%
4	4.30E+03	20.15%
5	1.11E+04	52.21%
6	1.20E+04	37.63%
7	2.55E+03	7.97%

5.4.3. Results for Optimized Second Configuration

The presentation and comparison of results in this section was carried out using the parameters for the optimized second configuration for both configurations. These values were obtained following the optimization process described in the Chapter Mathematical Model

Table 27:Optimal Parameters Second Configuration (Sphere-Sphere)

Optimal Parameters	
Buoy Radius [m]	2
Submerged Body Radius [m]	1
PTO Damping [Ns/m]	40000
Equivalent PTO Stiffness [N/m]	140000
Mooring Stiffness/ Floaters Interconnection Stiffness [N/m]	60000
b_{visc2} [Ns/m]	9.10E+03

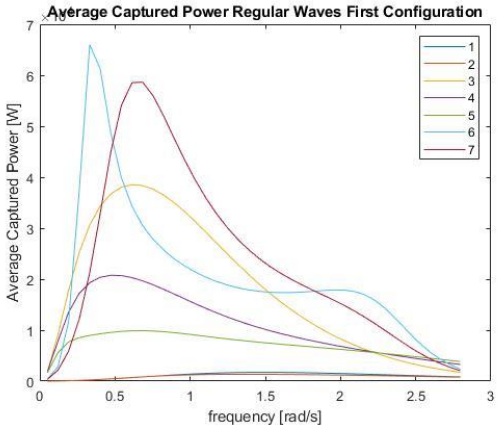

(a)

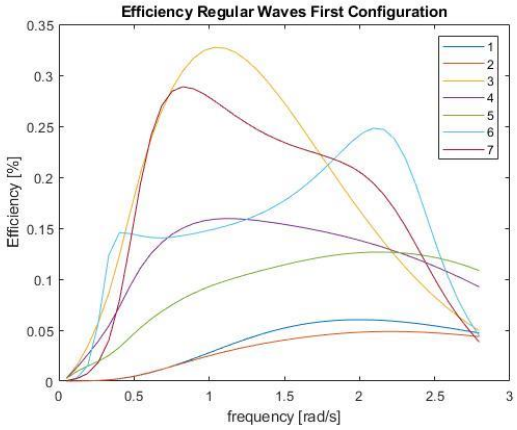

(b)

Figure 65:(a) Average Captured Power Regular Waves First Configuration (Sphere-Sphere), (b) Efficiency Regular Waves First Configuration (Sphere-Sphere)

Table 28:Absorbed Power and Efficiency for First Configuration in Irregular Waves (Sphere-Sphere)

Irregular Waves First Configuration		
Geometry	Absorbed Power [W]	Efficiency
1	1.81E+02	1.70%
2	1.64E+02	1.54%
3	5.32E+03	24.91%
4	2.77E+03	13.00%
5	1.52E+03	7.12%
6	4.68E+03	14.63%
7	7.34E+03	22.93%

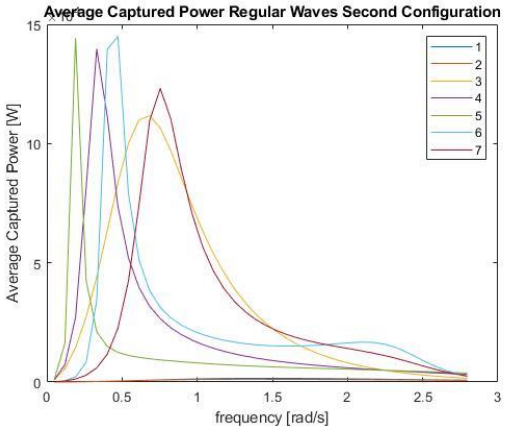

(a)

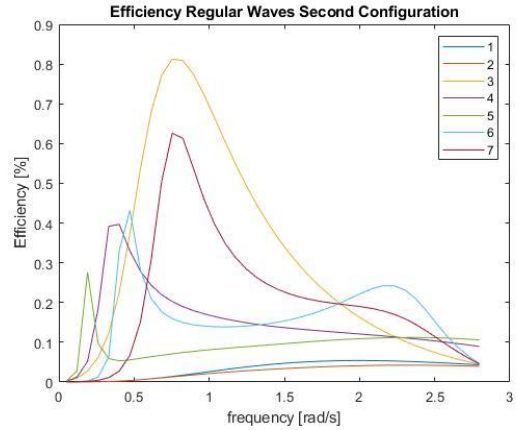

(b)

Figure 66:(a) Average Captured Power Regular Waves Second Configuration (Sphere-Sphere), (b) Efficiency Regular Waves Second Configuration (Sphere-Sphere)

Table 29:Absorbed Power and Efficiency for Second Configuration in Irregular Waves (Sphere-Sphere)

Irregular Waves Second Configuration		
Geometry	Absorbed Power [W]	Efficiency
1	1.69E+02	1.59%
2	1.44E+02	1.35%
3	1.28E+04	60.06%
4	4.91E+03	23.02%
5	1.50E+03	7.05%
6	6.79E+03	21.22%
7	1.09E+04	34.09%

5.4.4. Analyzes

First, when looking at the comparison between the two configurations using the parameters of the optimized first configuration it is possible to see that the second configuration is already slightly better. The maximum efficiency for the first configuration of the PTO is 46.67% against 52.21% for the second one.

Also, it is important to notice that in this case both configurations reach the optimum efficiency for different geometrical parameters (number 5 in Table 22 for the first optimization and number 3 for the second optimization).

It is important to notice that the second configuration reaches a higher efficiency in this case for a smaller buoy but a bigger submerged body.

Secondly, when comparing the two configurations using the optimized parameters of the second configuration it is possible to notice that the second configuration has also a higher value (in this case not slightly higher, but quite higher) than the first one, as it was expected, 60.06% for the second against 24.91% for the first.

It is important to notice that in this case both configurations reach the optimum efficiency for the same geometrical parameters (number 3 in Table 22).

Comparing just the power generated by the most efficient combination of geometrical parameters (which in this case makes sense as they have the same bodies dimensions), the second also has a higher value, 1.28E+04 W against 5.32E+03 W.

Thirdly, comparing the average efficiency of all geometrical configurations using both the optimized parameters of the first and second configuration, the second configuration presents better efficiency in both cases.

The average efficiency using the first optimized configuration parameters is 19.28% for the first configuration and 23.19% for the second.

Using the optimized parameters of the second configuration, the average efficiency for the first configuration is 12.26% against 21.20% for the second.

Finally, and most important (as usually when installing a wave energy converter, the optimum configuration is the one chosen), when comparing both optimized configurations the second configuration produces 60.06% efficiency against 46.67% in the first configuration, that represents an improvement of 13.39%, which is a good improvement in the operation of the WEC.

Now there is an interesting fact, even though the first optimized configuration has bigger bodies than the second (Table 30), is the second one that generates more power (that proofs that this optimization was indeed really good).

The second one generates 1.28E+04 W against 9.96E+03 W for the first one.

For this case (sphere-sphere) it is now proved that the second configuration is more efficient than the first one, being this the main goal of the present thesis, as it was already mentioned in the Section Objectives.

Table 30: Comparison Between Optimized Bodies for First and Second Configurations (Sphere-Sphere)

	First Configuration Optimized bodies	Second Configuration Optimized bodies
Buoy Radius [m]	2	2
Submerged Body Radius [m]	3	1

5.5. Analyzes of Absorbed Power

The goal of the present section is to analyze the graphics about absorbed power and efficiency generated so far. This was the moment selected to do it as in this part all of the graphics are already shown.

The peaks observed in the graphs of absorbed power (Figure 47(a)-47(a); Figure 55(a)-55(a); Figure 63(a)-63(a)) represents the natural resonant frequency of each of the systems.

This happens because when the incident wave (or any other external harmonic force) has its frequency in coincidence with the natural resonance frequency of the system a peak of energy absorption is observed. The more far away the frequency of the waves goes from this value, the absorption of energy decreases.

Systems can have different values of natural resonant frequencies as it depends on the system parameters. Looking at the graphs of absorbed power in the present thesis it is possible to see that different configurations have different values of natural resonant frequencies as it was expected (due to the fact that each of these systems has different parameters).

Another important consideration now is due to the fact that when dealing with irregular waves, usually the optimized system has a value of natural resonant frequency close to the value of the most common frequency that happens in the place considered (by looking at Figure 41 or Figure 42 it is possible to see that this frequency for the case of Azore-Pico is around 0.7 rad/s).

That happens because, as said before, the system generates the most energy if the frequency of the incoming waves coincides with the natural resonant frequency. So, if the frequency that occurs the most in a sea state is the same as the natural resonant frequency of this system, the systems will operate more time in the condition of resonance, consequently, operating more time at the peak of power absorption.

The optimized configurations in the present thesis are generally in accordance with that, as for example the case of optimized cylinder-sphere with the First PTO configuration, the natural resonant frequency of the system is around 0.7 rad/s as can be seen in Figure 47(a) (configuration number 4); or the case of optimized Sphere-Sphere for the second configuration of the PTO, the resonant frequency is also around 0.7 rad/s, as it can be seen in Figure 66(a) (configuration number 3).

It was realized that rising the size of the submerged body greatly decreases the value of resonant frequency. This happens mainly because of the great physical and added mass generated by the large volumes of the submerged body.

This can be seen in by looking at the difference in resonant frequency of the configuration 3 and 4 in the Figure 48(a). The only difference between these configurations is the radius of the submerged sphere (configuration 3 has 1 meter and configuration 4 has 3 meters). However, these configurations show huge difference when it comes to natural resonant frequency. Configuration 3 around 1.5 and configuration 4 around 0.6.

Another explanation that needs to be made is due to the fact that some graphs of efficiency/Power absorption show two peaks instead of one (configuration 2 in Figure 50(a)). The reason for this fact was studied and described by Bijun et al. (2014) and Rezanejad et al. (2018).

In their research it is shown that a two-body wave energy converter is a system with two natural frequencies. It is after that deduced an equation for efficiency that contains these two natural frequencies.

In order to find the optimum frequency, the zero value is applied to the derivate of the efficiency function with respect to the frequency. After some manipulations with the equations, it ends in a quadratic equation, in which the square of the positive roots corresponds to the optimum frequencies. Depending on the parameters of this equation, the solution can lead to three positive and one negative real value or one positive and one negative real values.

In the case of the equation having three positive and one negative real roots, the system will have two maxima and one minimum. These two maxima are the two peaks seen in the graphics.

In the case of the equation having one positive and one negative real roots, the system will have one maxima (the two maxima coincide at the same point, creating a single maxima). This value of maxima represents the only peak seen.

5.6. Comparison Between Optimal Configurations

The comparison between the optimized WEC of all the three geometrical configurations is presented here.

This was done in order to facilitate the visualizations of the results obtained and the analyzes, as it is better to analyze results if all of the data is showed together.

Table 31:Comparison of Optimal Design for all Geometrical Configurations (Cylinder-Sphere, Cylinder-Cylinder, Sphere-Sphere)

	First Configuration Optimized bodies	Second Configuration Optimized bodies
Geometrical Configuration	**Cylinder-Sphere**	
Buoy Radius [m]	2.5	1
Buoy Draft [m]	1	0.5
Submerged Body Radius [m]	3	1
Absorbed Power Irregular Waves [W]	1.26E+04	5.91E+03
Efficiency Irregular Waves	47.07%	55.43%
Geometrical Configuration	**Cylinder-Cylinder**	
Buoy Radius [m]	2.5	2.5
Buoy Draft [m]	2	1
Submerged Body Radius [m]	4	2.5
Submerged Body Heigth [m]	2.5	2
Absorbed Power Irregular Waves [W]	1.46E+04	1.86E+04
Efficiency Irregular Waves	54.86%	65.67%
Geometrical Configuration	**Sphere-Sphere**	
Buoy Radius [m]	2	2
Submerged Body Radius [m]	3	1
Absorbed Power Irregular Waves [W]	9.96E+03	1.28E+04
Efficiency Irregular Waves	46.67%	60.06%

As it can be seen in Table 31 all the efficiencies for the second configuration of the PTO optimized are higher than the first configuration. This means that it costs less money to generate energy in Pico-Azores using the second configuration (PTO between submerged body and sea bottom) instead of the first one (PTO between buoy and submerged body).

The wave energy converter that reached the best efficiency was the cylinder-cylinder for both the first and the second configuration of the PTO. However, the second most efficient was the sphere-sphere, for the case of second PTO configuration, and cylinder-sphere for the case of first PTO configuration.

Also, it is possible to see that the second configuration of the PTO is optimized always for smaller bodies (both floater and submerged body, exception made for the case of cylinder-cylinder in which the size of the buoy is the same) in comparison with the first configuration, this is even more noticed in the case of the submerged body.

For the case cylinder-sphere, the size of the submerged sphere goes from 3 meters radius (first configuration of the PTO) to 1 meter (second configuration of the PTO).

For cylinder-cylinder it goes from 4 meters of radius and 2.5 meters of height (for the first PTO configuration) to 2.5 meters radius and 2 meters height (second configuration of the PTO).

For the case sphere-sphere it goes from 3 meters radius (for the first PTO configuration) to 1 meter (for the second PTO configuration).

It is also possible to notice that the second configuration is always optimized for smaller values of b_{visc2}. This is mathematically explained by the fact previously mentioned that the second configuration is always optimized for smaller submerged bodies, and by looking at the equation 27 in the chapter Mathematical Model ($b_{visc2} = 0.5\rho A_c c_d \frac{8}{3\pi} V_{max}$) it is possible to see that this calculation depends on the area of the submerged body in the heave direction (A_c), and as said, the second configuration is always optimized for a smaller submerged body. A possible physical explanation for this fact is that the power generated by the second configuration depends only on the heave movement of the submerged body, so the more it moves the better, while the first configuration generates energy by a combination of the movements of the buoy and the submerged body. This is explained in details and showed in the equations 36 and 37 of the chapter Mathematical Model (for the first configuration of the PTO $P_{avg}(\omega) = 0.5\omega^2 c_{pto} abs(X_1 - X_2)$ and for the second $P_{avg}(\omega) = 0.5\omega^2 c_{pto} abs(X_2)$, in which $X_1 and\ X_2$ are the displacement. So, it makes perfect sense that the optimization of the second configuration takes more into consideration the reduction of this coefficient while the one for the first configuration doesn't.

Now, analyzing all the optimized data together, it is possible to notice that the first configuration of the PTO produced an average efficiency of 49.53%, while the second configuration of the PTO produced an average efficiency of 60.39%. That means that using the second configurations instead of the first one generates an average improvement in the efficiency of the optimized data of 10.85%.

Comparing all the cases and efficiencies calculated (not just the optimized ones) in the present thesis it is possible to notice that the second configuration of the PTO still more efficient than the first one. The second configuration has an average efficiency of 24.62% while the first one has an efficiency of 18.17%. So, the second configuration is 6.45% more efficient than the first one considering all the cases analyzed.

Also, as it was said before in the analyzes of each different configuration, comparing just all the cases for each configuration (cylinder-sphere, cylinder-cylinder, and sphere-sphere) the second configuration of the PTO is still more efficient in all the cases. For cylinder-sphere 17.40% against 11.86%, for cylinder-cylinder 34.27% against 26.89% and for the case of sphere-sphere 22.19% against 15.77%. This means that the second configuration is indeed more efficient than the first one for all the cases analyzes. This final conclusion proofs the starting objective of the present thesis previously described.

Chapter 6. Conclusion

The present study was carried out in order to compare two different configurations of wave energy converters (PTO in between floater and submerged body; and PTO in between submerged body and sea bottom) and decide which one is better in terms of efficiency of harvesting energy (as having a higher efficiency means cheaper costs for generating energy).

The initial desire of the thesis was to prove that the second configuration is more efficient (and so produce energy in a cheaper way if all other costs are assumed constant) than the first configuration.

The analyzes was carried out firstly using NEMOH to model different structures of the wave energy converters and obtain the hydrodynamical coefficients. Followed by the development of a dynamic model that optimizes the system and compare the maximum efficiencies and power absorbed for the two configurations, all the results were presented in several tables in the Chapter 5.

The analyzes was carried out for three different geometrical configurations (cylinder-sphere, cylinder-cylinder, sphere-sphere for the floater and the submerged body respectively) placed in a specific area of the ocean, Pico-Azores-Portugal.

After the analyzes was carried out and the results compared, it was concluded (as it was desired in the begging of the thesis) that the second configuration is more efficient than the first one for all three geometrical configurations. The average difference of efficiency between the two configurations is 10.85%. That means that, if considering all the other costs (for instance, installation) constant, the second configuration can generate energy with less costs, being this of paramount importance as the cost of energy is one of the main barriers for the usage of wave energy converters nowadays.

This is the main barrier nowadays because wave energy is generally clean, so it doesn't pollute as much as conventional ways of generating energy (as coal or fuel for instance).

That means that if somehow this energy could be harvested in a cheaper way it would be way more used all over the globe and it would also prevent the excess of pollution caused by the conventional ways of generating energy (being this one of the biggest current problems of the world)

It was also noticed that the second configuration is optimized for smaller bodies than the first one. For example, in the case cylinder-sphere the first configuration is optimized for buoy radius of 2.5m, buoy draft of 1m and submerged body of 3m; and the second configuration is optimized for buoy radius of 1m, buoy draft of 0.5m and submerged body of 1m.

The work presented in this thesis is expected to contribute to the understanding of the effect of the variation of the design variables of a WEC on its performance.

For the future work it is suggested to improve the model by taking into consideration some non-linear effects. This can be done be creating models using not just the frequency domain (as it was done in the present thesis) but also using the time domain. The time domain presents some advantages if the effect of nonlinear forces wants to be considered. And, by considering these effects it is possible to represent and analyze for example higher order waves, complex mooring, non-linear wave excitation forces.

Also, in future works, the analyzes should be carried out for the same configurations but other areas in the ocean (as in the present thesis just the region of Pico-Azores was considered). By doing these the results are more reliable, once it is guaranteed that the second configuration is indeed more efficient than the first one no matter were in the ocean the analyzes is being made.

Another possible addition for the present work to be done in the future is taking into consideration the effect of the wind, once in some parts of the ocean this effect could be quite high and could

be taken into consideration for a more reliable conclusion. Another possible addition for the present work is to implement some control methods and check if after this the second configuration still is more efficient.

Although all of these additions that could be done in future works would improve the reliability of the conclusions, they would also represent more computational time and capacity, combined with more complex analyzes involving probably different software's and equations in order to take care of the non-linearities that would appear.

References

Aderinto, Tunde & Li, Hua. (2018). Ocean Wave Energy Converters: Status and Challenges. Energies. 11. 1250. 10.3390/en11051250.

Al Shami, E., Wang, X., Zhang, R. and Zuo, L., 2019. A parameter study and optimization of two body wave energy converters. *Renewable energy*, *131*, pp.1-13.

Al Shami, E., Wang, X. and Ji, X., 2019. A study of the effects of increasing the degrees of freedom of a point-absorber wave energy converter on its harvesting performance. *Mechanical Systems and Signal Processing*, *133*, p.106281.

Al Shami, E., Zhang, R. and Wang, X., 2019. Point absorber wave energy harvesters: A review of recent developments. *Energies*, *12*(1), p.47.

Ahamed, R., McKee, K. and Howard, I., 2020. Advancements of wave energy converters based on power take off (PTO) systems: A review. *Ocean Engineering*, *204*, p.107248.

All Answers Ltd. November 2018. Marine Energy Generating Devices & their Suitability for Ireland's Coastline. [online]. Available from: https://ukdiss.com/examples/marine-energy-ireland.php?vref=1 [Accessed 10 February 2021].

Aw-energy.com. 2021. *WaveRoller – AW-Energy Oy*. [online] Available at: <https://aw-energy.com/waveroller/> [Accessed 3 February 2021].

Babarit, A. and G. Delhommeau (2015). "Theoretical and numerical aspects of the open source BEM solver NEMOH." 11th European Wave and Tidal Energy Conference (EWTEC2015).

Bacelli, G., Ringwood, J.V. and Gilloteaux, J.C., 2011. A control system for a self-reacting point absorber wave energy converter subject to constraints. *IFAC Proceedings Volumes*, *44*(1), pp.11387-11392.

Beatty, S.J., Hall, M., Buckham, B.J., Wild, P. and Bocking, B., 2015. Experimental and numerical comparisons of self-reacting point absorber wave energy converters in regular waves. *Ocean Engineering*, *104*, pp.370-386.

Bijun Wu, Xing Wang, Xianghong Diao, Wen Peng, Yunqiu Zhang, Response and conversion efficiency of two degrees of freedom wave energy device, Ocean Engineering, Volume 76, 2014, Pages 10-20

Bolin, David, et al. "STATISTICAL PREDICTION OF GLOBAL SEA LEVEL FROM GLOBAL TEMPERATURE." *Statistica Sinica*, vol. 25, no. 1, 2015, pp. 351–367. *JSTOR*, www.jstor.org/stable/24311020. Accessed 25 July 2021.

Bozzi, S., Miquel, A.M., Antonini, A., Passoni, G. and Archetti, R., 2013. Modeling of a point absorber for energy conversion in Italian seas. *Energies*, *6*(6), pp.3033-3051

Cengel, Y. A, Cimbala, J. M. (2010). Fluid Mechanics Fundamentals and Application. 2nd Ed

Cheng, Z., Yang, J., Hu, Z. and Xiao, L., 2014. Frequency/time domain modeling of a direct drive point absorber wave energy converter. *Science China Physics, Mechanics and Astronomy*, *57*(2), pp.311-320.

Christian-D. Schönwiese, (1994) Analysis and prediction of global climate temperature change based on multiforced observational statistics, Environmental Pollution, Volume 83, Issues 1–2,

Cruz J (2008) Ocean Wave Energy: current status and future perspectives. Springer, Heidelberg p. 423.

Emec.org.uk. 2021. *Wave devices : EMEC: European Marine Energy Centre*. [online] Available at: <http://www.emec.org.uk/marine-energy/wave-devices/> [Accessed 15 August 2020].

Emec.org.uk. 2017. *Pelamis Wave Power : EMEC: European Marine Energy Centre*. [online] Available at: <http://www.emec.org.uk/about-us/wave-clients/pelamis-wave-power/> [Accessed 12 July 2020].

Engström, J., Eriksson, M., Isberg, J. and Leijon, M., 2009. Wave energy converter with enhanced amplitude response at frequencies coinciding with Swedish west coast sea states by use of a supplementary submerged body. *Journal of Applied Physics*, *106*(6), p.064512.

Falcão A. F. O. (2010) Wave Energy Utilization: A Review of the technologies. Renewable and Sustainable Energy Reviews, Volume 14, Issue 3, 2010, p. 899-918,

Falcão, A.F. and Rodrigues, R.J.A., 2002. Stochastic modelling of OWC wave power plant performance. *Applied Ocean Research*, *24*(2), pp.59-71.

Farrok, O., Ahmed, K., Tahlil, A.D., Farah, M.M., Kiran, M.R. and Islam, M., 2020. Electrical power generation from the oceanic wave for sustainable advancement in renewable energy technologies. *Sustainability*, *12*(6), p.2178.

Folley, M., Whittaker, T. and Osterried, M., 2004, January. The oscillating wave surge converter. In *The Fourteenth International Offshore and Polar Engineering Conference*. International Society of Offshore and Polar Engineers.

Getzin S., Yizhaq H., Bell B., et al. Discovery of fairy circles in Australia supports self-organization theory. Proc. Natl. Acad. Sci.2016; 113: 3551-3556

Getzin S., Wiegand K., Wiegand T., et al. Adopting a spatially explicit perspective to study the mysterious fairy circles of Namibia. Ecography 2015; 38: 1-11.

Giorgio Bacelli, John V. Ringwood, Jean-Christophe Gilloteaux, A control system for a self-reacting point absorber wave energy converter subject to constraints, IFAC Proceedings Volumes, Volume 44, Issue 1, 2011, Pages 11387-11392

Goda, Y., 2010. *Random seas and design of maritime structures* (Vol. 33). World Scientific Publishing Company.

Guedes Soares, C., Bhattacharjee, J., Tello, M. and Pietra, L., 2012. Review and classification of wave energy converters. *Maritime Engineering and Technology. London: Taylor & Francis Group*, pp.585-594

Harris, Rob & Johanning, Lars & Wolfram, Julian. (2006). Mooring systems for wave energy converters: A review of design issues and choices. Proceedings of the Institution of Mechanical Engineers. Part B: Journal of Engineering Manufacture. 220. 159-168.

Hausfather, Z., Drake, H. F., Abbott, T., & Schmidt, G. A. (2020). Evaluating the performance of past climate model projections. Geophysical Research Letters, 47, e2019GL085378.

Jaya Muliawan, M., Gao, Z., Moan, T. and Babarit, A., 2013. Analysis of a two-body floating wave energy converter with particular focus on the effects of power take-off and mooring systems on energy capture. *Journal of Offshore Mechanics and Arctic Engineering*, *135*(3).

Jiejie Sun, Wenxing Jiao, Qian Wang, Tongli Wang, Hongqiang Yang, Jiaxin Jin, Huili Feng, Jiahuan Guo, Lei Feng, Xia Xu, Weifeng Wang, Potential habitat and productivity loss of Populus deltoides industrial forest plantations due to global warming, Forest Ecology and Management, Volume 496, 2021

Kalofotias, F., 2017. Manual for the open source potential solver: NEMOH.

Liang, C. and Zuo, L., 2016, September. On the dynamics and design of a two-body wave energy converter. In *Journal of Physics: Conference Series* (Vol. 744, No. 1, p. 012074). IOP Publishing.

Matos, A., Madeira, F., Fortes, C.J.E.M., Didier, E., Poseiro, P. and Jacob, J., 2015. Wave energy at Azores islands. *Proc., SCACR*.

Mørk, G., et al. (2010). Assessing the Global Wave Energy Potential. ASME 2010 29th International Conference on Ocean, Offshore and Arctic Engineering.

OES (2016). Annual Report 2016. Available at: https://report2016.ocean-energy-systems.org (Accessed: 9 January 2021).

OES (2017). International Vision for Ocean Energy Report 2017. Available at: https://testahemsidaz2.files.wordpress.com/2017/03/oes-international-vision.pdf (Accessed: 9 January 2021).

Oikonomou, C., 2018. *Numerical hydrodynamic analysis of wave energy converter arrays with inter-body mooring connections with the spar-buoy OWC as a case study* (Doctoral dissertation, Lancaster University).

Penalba, M., Kelly, T. and Ringwood, J., 2017. Using NEMOH for modelling wave energy converters: A comparative study with WAMIT.

Rezanejad, K., Guedes Soares, C., (2018) Enhancing the primary efficiency of an oscillating water column wave energy converter based on a dual-mass system analogy, Renewable Energy, Volume 123, 2018, Pages 730-747

Ricci, P., 2012. Modelling, optimization and control of wave energy point-absorbers [PhD thesis]. *Instituto Superior Técnico*.

Ritchie, H., 2017. *Energy Production and Consumption*. [online] Our World in Data. Available at: <https://ourworldindata.org/energy-production-consumption> [Accessed 9 June 2020].

Ruezga, A., 2019. Buoy Analysis in a Point-Absorber Wave Energy Converter. *IEEE Journal of Oceanic Engineering*, *45*(2), pp.472-479.

Sang, Y., Karayaka, H.B., Yan, Y., Zhang, J.Z., Bogucki, D. and Yu, Y.H., 2017. A rule-based phase control methodology for a slider-crank wave energy converter power take-off system. *International Journal of Marine Energy*, *19*, pp.124-144.

Shadman, M., Avalos, G.O.G. and Estefen, S.F., 2021. On the power performance of a wave energy converter with a direct mechanical drive power take-off system controlled by latching. *Renewable Energy*, *169*, pp.157-177.

Shadman, M., Estefen, S.F., Rodriguez, C.A. and Nogueira, I.C., 2018. A geometrical optimization method applied to a heaving point absorber wave energy converter. *Renewable energy*, *115*, pp.533-546.

Siow, C.L., Koto, J., Abyn, H. and Khairuddin, N., 2014. Linearized morison drag for improvement semi-submersible heave response prediction by diffraction potential. *Journal of Ocean, Mechanical and Aerospace Science and Engineering*, *6*, pp.8-16.

Tamir Klein, William R.L. Anderegg, (2021) A vast increase in heat exposure in the 21st century is driven by global warming and urban population growth, Sustainable Cities and Society, Volume 73

Vicente, Pedro & Falcao, Antonio & Justino, Paulo. (2011). Optimization of Mooring Configuration Parameters of Floating Wave Energy Converters. Proceedings of the International Conference on Offshore Mechanics and Arctic Engineering - OMAE. 5. 10.1115/OMAE2011-49955.

Vidhee Avashia, Amit Garg, Implications of land use transitions and climate change on local flooding in urban areas: An assessment of 42 Indian cities, Land Use Policy, Volume 95, 2020

Walton, R., 2019. Global electricity consumption to rise 79 percent higher by 2050, EIA says | Power Engineering. [online] Power Engineering. Available at: <https://www.power-eng.com/renewables/global-electricity-consumption-to-rise-79-percent-higher-by-2050-eia-says/> [Accessed 7 June 2020].

Wang, L., Lin, M., Tedeschi, E., Engström, J. and Isberg, J., 2020. Improving electric power generation of a standalone wave energy converter via optimal electric load control. *Energy*, *211*, p.118945.

Water Wave Mechanics for Engineers and Scientists – pg.98

Zhao, X.L., Ning, D.Z., Zou, Q.P., Qiao, D.S. and Cai, S.Q., 2019. Hybrid floating breakwater-WEC system: A review. *Ocean Engineering*, *186*, p.106126.

Zheng Chen, Yong-Ping Wu, Guo-Lin Feng, Zhong-Hua Qian, Gui-Quan Sun (2021) Effects of global warming on pattern dynamics of vegetation: Wuwei in China as a case, Applied Mathematics and Computation, Volume 390